X-ray imaging for environmental science

Chris Jacobsen
Associate Division Director, X-ray Science Division, Advanced Photon Source
Professor, Physics & Astronomy, Northwestern University

Argonne NATIONAL LABORATORY | Advanced Photon Source

NORTHWESTERN UNIVERSITY

U.S. DEPARTMENT OF ENERGY

X-ray refractive index

Above the plasma frequency:

$$n = 1 - \frac{n_a r_e}{2\pi}\lambda^2 (f_1 + if_2) = 1 - \alpha\lambda^2 (f_1 + if_2)$$

Phase velocity is faster than light in vacuum!

$$v_p = \frac{w}{k} \approx c\left(1 + \alpha\, f_1 \lambda^2\right)$$

But group velocity is OK:

$$v_g = \frac{dw}{dk} \approx c\left(1 - \alpha\, f_1 \lambda^2\right)$$

Prisms refract x rays the opposite way from visible light!

Phase is advanced rather than retarded!

Total internal reflection becomes external, with critical angle

$$\theta_c \approx \sqrt{2\alpha\, \lambda^2 f_1}$$

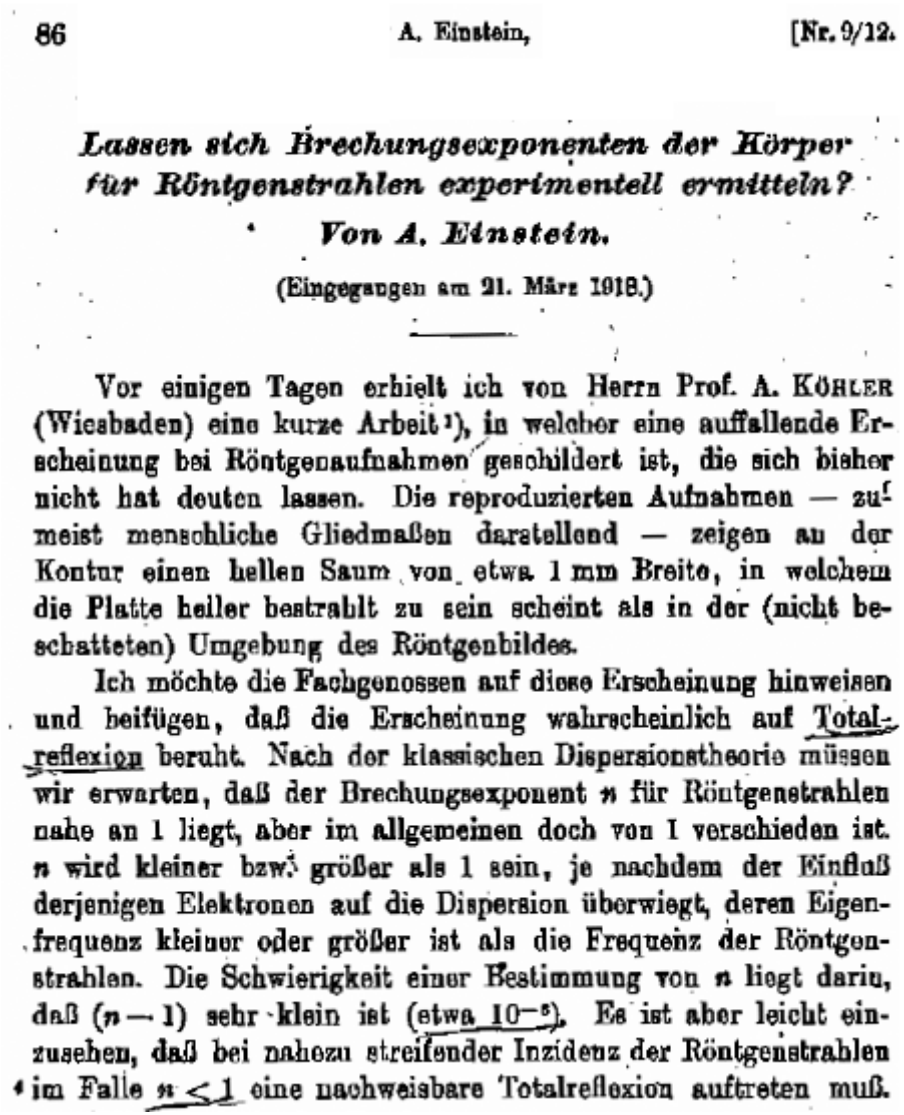

86 A. Einstein, [Nr. 9/12.

Lassen sich Brechungsexponenten der Körper für Röntgenstrahlen experimentell ermitteln?

Von A. Einstein.

(Eingegangen am 21. März 1918.)

Vor einigen Tagen erhielt ich von Herrn Prof. A. KÖHLER (Wiesbaden) eine kurze Arbeit[1]), in welcher eine auffallende Erscheinung bei Röntgenaufnahmen geschildert ist, die sich bisher nicht hat deuten lassen. Die reproduzierten Aufnahmen — zumeist menschliche Gliedmaßen darstellend — zeigen an der Kontur einen hellen Saum von etwa 1 mm Breite, in welchem die Platte heller bestrahlt zu sein scheint als in der (nicht beschatteten) Umgebung des Röntgenbildes.

Ich möchte die Fachgenossen auf diese Erscheinung hinweisen und beifügen, daß die Erscheinung wahrscheinlich auf Totalreflexion beruht. Nach der klassischen Dispersionstheorie müssen wir erwarten, daß der Brechungsexponent n für Röntgenstrahlen nahe an 1 liegt, aber im allgemeinen doch von 1 verschieden ist. n wird kleiner bzw. größer als 1 sein, je nachdem der Einfluß derjenigen Elektronen auf die Dispersion überwiegt, deren Eigenfrequenz kleiner oder größer ist als die Frequenz der Röntgenstrahlen. Die Schwierigkeit einer Bestimmung von n liegt darin, daß $(n-1)$ sehr klein ist (etwa 10^{-5}). Es ist aber leicht einzusehen, daß bei nahezu streifender Inzidenz der Röntgenstrahlen im Falle $n < 1$ eine nachweisbare Totalreflexion auftreten muß.

X rays

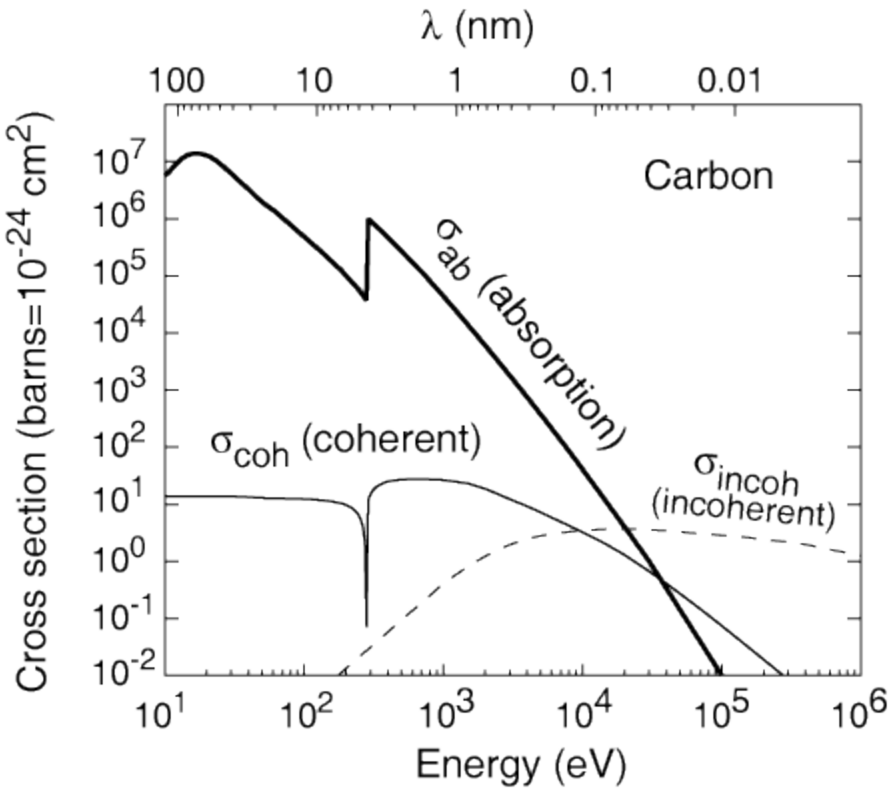

- Absorption dominates
- Inelastic scattering is weak
- No multiple scattering

Electrons

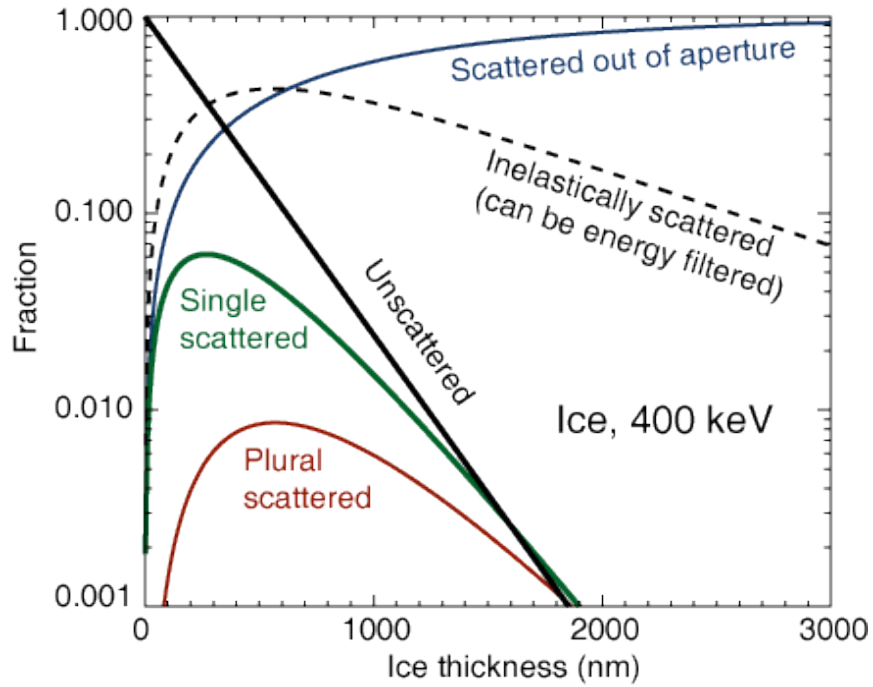

- Inelastic scattering dominates (energy filters)
- Multiple scattering often present
- High contrast from small things

X rays are better than electrons for thick specimens

- Electrons: silicon atom columns, molecules, viruses... HADF exceptions!
- X rays: cells, tissues, nanocomposites... Flash imaging exceptions!

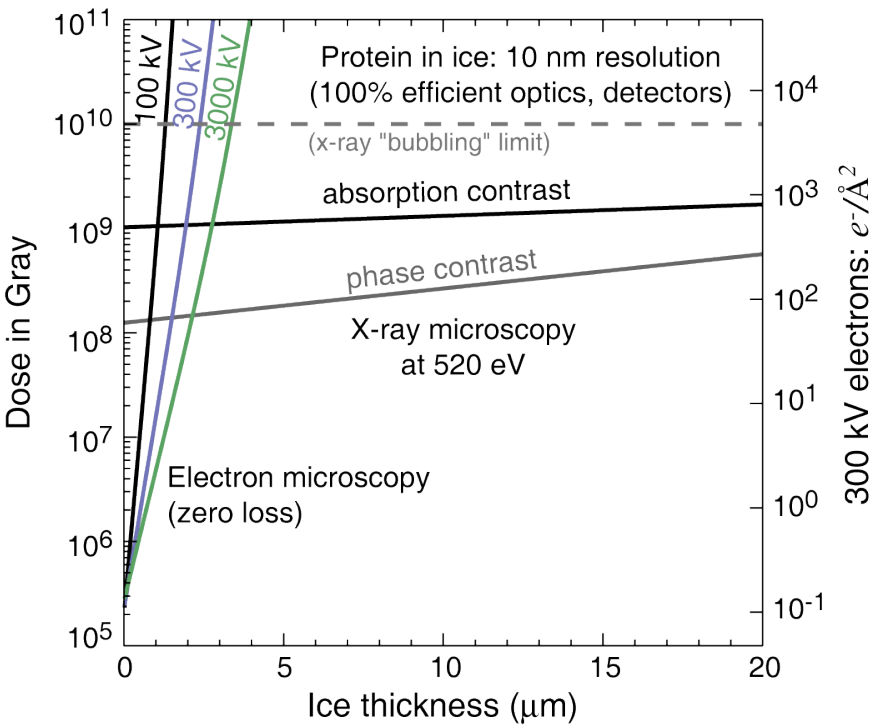

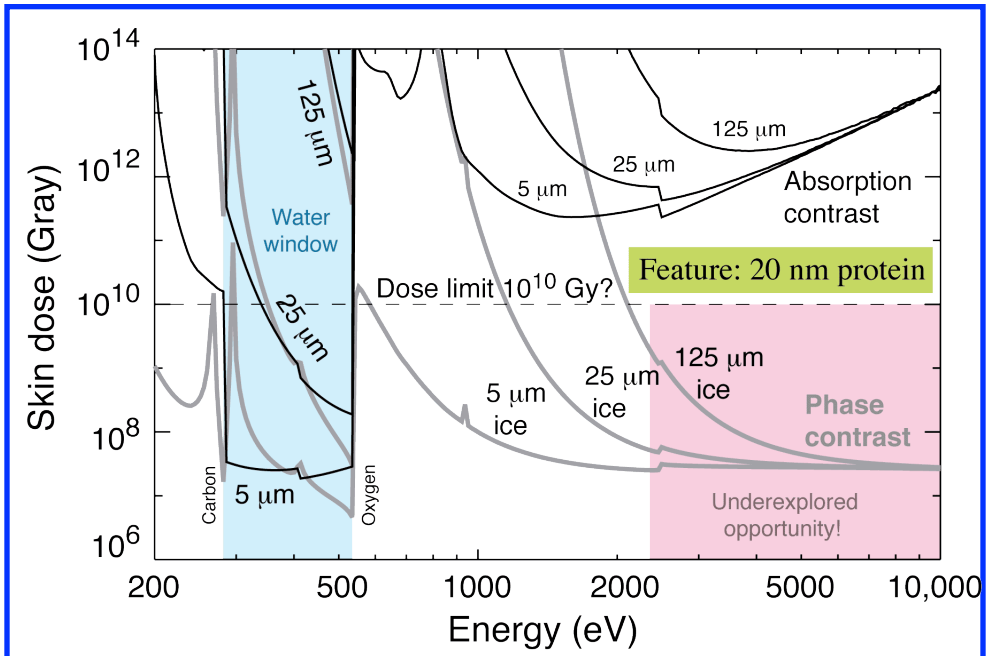

Phase contrast is important!

These plots: based on Jacobsen, Medenwaldt, and Williams, in **X-ray Microscopy & Spectromicroscopy** (Springer, 1998). See also Sayre *et al.*, *Science* **196**, 1339 (1977).

Resolution comes at a cost in exposure

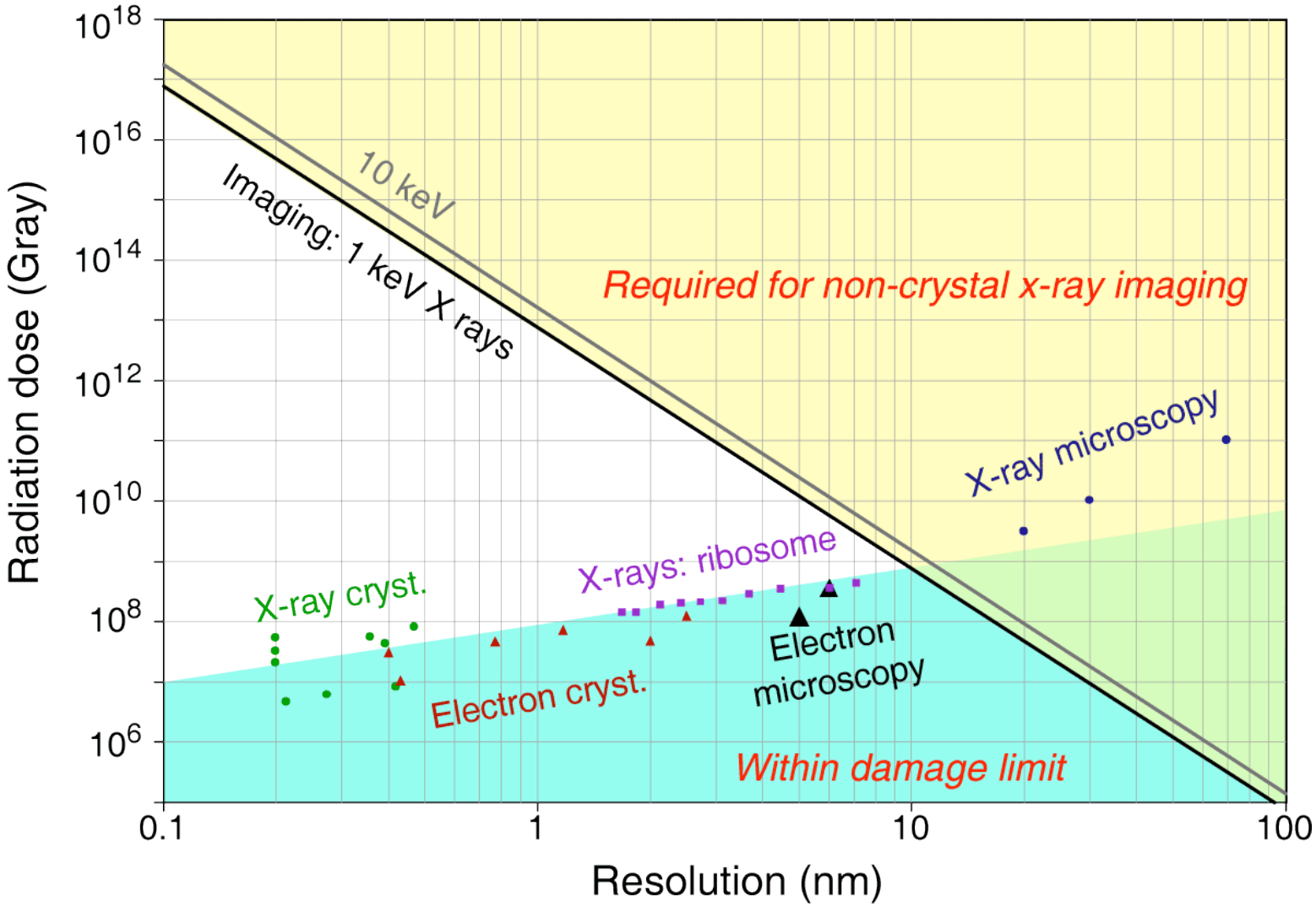

Assumption: 100% efficient microscopes! This plot: Howells *et al.*, *J. Electr. Spectr. Rel. Phen.* **170**, 4 (2009). See also Shen *et al.*, *J. Sync. Rad.* **11**, 432 (2004).

X-ray focusing: Fresnel zone plates

- Refraction is weak, and accompanied by absorption.
- Reflection is at grazing incidence: figure, finish, alignment....
- Diffraction: well suited to nanofocusing
- Largest diffraction angle is given by outermost (finest) zone width dr_N as $\theta=\lambda/(2dr_N)$
- Rayleigh resolution is 0.61 $\lambda/(\theta)$ $=1.22dr_N$
- Zones must be positioned to ~1/3 width over diameter (10 nm in 100 μm, or 1:10^4)

Diameter *d*, outermost zone width dr_N, focal length *f*, wavelength λ:

$$d\ dr_N = f\ \lambda$$

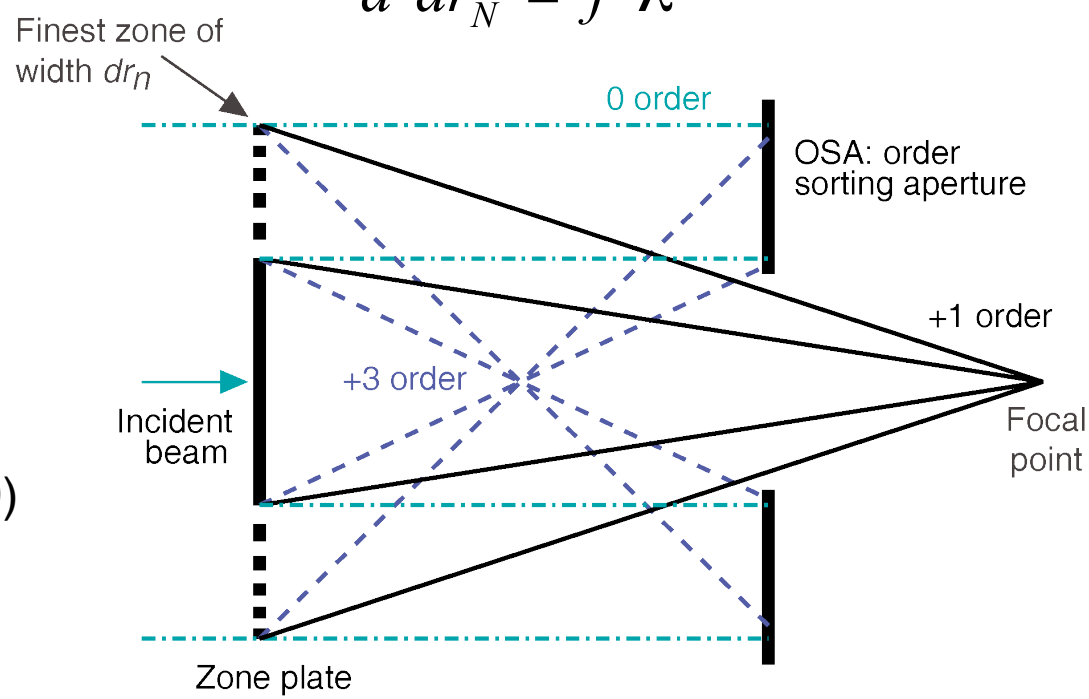

Central stop and order sorting aperture (OSA) to isolate first order focus

Zone plate efficiency and thickness

- For binary zones, 1:1 mark:space ratio.
- See Kirz, *J. Opt. Soc. Am.* **64**, 301 (1974)

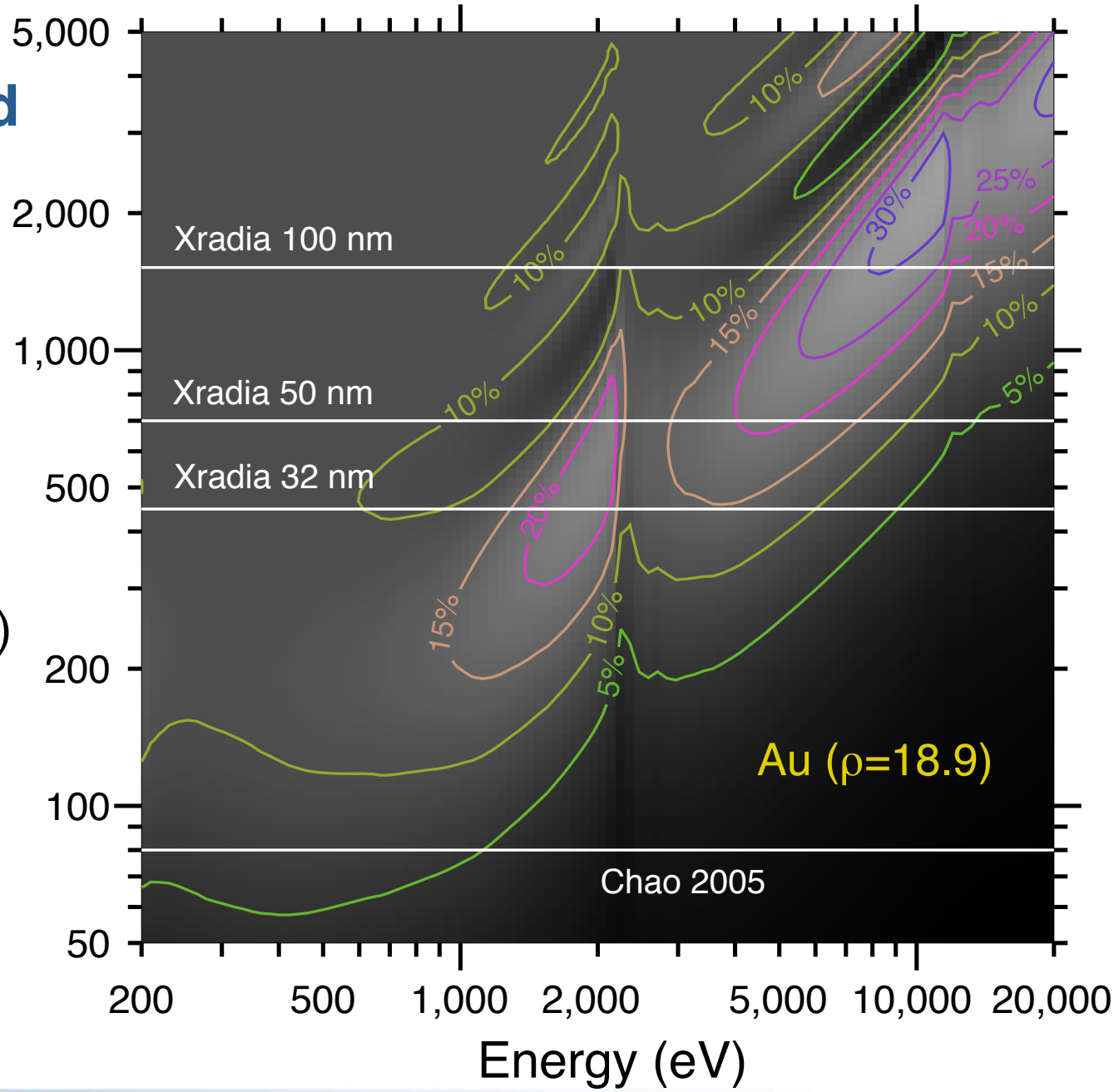

Zone plates by electron beam lithography

- Electron beam lithography: produces the finest possible structures (other than what nature can be persuaded to make by itself)
- M. Lu, A. Stein (PhD 2002; now BNL), S. Spector (PhD 1998; now Lincoln Lab), C. Jacobsen (Stony Brook)
- D. Tennant (Lucent/New Jersey Nanotech Consortium; now Cornell CNF)
- JEOL JBX-9300FS: 1 nA into 4 nm spot, 1.2 nm over 500 μm, 100 keV

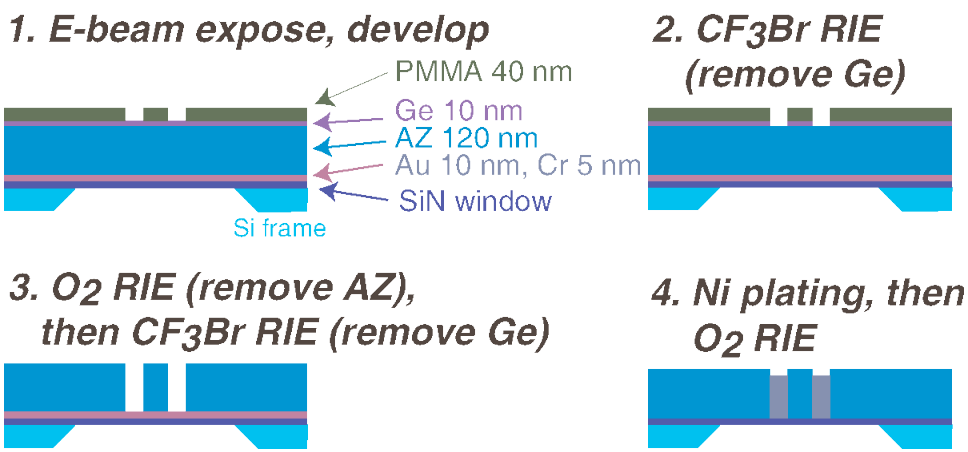

A. Stein and JBX-9300FS

X-ray optics: best published resolution

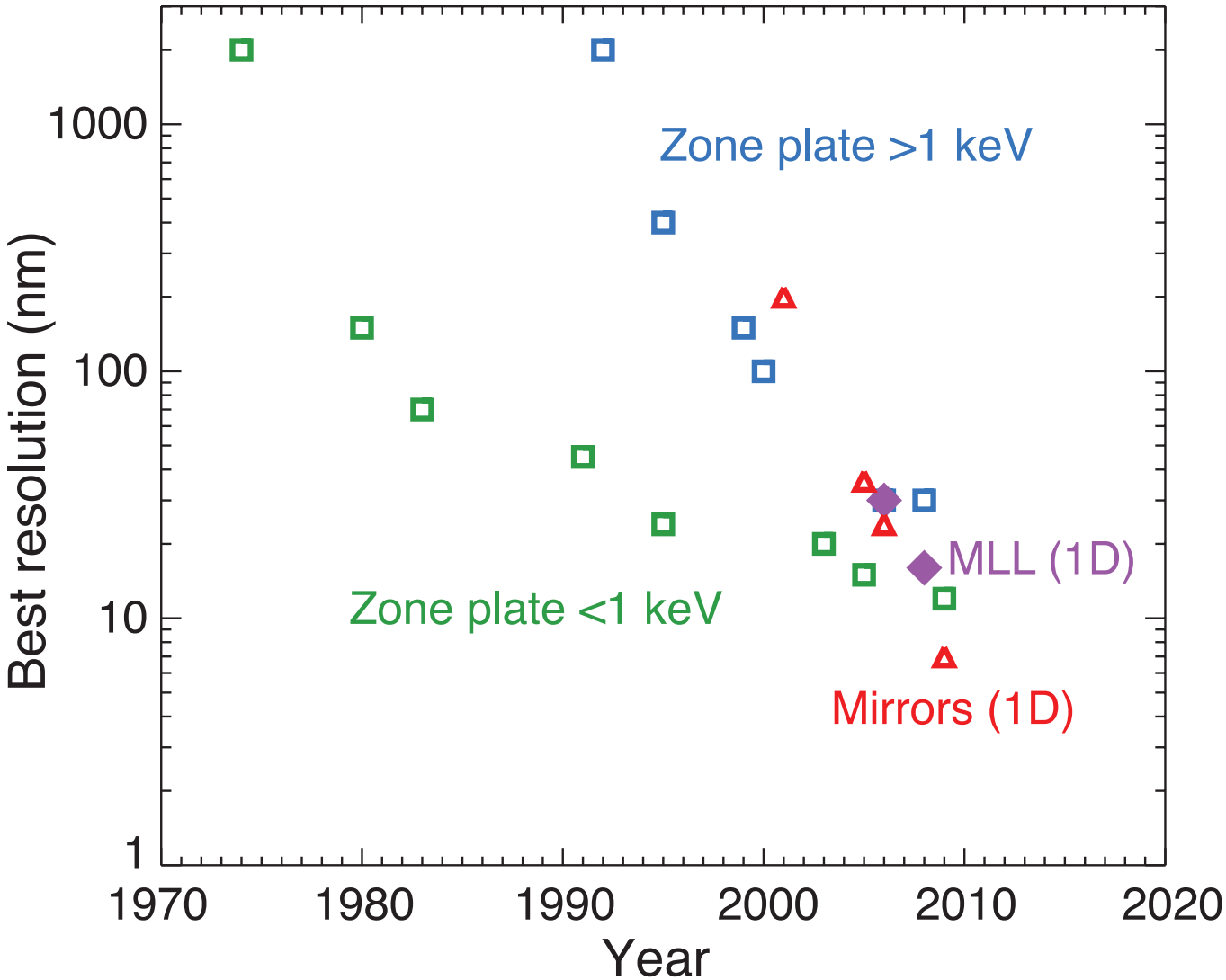

Laboratory x-ray sources

- Limited in brightness (photons per area per angle) due to melting of the target.
- Emit into 2π, and continuum spectrum plus fluorescence lines

Synchrotron radiation

- General Electric, Schenectady, New York; April 24, 1947
- Herb Pollock: “On April 24, Robert Langmuir and I were running the machine and as usual were trying to push the electron gun and its associated pulse transformer to the limit. Some intermittent sparking had occurred and we asked the technician to observe with a mirror around the protective concrete wall. He immediately signaled to turn off the synchrotron as `he saw an arc in the tube.’ The vacuum was still excellent, so Langmuir and I came to the end of the wall and observed.”

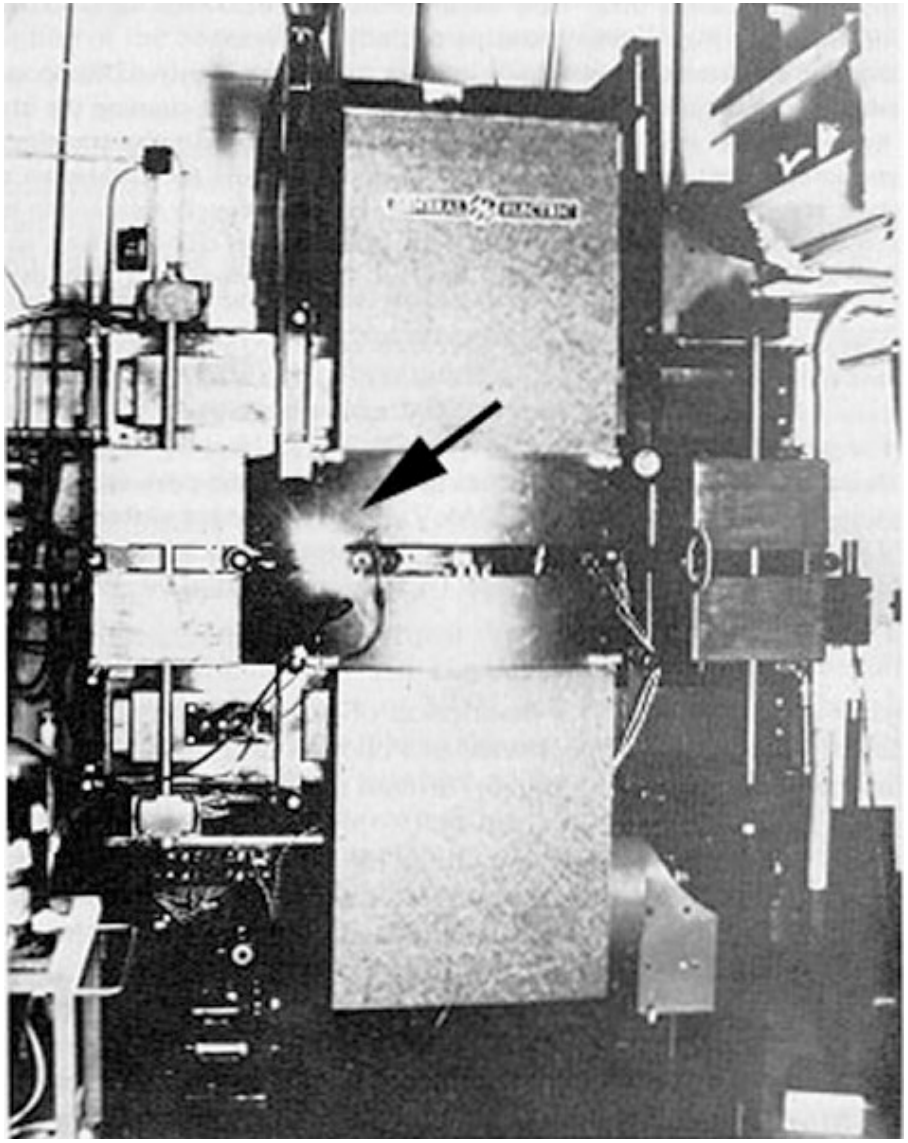

Modern x-ray beams

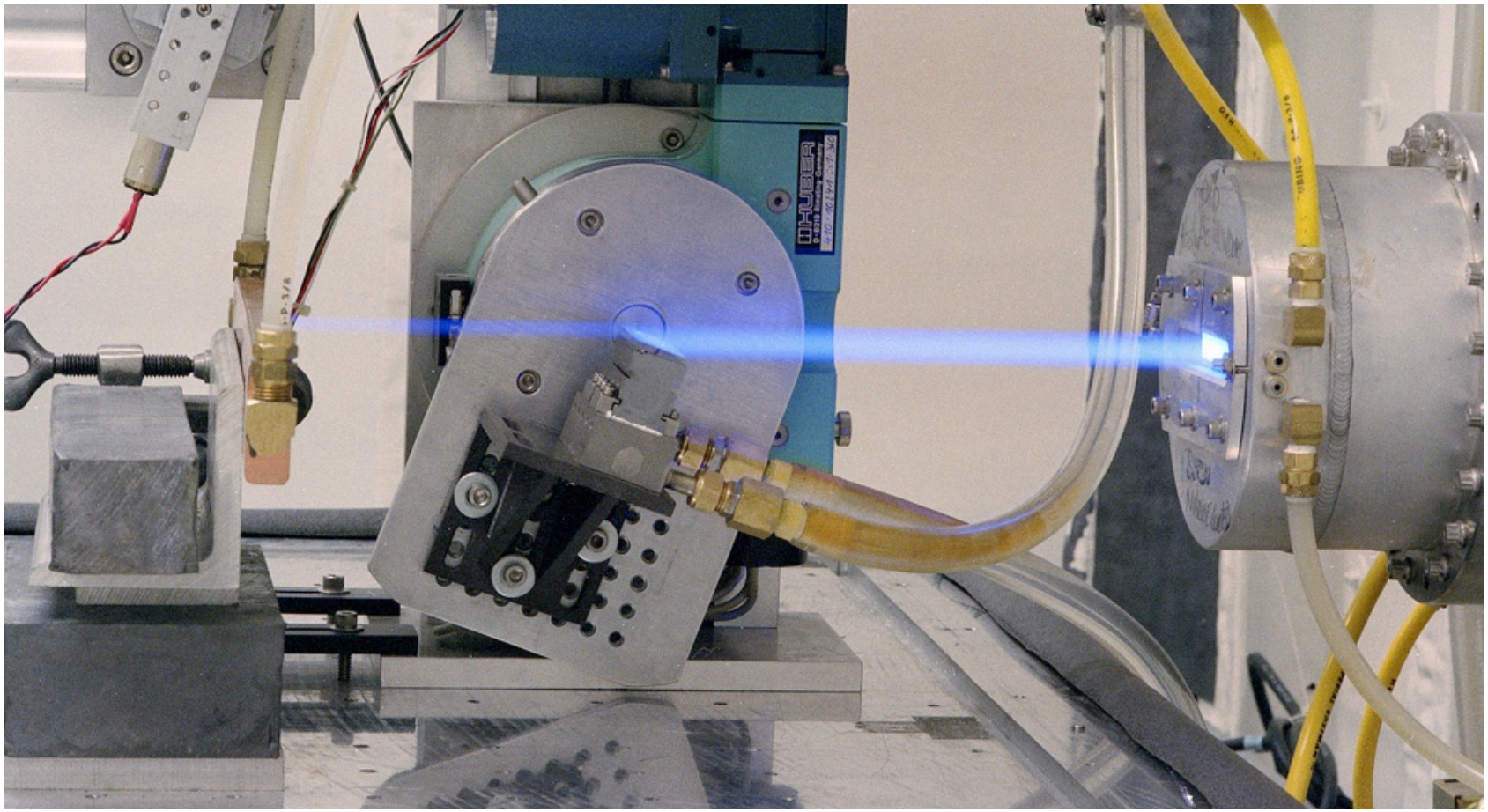

The Advanced Photon Source (APS): 7 GeV, 1.1 km circumference

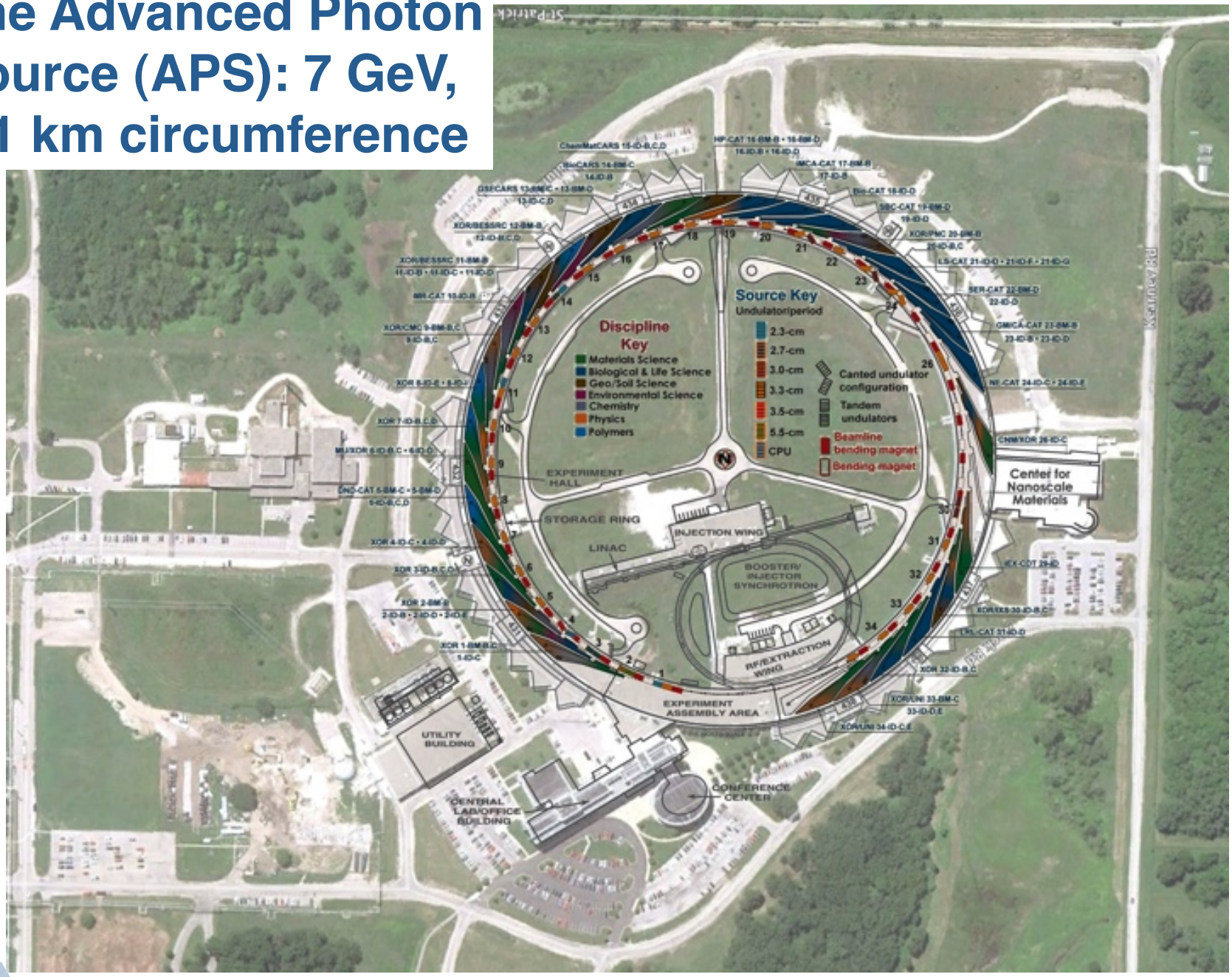

Beamlines at the APS

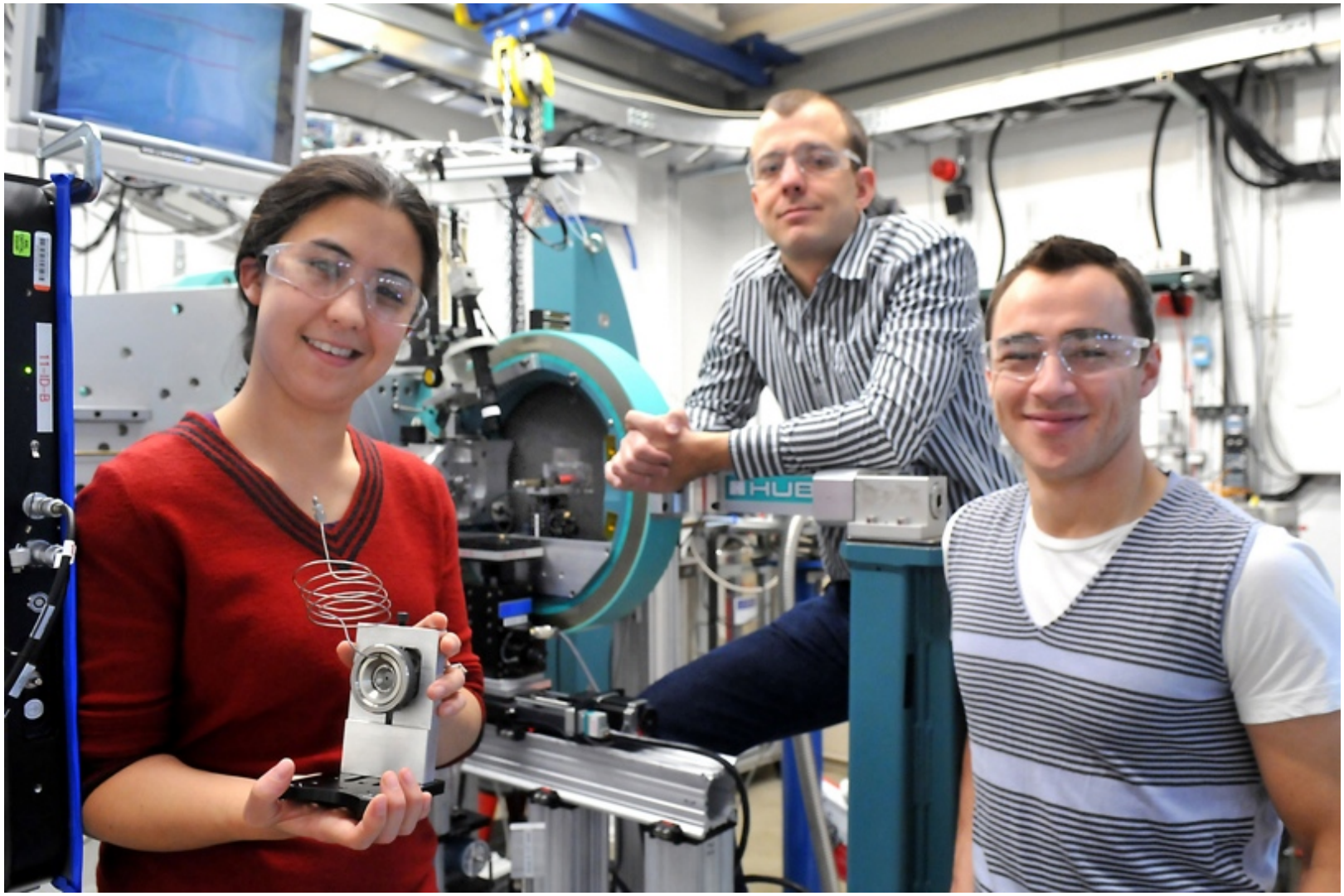

http://www.aps.anl.gov/Upgrade/Resources/Technical_Information/files/BrightnessTuningCurves_NSLSII_vs_APS.pdf

APS undulators: 200 mA, 4.8 meters long

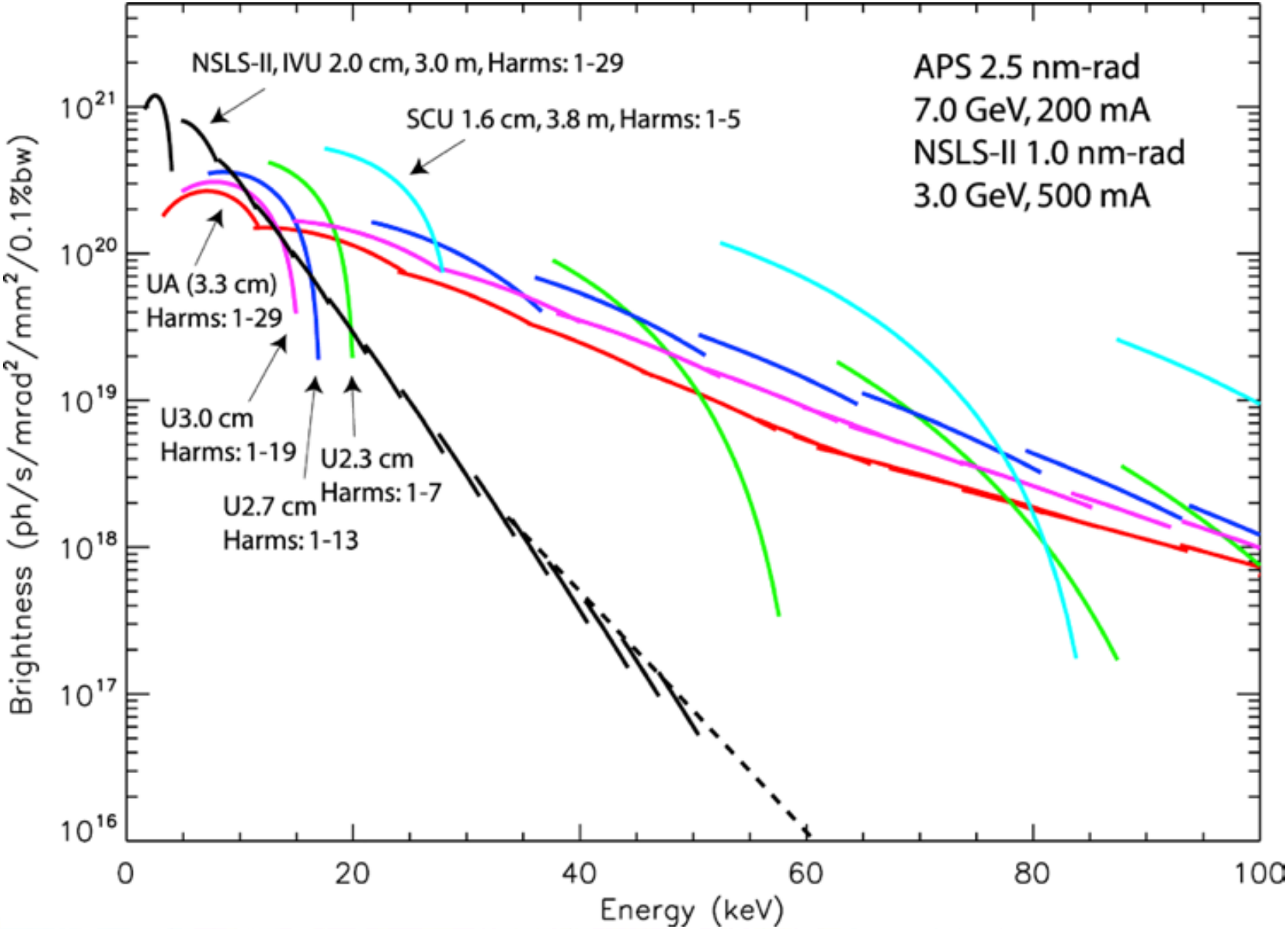

Imaging and microscopy at Argonne

- Imaging group (Francesco De Carlo)
  - 1-2 um resolution automated tomography
  - Ultrafast imaging down to 150 psec
  - Transmission x-ray microscope: 50 nm resolution tomography
- Microscopy group (Stefan Vogt)
  - X-ray fluorescence microprobes at <100 nm resolution
  - Microdiffraction studies of strain
  - Coherent diffraction imaging
- Center for Nanoscale Materials
  - Nanoprobe with 30-50 nm resolution
- LS-CAT (Wayne Anderson)
  - Bio nanoprobe (NIH funding to Gayle Woloschak) for 50 nm cryo fluorescence
- Imaging Institute?
  - Bring together microscopy at APS, scanned probe imaging at CNM, Electron Microscopy Center, plus computation.

Ultrafast imaging of fuel injector sprays

- 13.3 keV, 0.3 keV bandpass
- Wang *et al.*, *Nature Physics* **4**, 305 (2008)

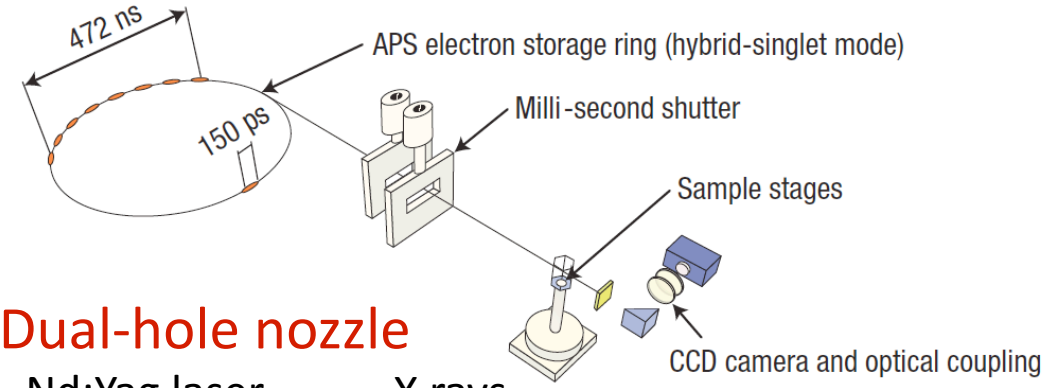

Single-hole nozzle

Nd:Yag laser X rays

Dual-hole nozzle

Nd:Yag laser X rays

20 µsec

1500 µsec

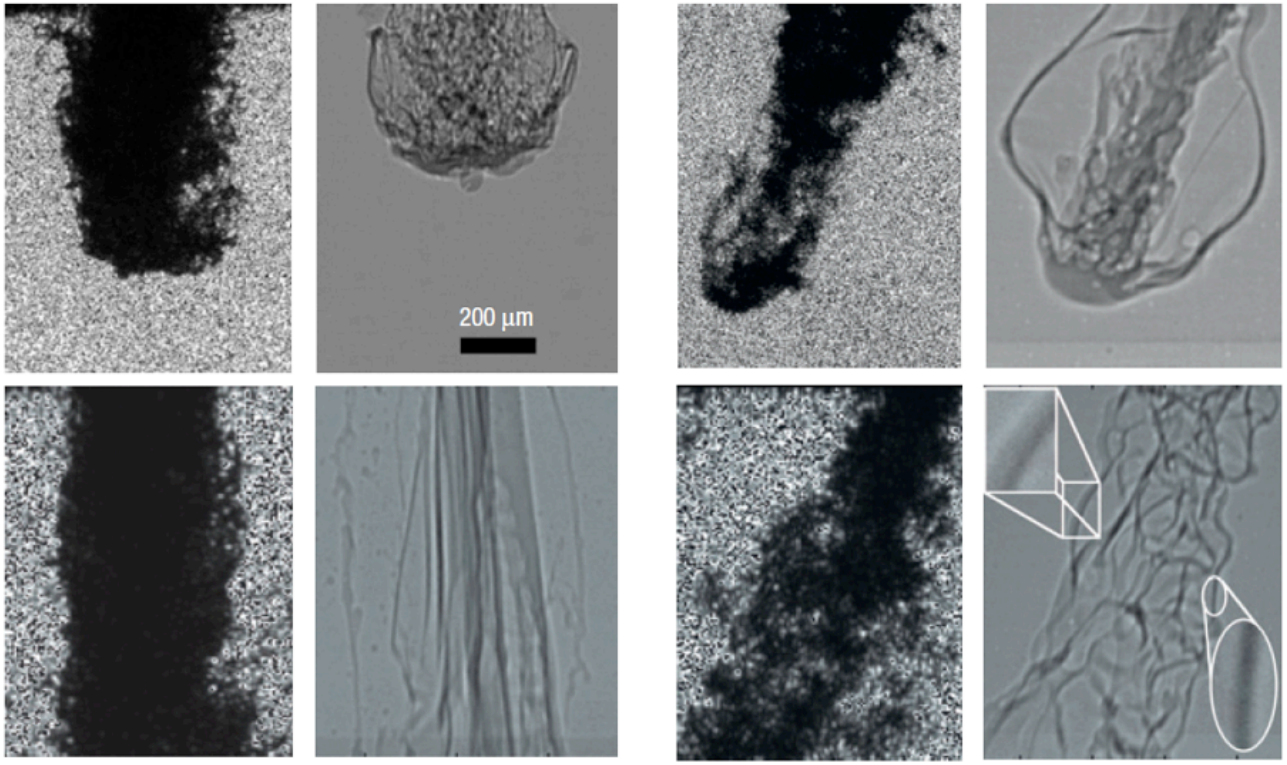

20 µsec

1500 µsec

APS, Mayo Clinic, Visteon Corp.

- Ductile shear zones: where minerals (and earthquakes) are born.
- Pores, mica phase, oxides plus epidote (correlative SEM)
- Pore sheets parallel to mylonitic foliation (dynamic recrystallization)
- Field of view: 1600×1600×800 µm
- 30 minutes data collection, 20 keV

Fusseis, Regenauer-Lieb, Liu, Hough, and De Carlo, *Nature* **459**, 974 (2009)
University of Western Australia/CSIRO/APS.

- High-strain shear zone: zoom in on pores
- Shows that pores are non-percolating
- Field of view: 160×160×160 µm, at 1.3 µm resolution
- Note: automation allowed 52 full cubes to be sampled

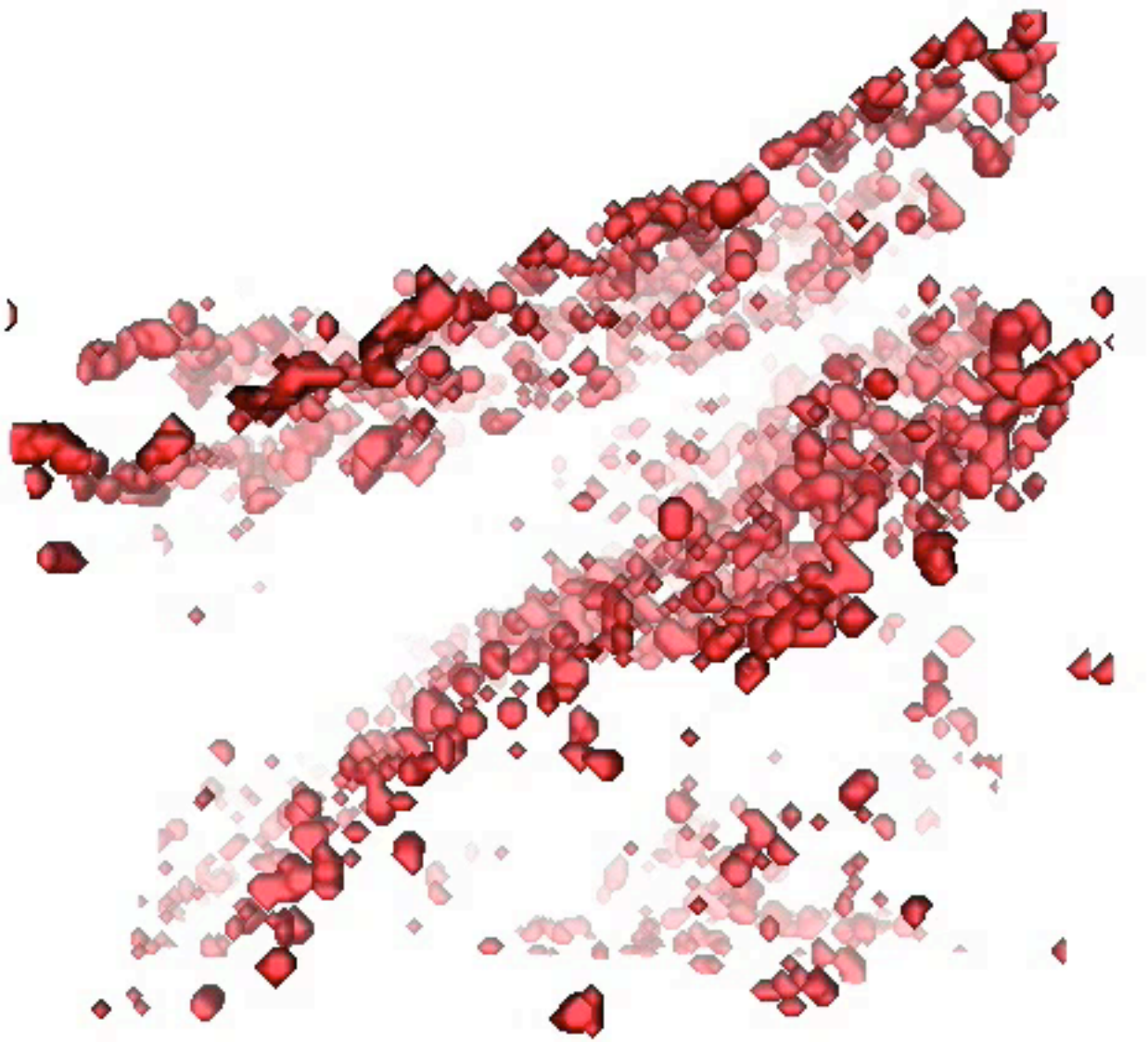

Fusseis, Regenauer-Lieb, Liu, Hough, and De Carlo, *Nature* **459**, 974 (2009)
University of Western Australia/CSIRO/APS.

Zone plate nanotomography of fuel cell materials

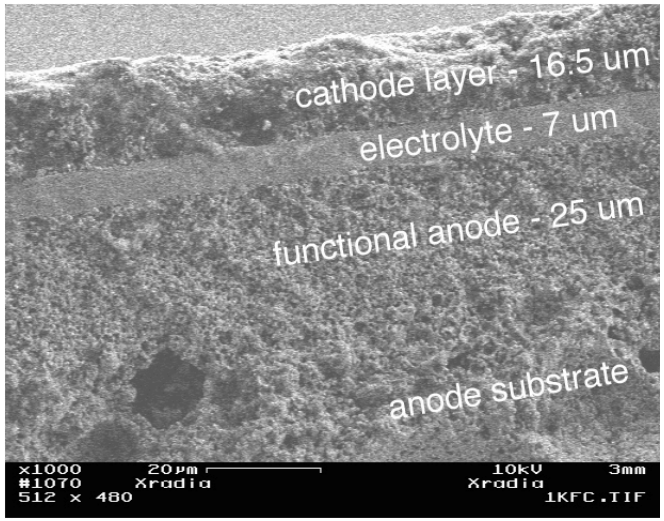

SEM Image

- The performance of a solid oxide fuel cell depends critically on the porosity of the cathode, electrolyte, and anode at their interface – three-phase interface (TPI).
- X-ray nano-CT non-destructively obtains 3D porous structure, elemental mapping, and chemical speciation - imaged *in operando*
- Steve Wang *et al., APS & MSD, Argonne*

TXM/nanoCT Images

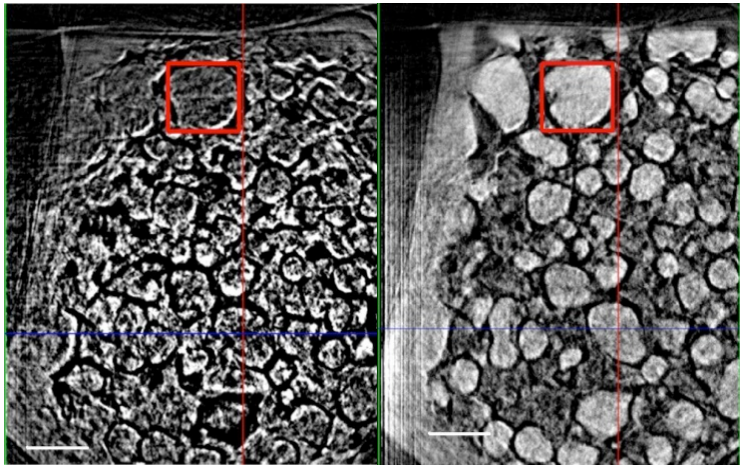

Below Ni edge Above Ni edge

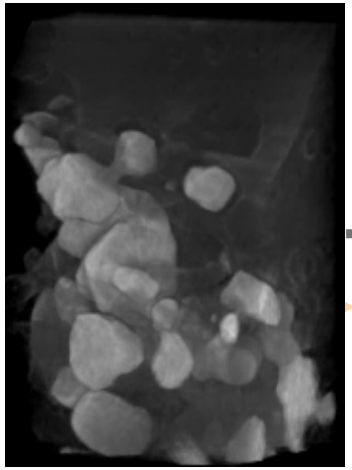

3D Ni structure

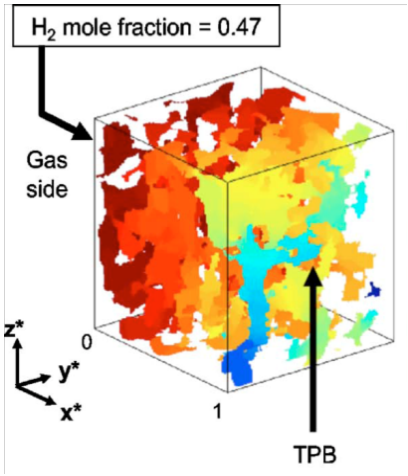

Function prediction

In situ measurement of strain in Silicon-On-Insulator (SOI)

- Strain in SOI increases mobility of holes and electrons, improving performance. Very important as 30 nm node is implemented, but strain is heterogenuous.
- Electron diffraction: requires thinning. X-ray diffraction: *in situ*

SOI/SiC system ($a_{Si} > a_{SiC}$)

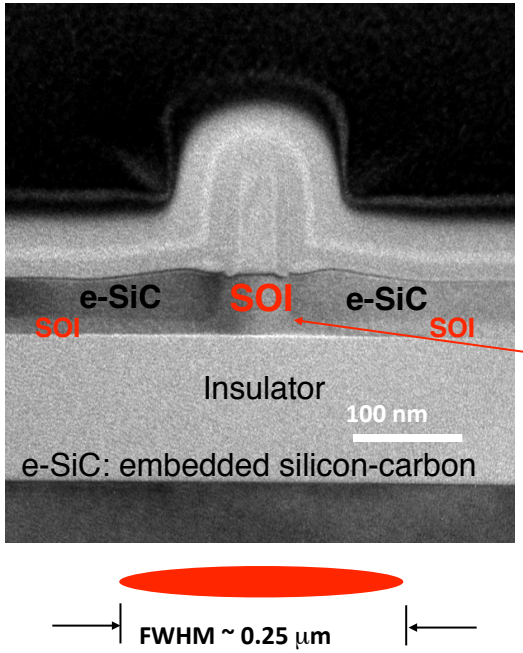

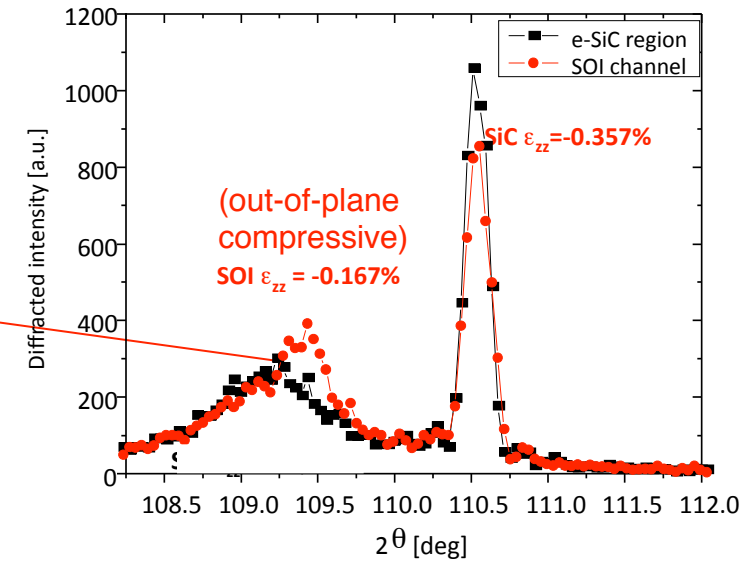

e-SiC region: 0.8 μm away

Measured strain in SOI channel is 95% of expected value; altered by constraint of overlying gate

Murray, Ren, Ying, Polvino, Noyan, and Cai, *Appl. Phys. Lett.* **94**, 063502 (2009). IBM, Columbia University, APS.

Metallic phases and corrosion

- US loses 4% of annual gross national product to corrosion.
- Nuclear power plants: harsh conditions, high consequence for failure
- Nuclear power: low-carbon electrical energy

Containment vessel, Davis-Besse nuclear power station, Ohio, March 2002

Stewart Brand:
anti-nuclear in 1969
pro-nuclear today

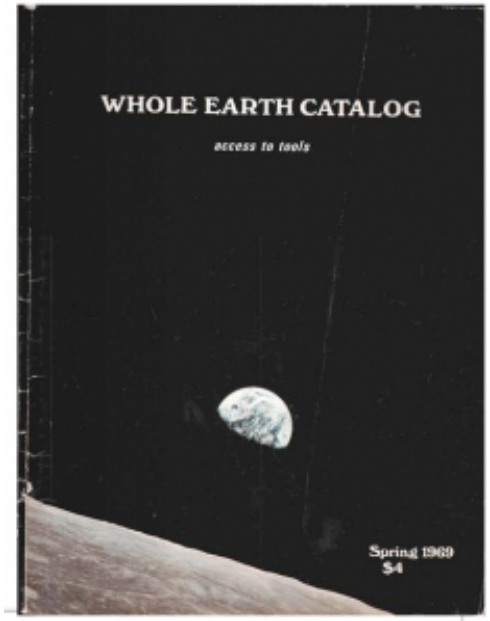

X-ray microdiffraction: phase changes in depth

- Alloy 321 exposed to metal-dusting gas for 1130 hours

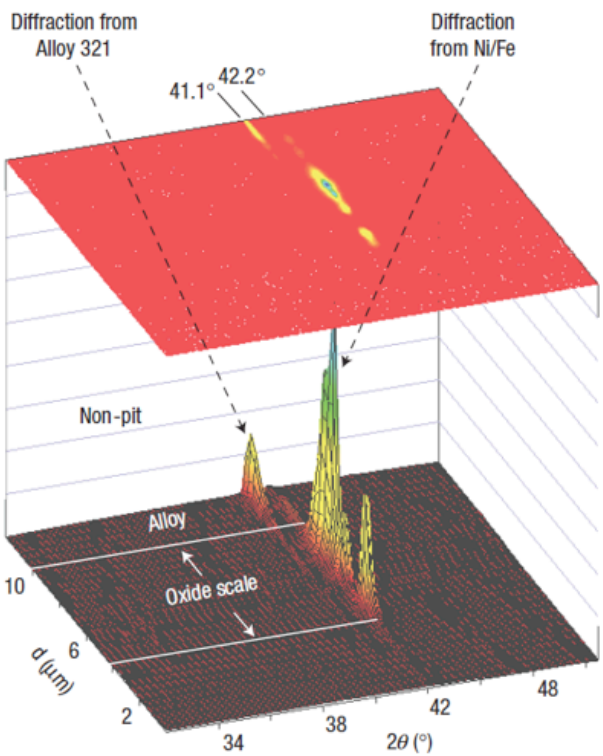

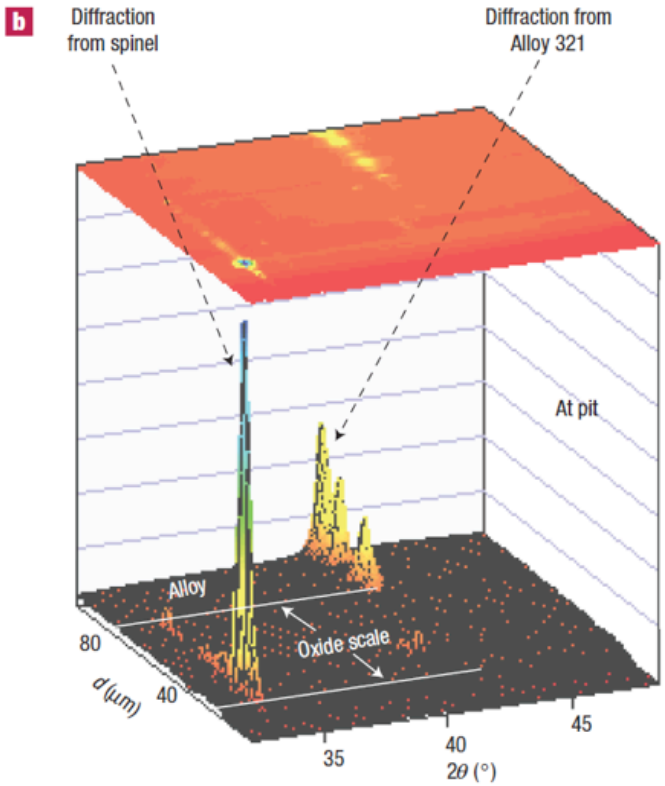

Oxide scale areas hint at embedded Ni/Fe particles

Pits show spinel phase, but no metallic network

Zeng, Natesan, Cai, and Darling, *Nature Materials* **7**, 641 (2008).
ANL nuclear materials, APS, CNM.

Oxide scale shows metal networks that may be a path for carburization!

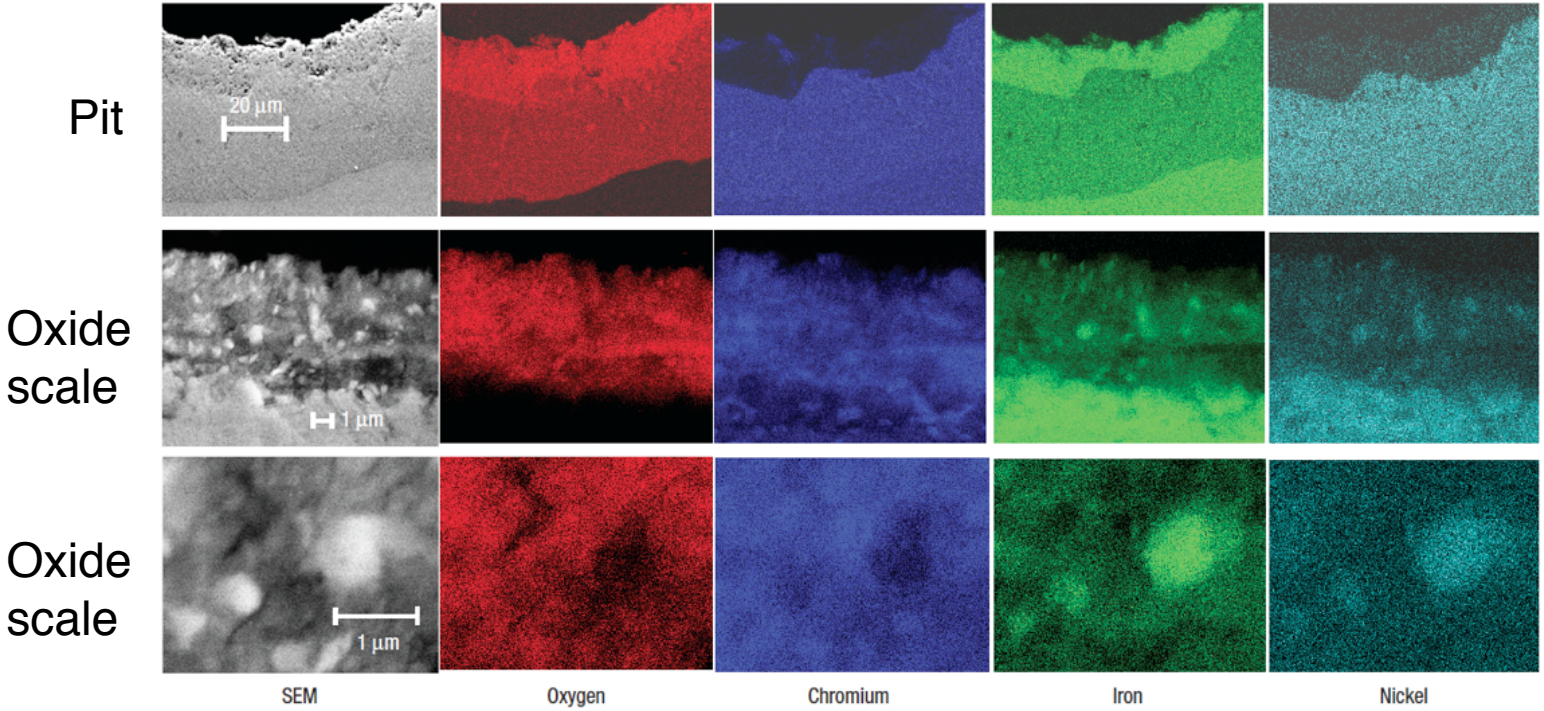

The pits are not the problem! Oxide scales lead to weakening

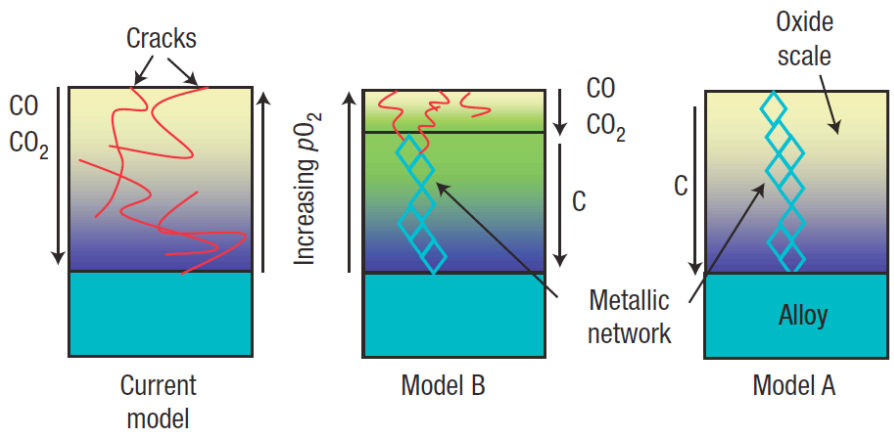

Zeng, Natesan, Cai, and Darling, *Nature Materials* **7**, 641 (2008).
ANL nuclear materials, APS, CNM.

Comparison of trace element detection methods

X-ray fluorescence offers part-per-billion sensitivity with reduced radiation damage

May not represent latest electron microprobe developments!

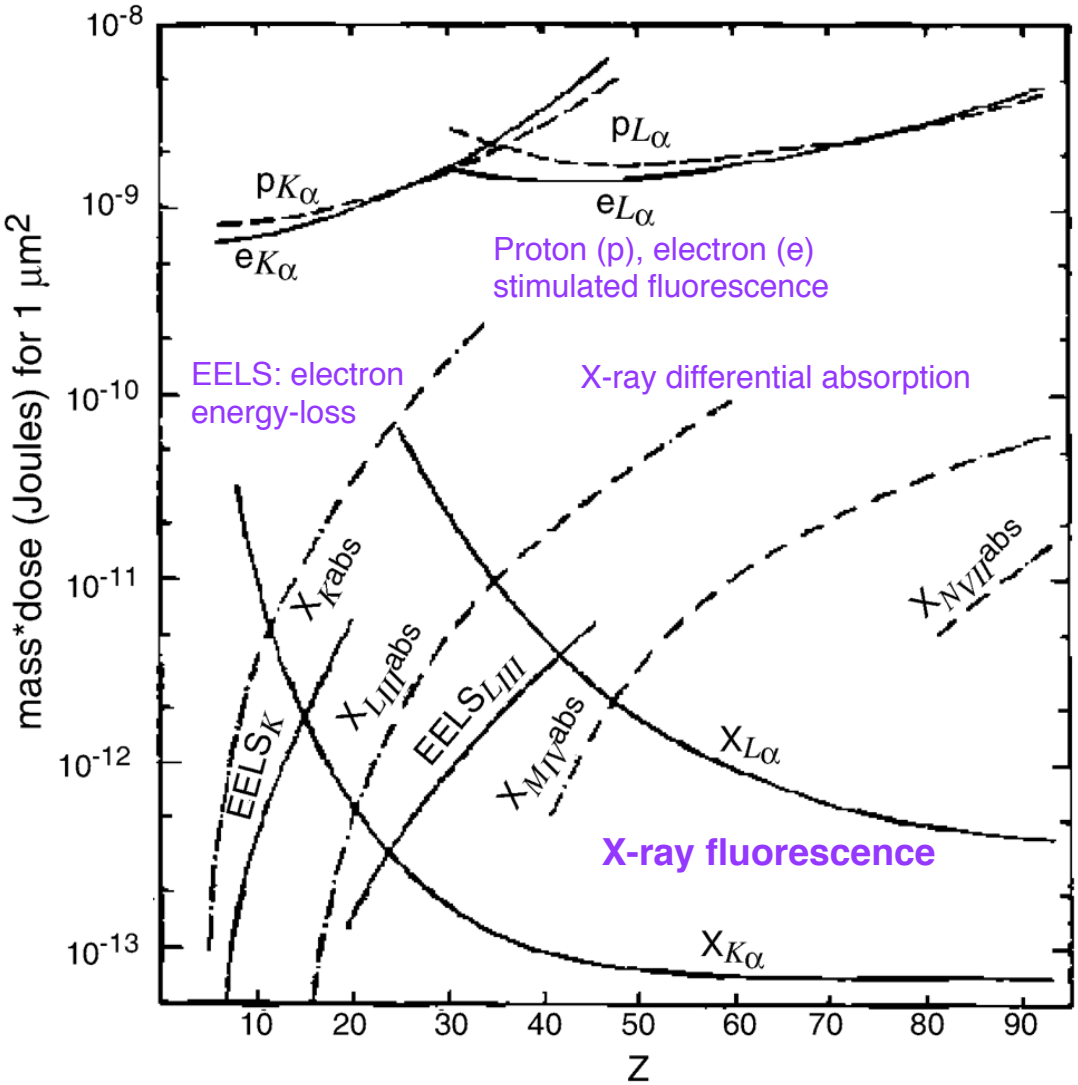

J. Kirz, in *Scanning Electron Microscopy* **2**, 1980, p. 239.
Hard-to-find reprint:
http://tinyurl.com/2fx94m6

Global carbon cycle

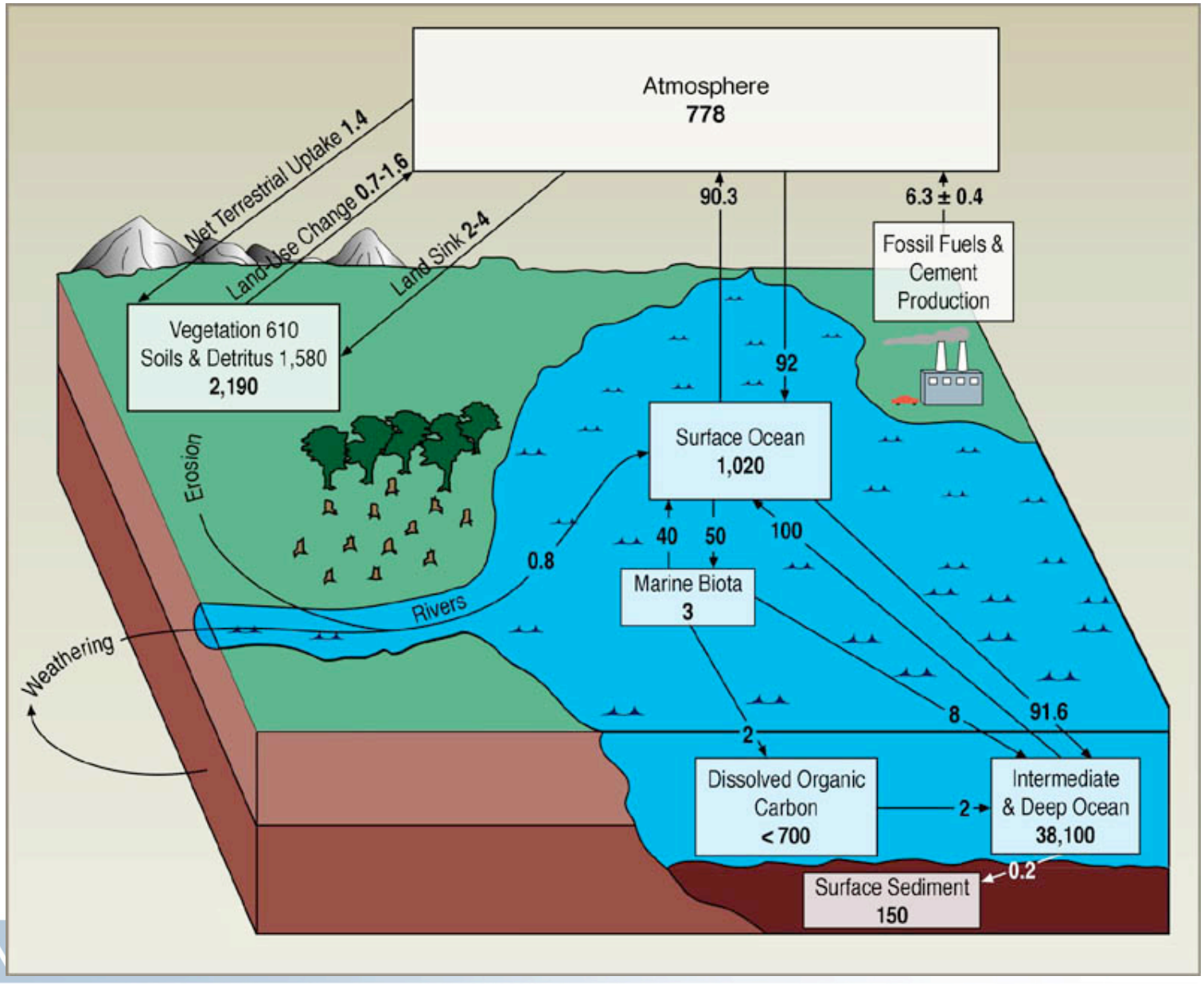

petagrams, petagrams/year (climatescience.gov)

Analyzing full spectra

- Peaks from trace elements can be on shoulders of strong peaks from common elements.
- Setting simple energy windows can give poor quantitation. Record full spectrum and do curve-fitting!
- Wavelength dispersive detectors can help – but often with lower collection solid angle
- This example: Twining *et al.*, *Anal. Chem.* **75**, 3806 (2003). Also ESRF, elsewhere.
- Analysis approach: Vogt, Maser, and Jacobsen, *J. Phys. IV* **104**, 617 (2003).

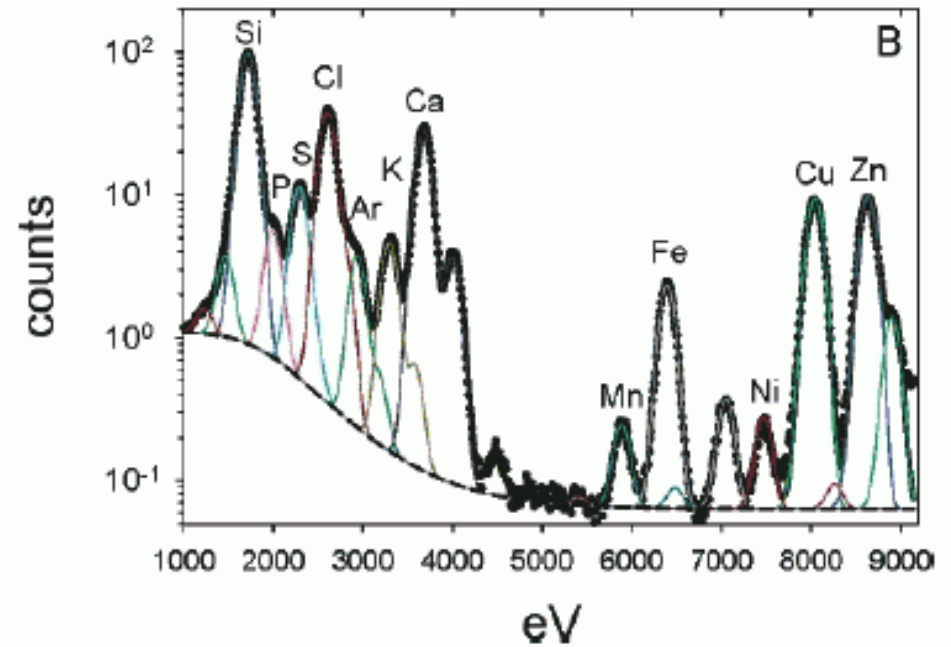

Figure 1. Fluorescence spectra for the marine diatom *T. weissflogii*. Pixel-averaged spectra for the target cell and a neighboring background region are plotted in (A). The Kα peaks of the major bioactive elements are indicated above the peaks. (B) displays the fit of the EMG model to the cell spectrum. The sigmoidal baseline is shown as a dotted line, the overall model is black, and the Kα and Kβ peaks for each element are displayed in various other colors.

Iron and carbon in the ocean

- Seed Southern Pacific with bioavailable iron to increase CO_2 uptake?
- Requires understanding of iron and carbon uptake in phytoplankton; combine fluorescence with phase contrast.

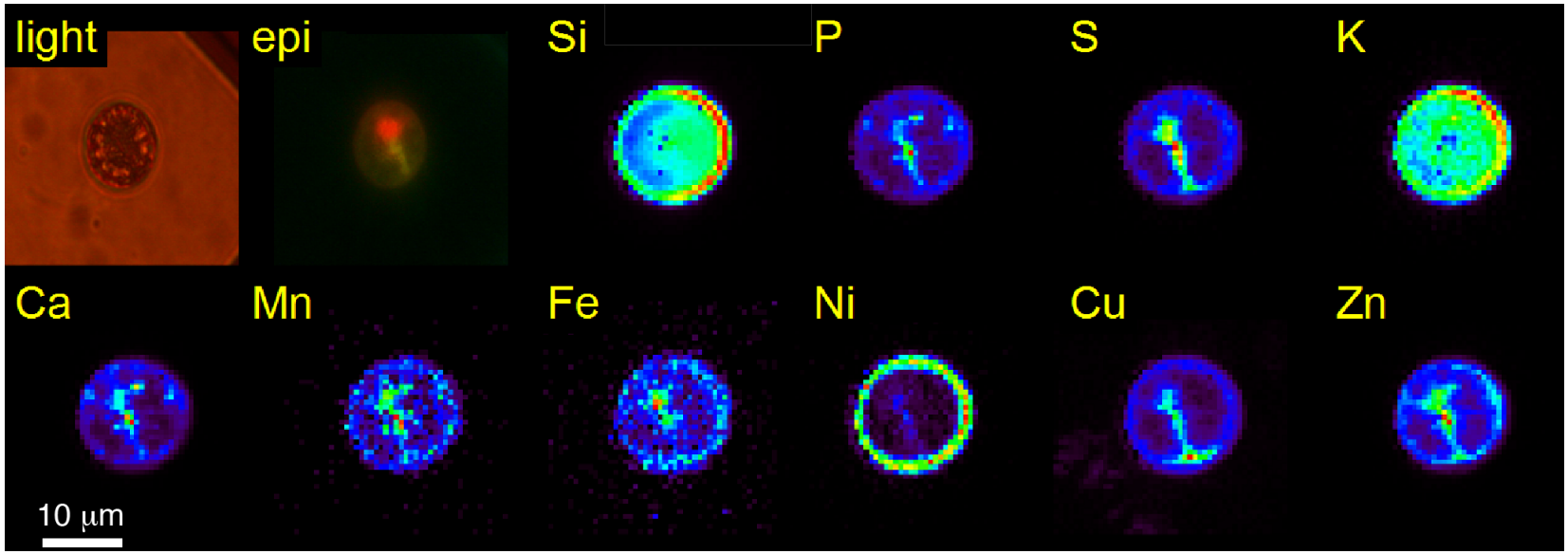

B. Twining, S. Baines, N. Fisher, J. Maser, S. Vogt, C. Jacobsen, A. Tovar-Sanchez, and S.Sañudo-Wilhelmy, *Anal.. Chem.* **75**, 3806 (2003)

Cruising the Southern Pacific

Cruising the Southern Pacific

What's missing? Phase contrast for low-Z

- Segmented x-ray detector (Stony Brook, BNL, Max Planck silicon lab).
- Acquire simultaneously with fluorescence
- Fourier filtering, Fourier integration for absolute phase contrast.
- Sensitivity: ~π/180.

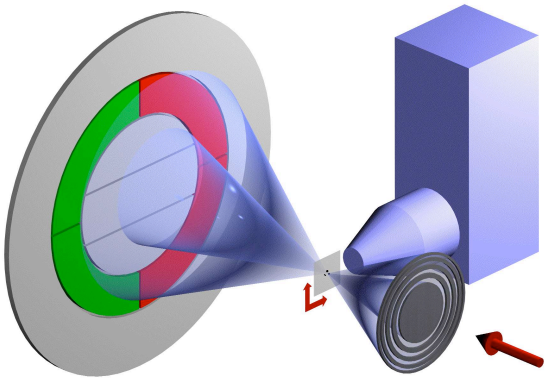

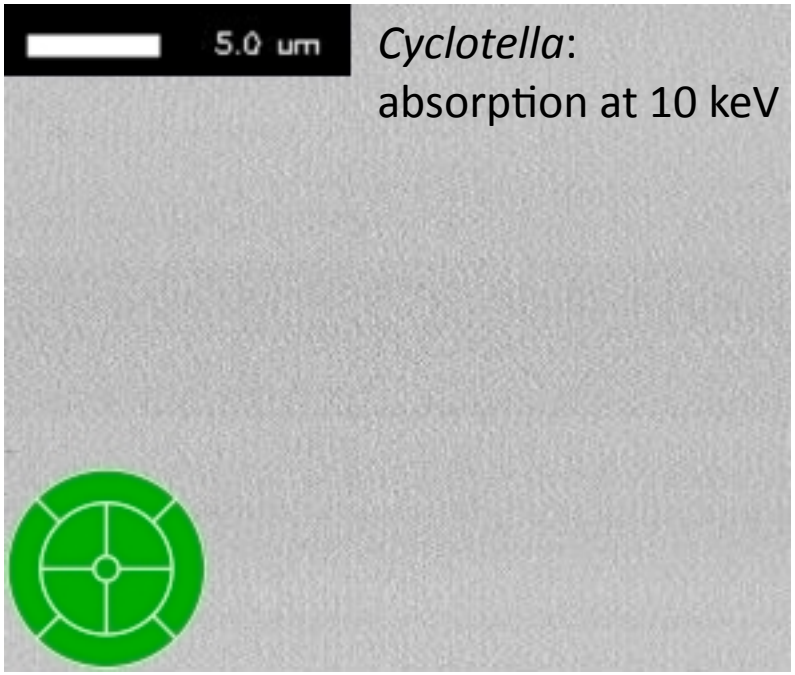

Hornberger *et al.*, *Ultramic.* **107**, 644 (2007); Feser *et al.*, *Nucl. Inst. Meth. A* **565**, 841 (2006); de Jonge *et al.*, *Phys. Rev. Lett.* **100**, 163902 (2008)

What's missing? Phase contrast for low-Z

- Segmented x-ray detector (Stony Brook, BNL, Max Planck silicon lab).
- Acquire simultaneously with fluorescence
- Fourier filtering, Fourier integration for absolute phase contrast.
- Sensitivity: ~π/180.

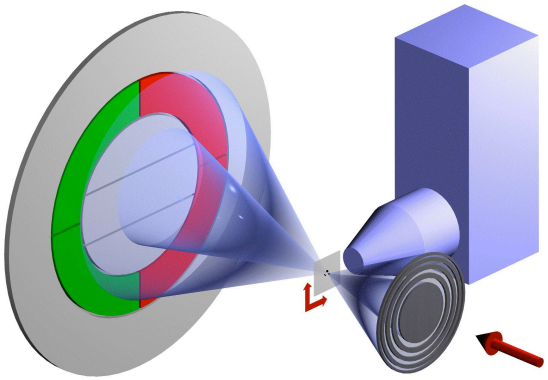

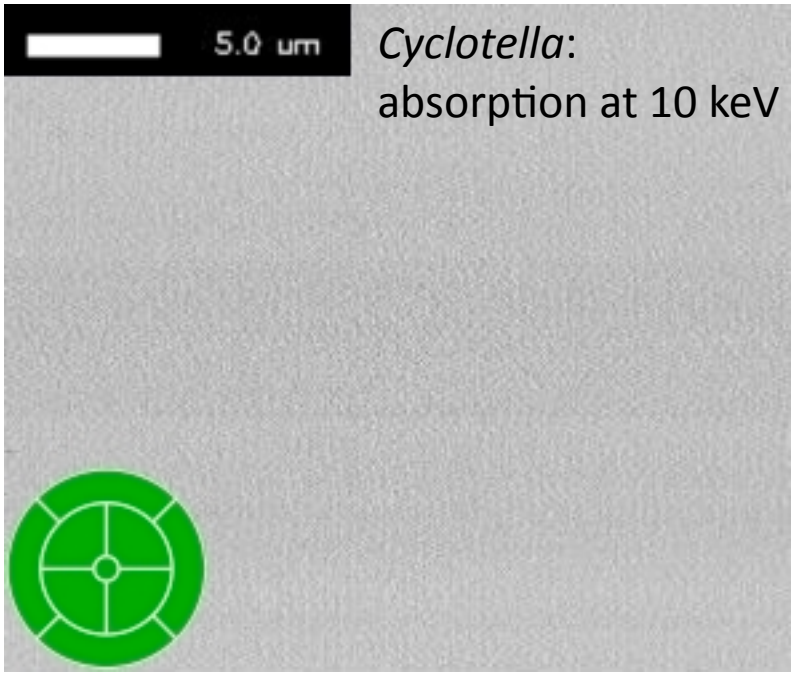

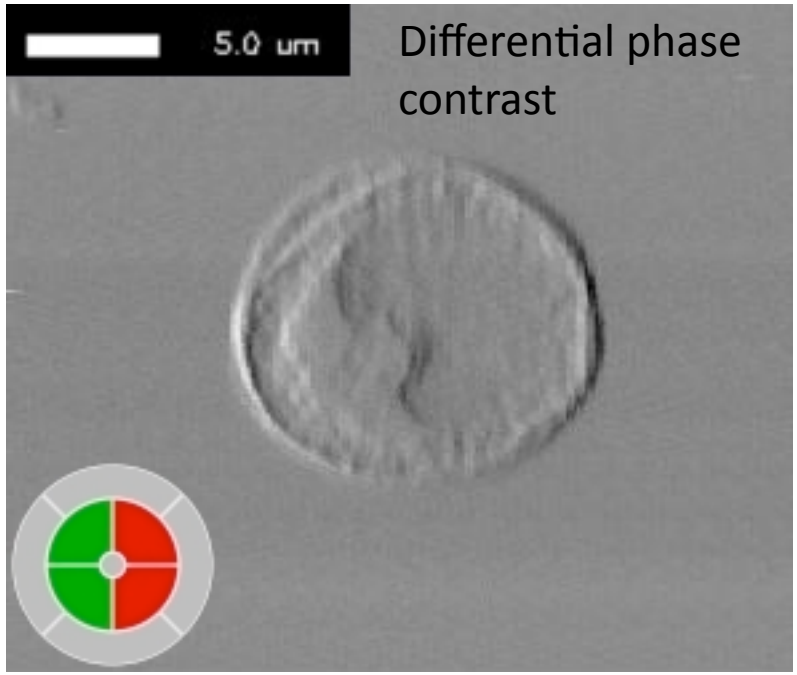

Hornberger *et al.*, *Ultramic.* **107**, 644 (2007); Feser *et al.*, *Nucl. Inst. Meth. A* **565**, 841 (2006); de Jonge *et al.*, *Phys. Rev. Lett.* **100**, 163902 (2008)

Polystyrene spheres at 10 keV: quantitative

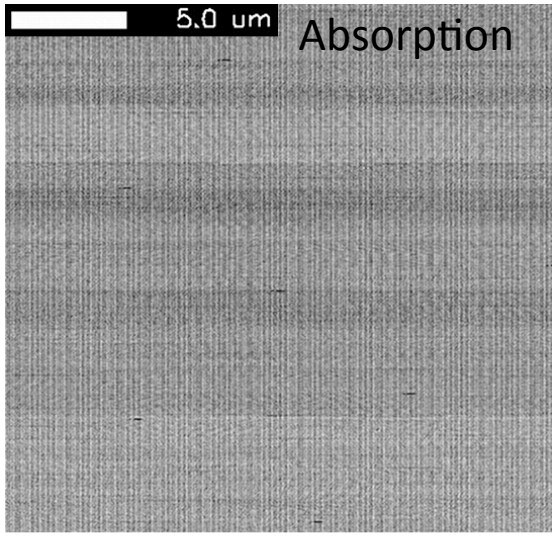

- 50 nm steps, 10 msec pixel clock
- Reconstructed values agree within 2% of Henke tabulation
- Sensitivity: $\pi/180$
- C. Holzner *et al.*

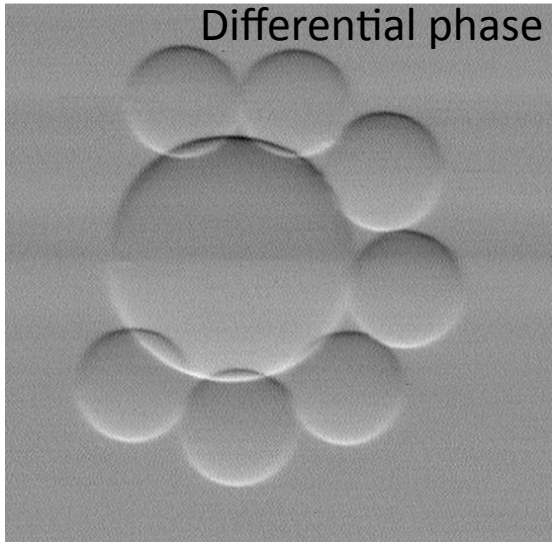

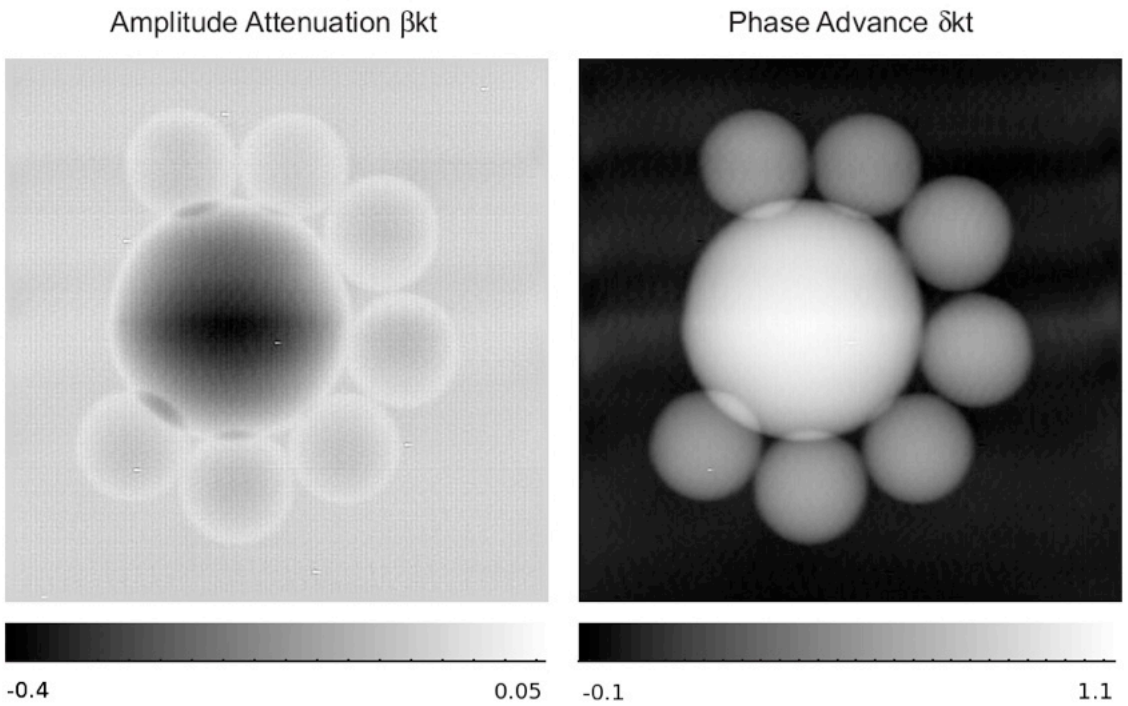

Fourier filtering applied to Zernike phase contrast

- Xradia lab system, 8.04 keV, stained bone sample

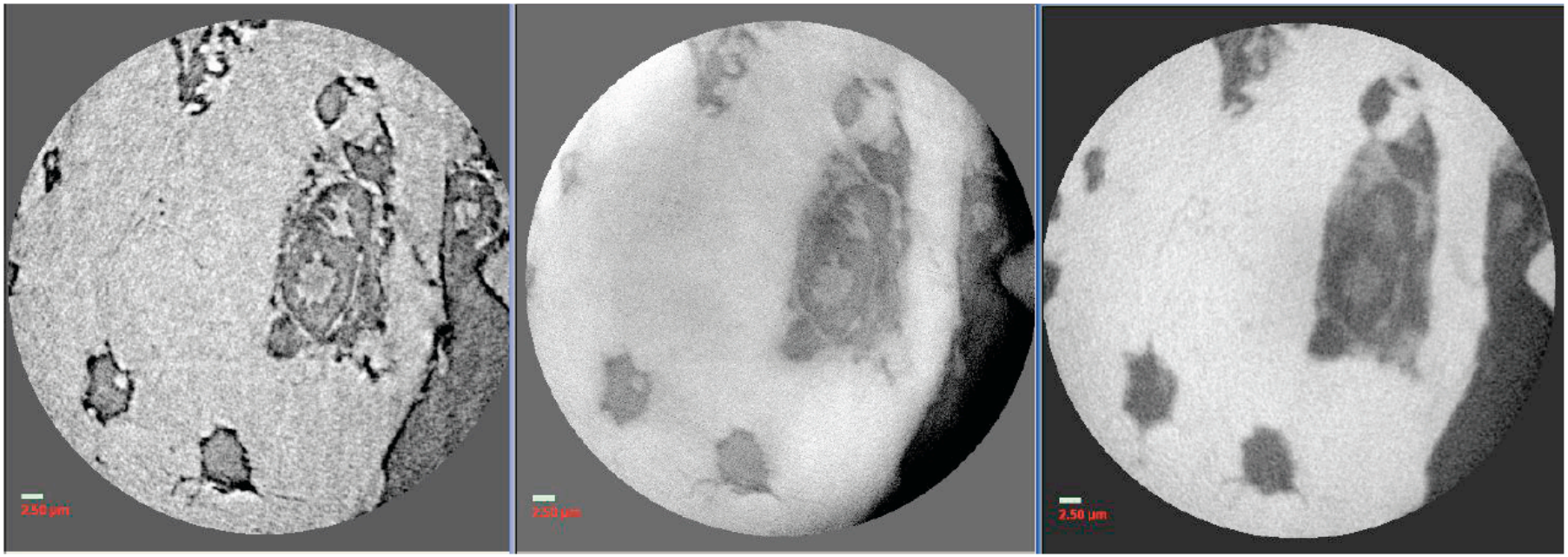

Zernike filtered Zernike absorption

- C. Holzner (manuscript in preparation)

Zernike phase contrast

- You don't need a fully coherent source for phase contrast!
- As many coherent "modes" as pixels in detector

Change phase into intensity by mixing with a reference wave

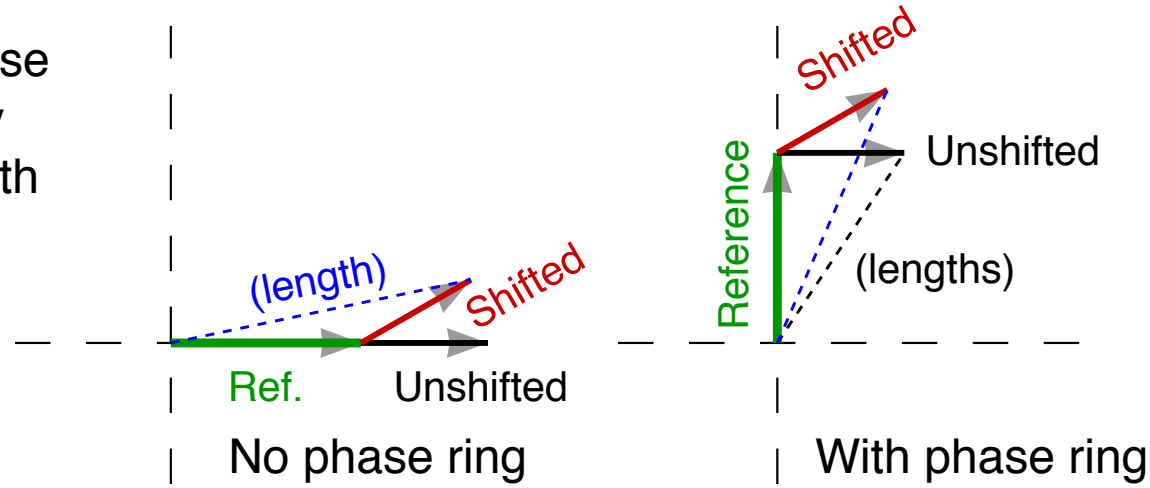

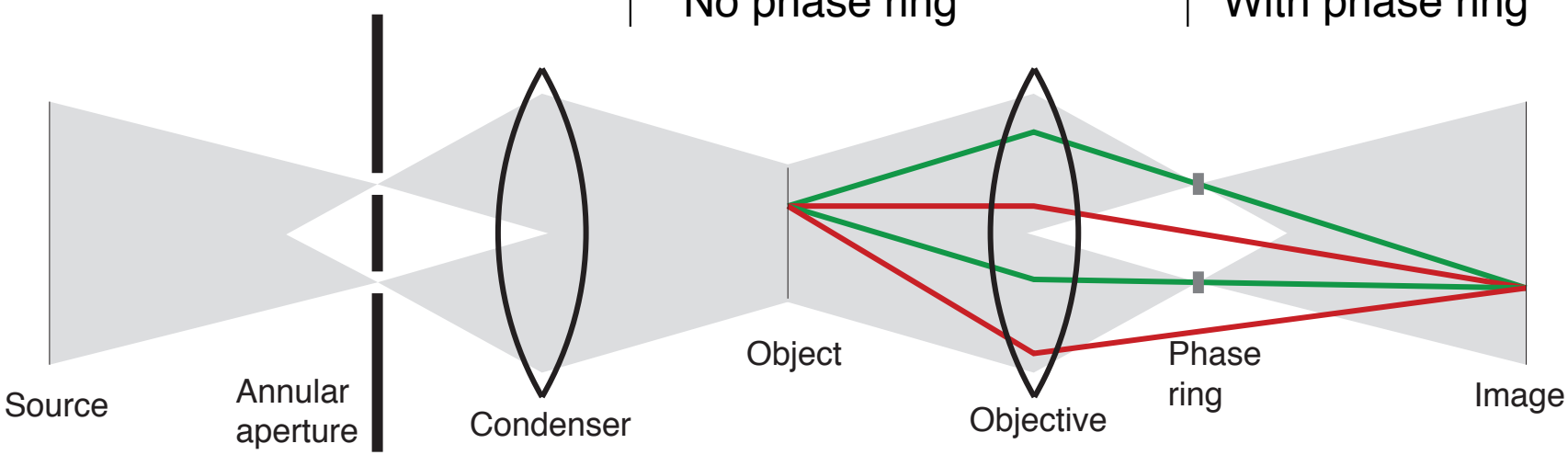

Zernike in a full field microscope

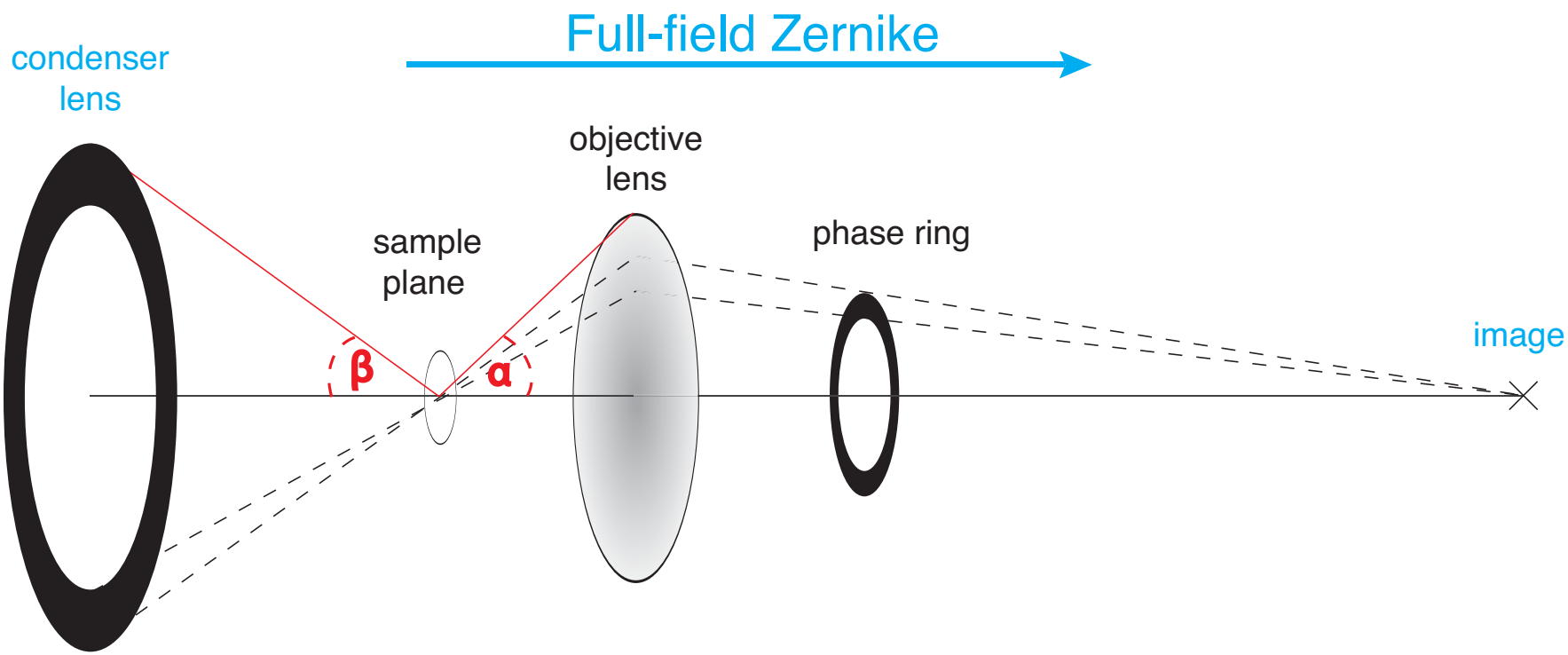

Zernike in a scanning x-ray microscope!

Reciprocity. Suggested by Wilson & Sheppard (1984); US Patent 4,953,188, Siegel, Schmahl, and Rudolph (1990); but not realized.

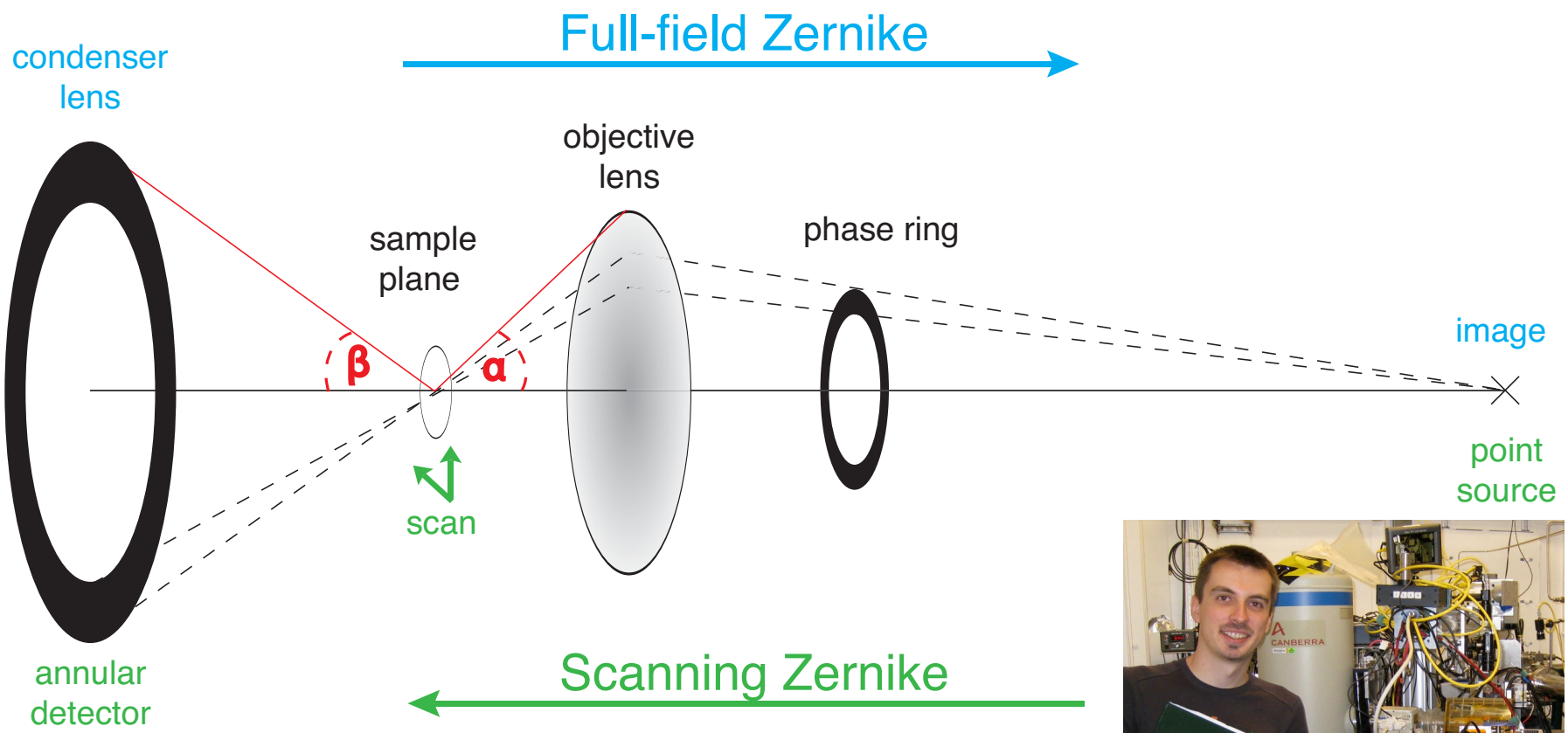

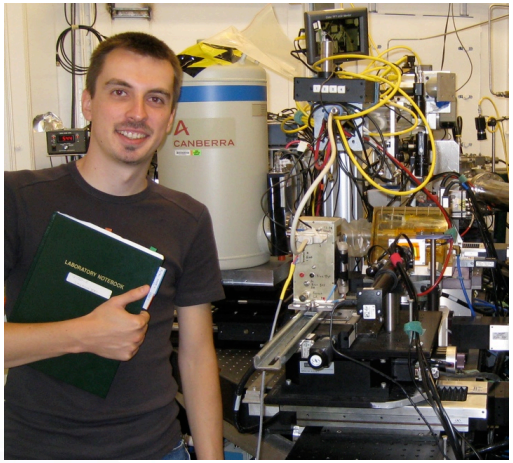

C. Holzner, M. Feser, B. Hornberger, S. Vogt, C. Jacobsen, *Nature Physics* **6**, 883 (2010)

Examples of phase contrast in microprobes

Zinc in Z bands in muscle:
with B. Palmer, U. Vermont

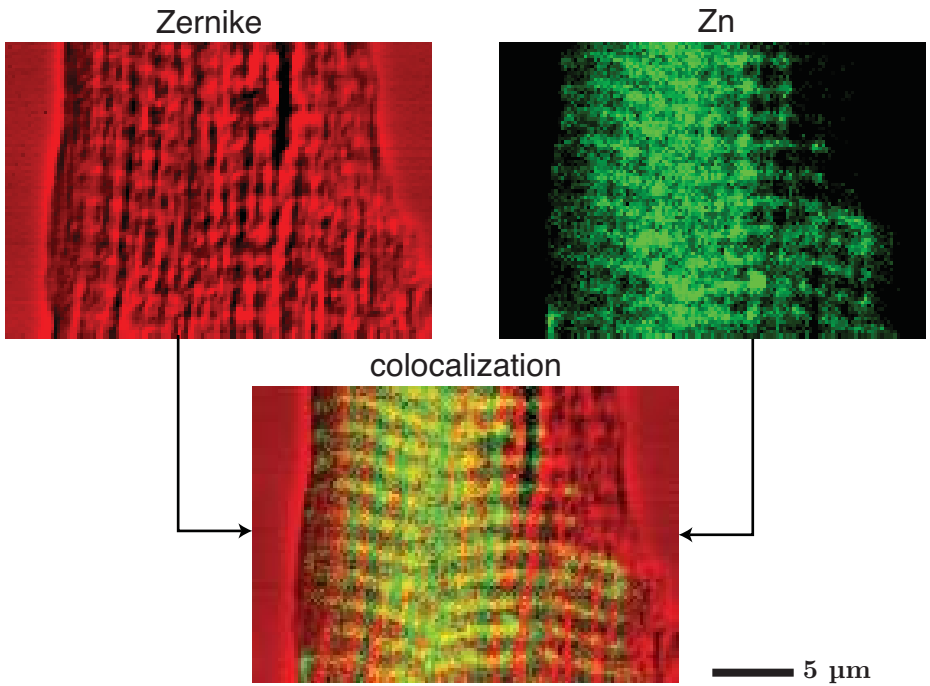

3T3 fibroblast at 10 keV

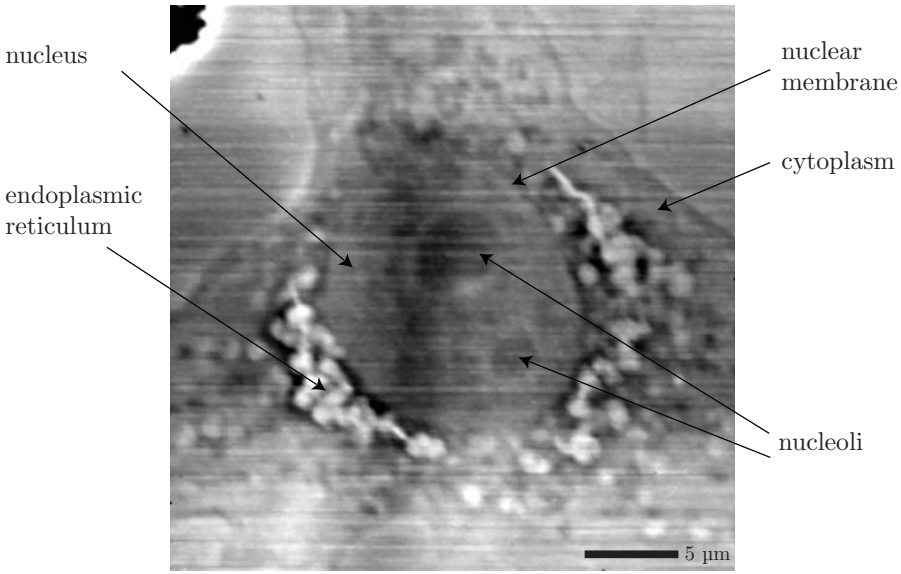

Phase contrast tomography of Cyclotella (marine protist)

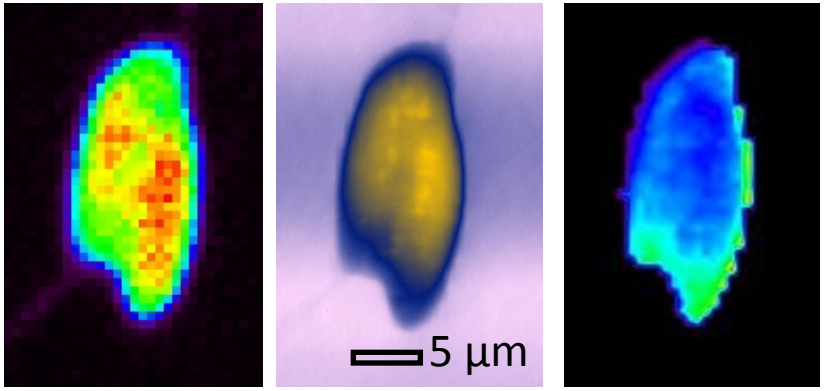

Sulfur content | Protist mass | Sulfur concentration

Quantitative 3D fluorescence of a diatom

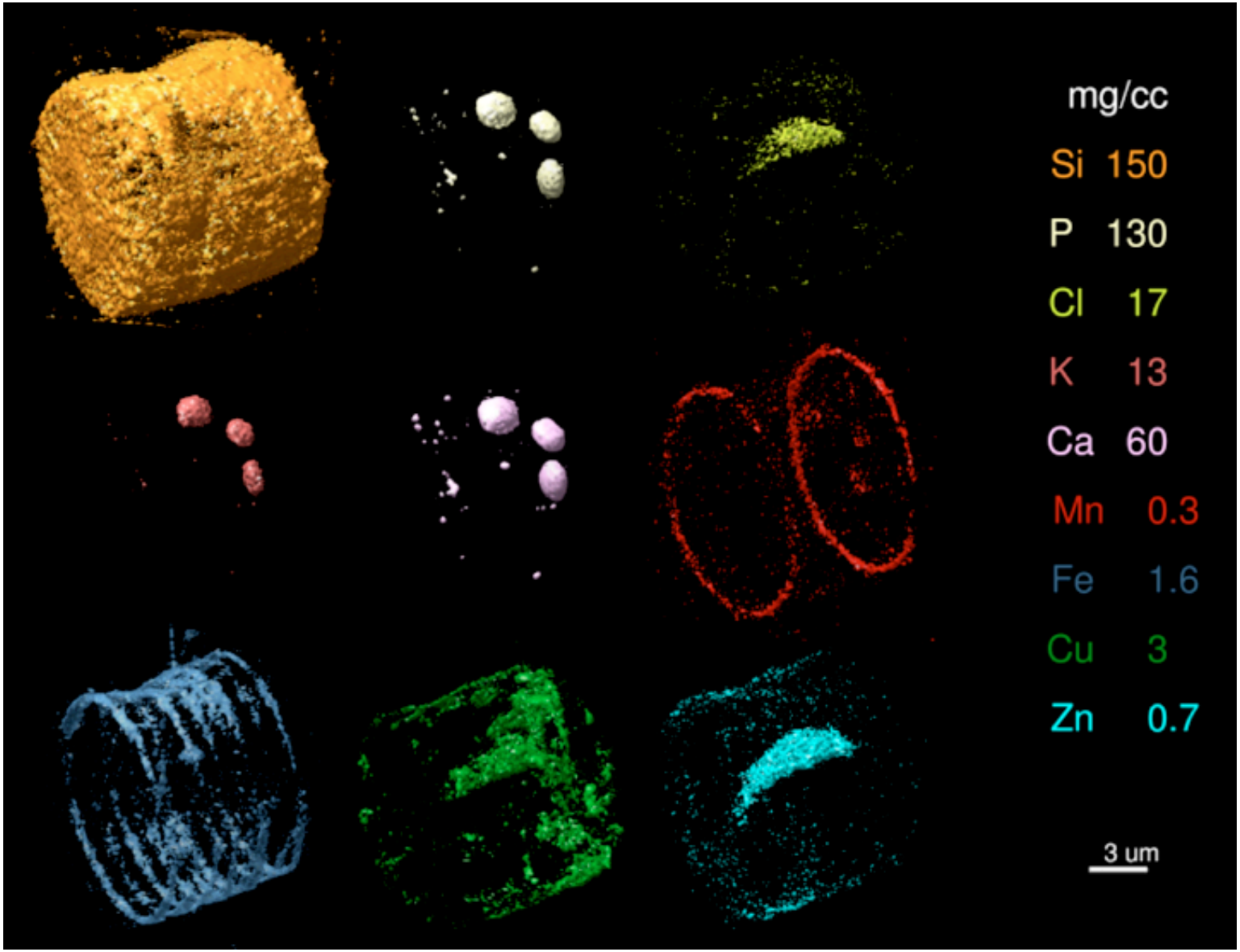

M. de Jonge, C. Holzner, S. Baines, B. Twining, K. Ignatyev, J. Diaz, D. Howard, A. Miceli, I. McNulty, C. Jacobsen, S. Vogt, *Proc. Nat. Acad. Sci.* **107**, 15676 (2010)

Fluorescence tomography

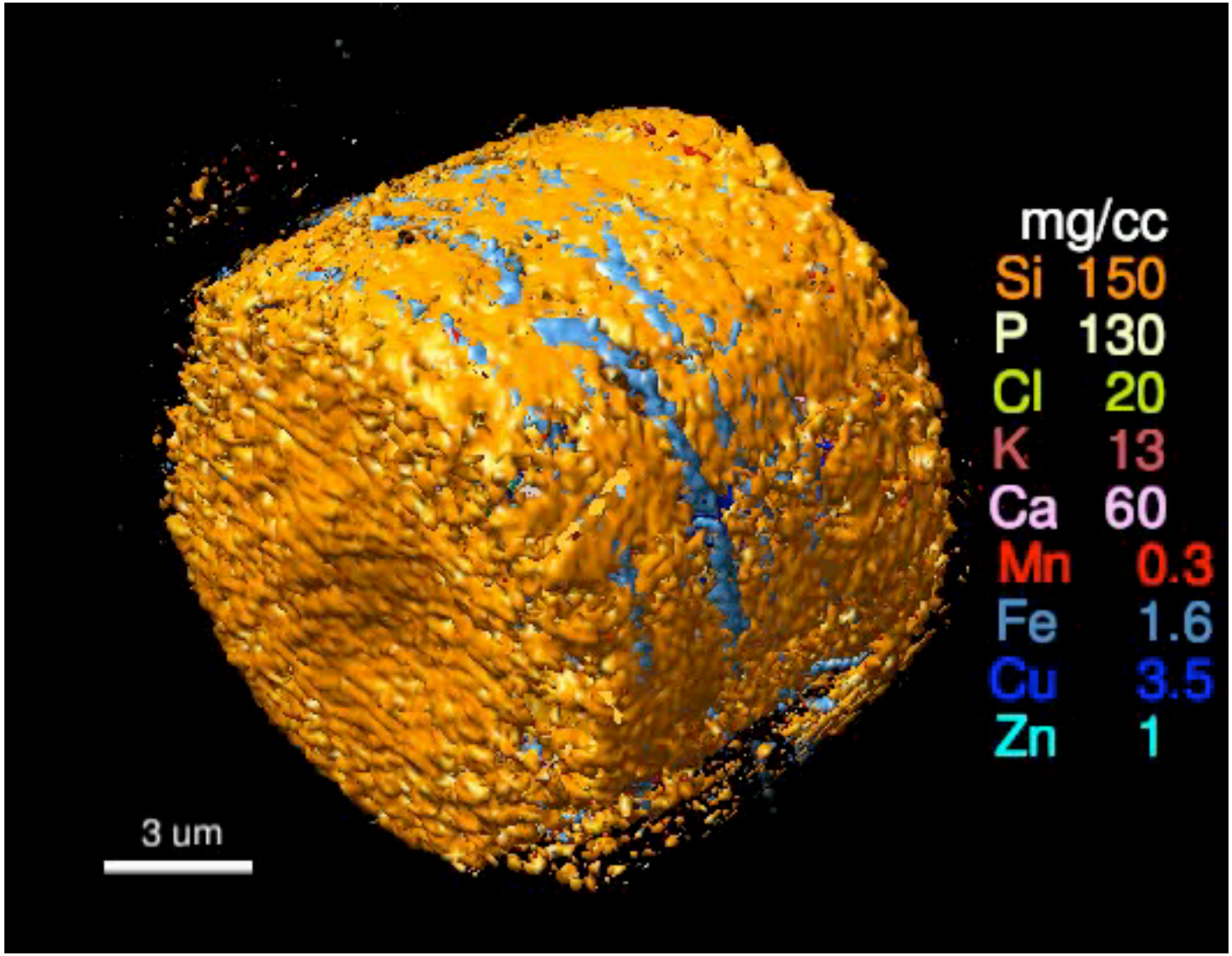

de Jonge *et al.*, *Proc. Nat. Acad. Sci.* **107**, 15676 (2010). Next: phase contrast for alignment, dose fractionation for fluorescence.

Zone plate microscopes

TXM

- Incoherent illumination
- Pixels in parallel: fast
- Higher dose to specimen: ~1-10% optic *after*
- Can work with lab sources

STXM ("sticks-em")

- Coherent illumination
- Pixels in serial: slower
- Lower dose to specimen: optic *before*
- More modalities: fluorescence etc.

TXM: transmission x-ray microscope

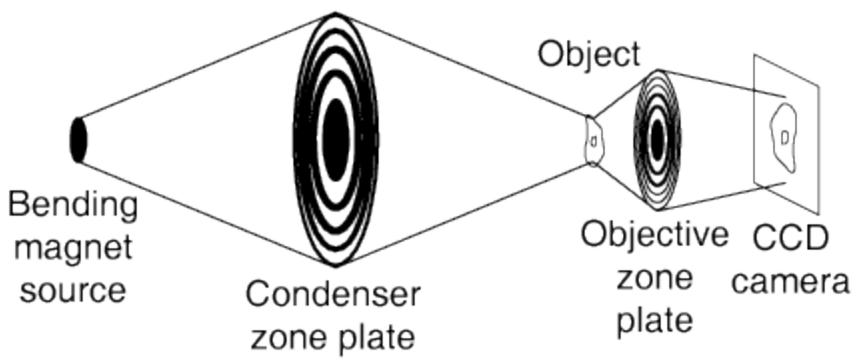

STXM: scanning transmission x-ray microscope

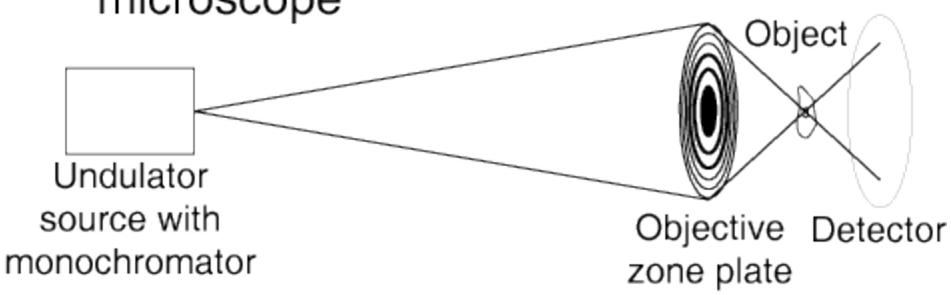

Soft x-ray tomography in a TXM

National Center for X-ray Tomography (UCSF/LBL): Larabell, Le Gros *et al.*

Parkinson *et al.*, *J. Struct. Bio.* **162**, 380 (2008): fission yeast *Schizosaccharomyces pombe*. Color coding by density: Nuclei, mitochondria, vacuoles…

40-50 nm resolution 2D;
70 nm resolution 3D

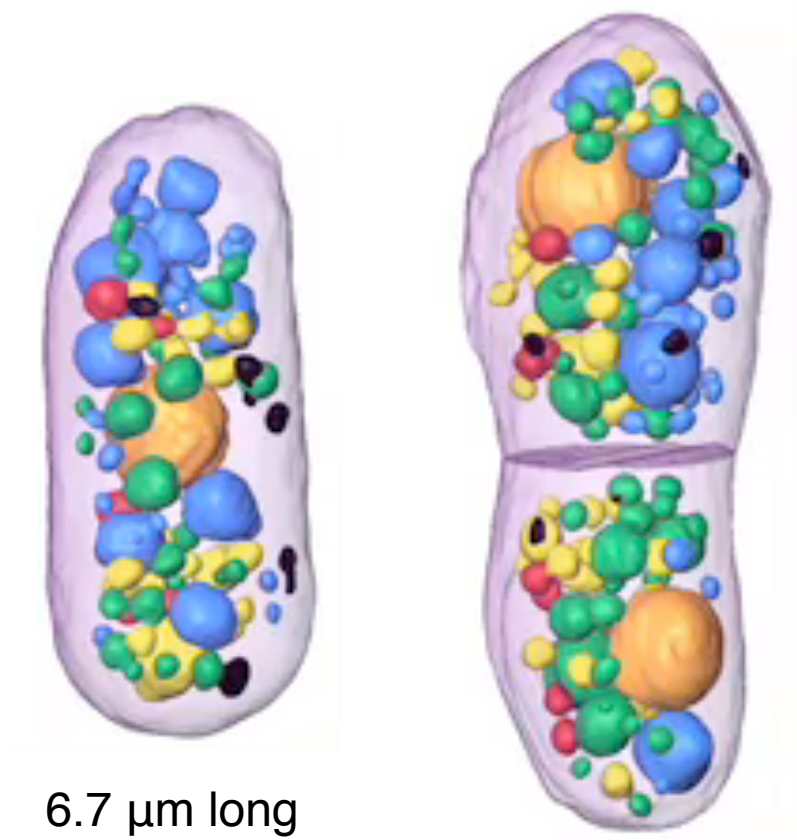

6.7 µm long

Anilao, Philippines, 17-Oct-2010

Anilao, Philippines, 17-Oct-2010

Near-edge absorption fine structure (NEXAFS) or X-ray absorption near-edge structure (XANES)

- Fine-tuning of the x-ray energy near an atom's edge gives sensitivity to the chemical bonding state of atoms of that type
- First exploitation for chemical state transmission imaging: Ade *et al.*, *Science* **258**, 972 (1992) – Stony Brook/X1A

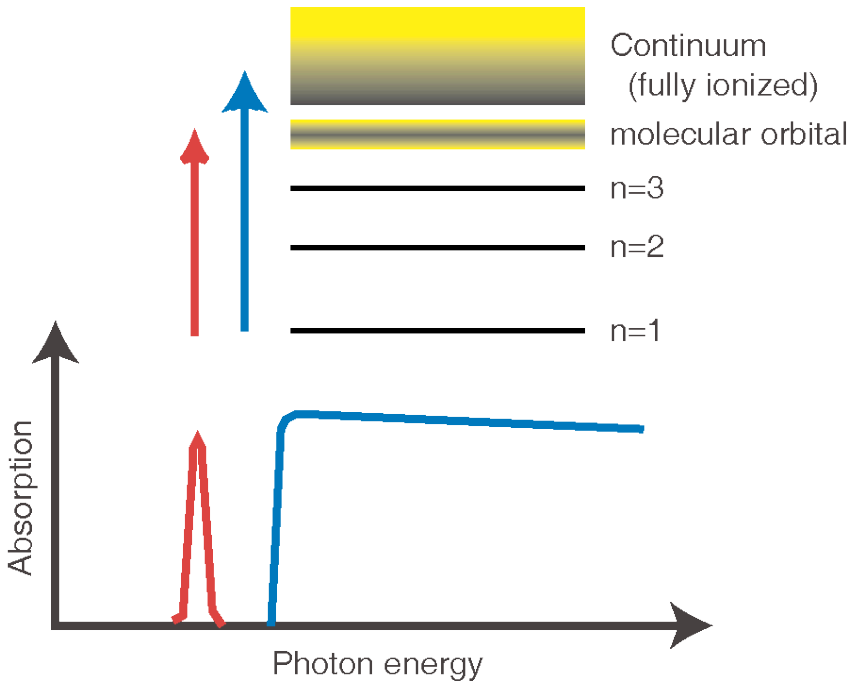

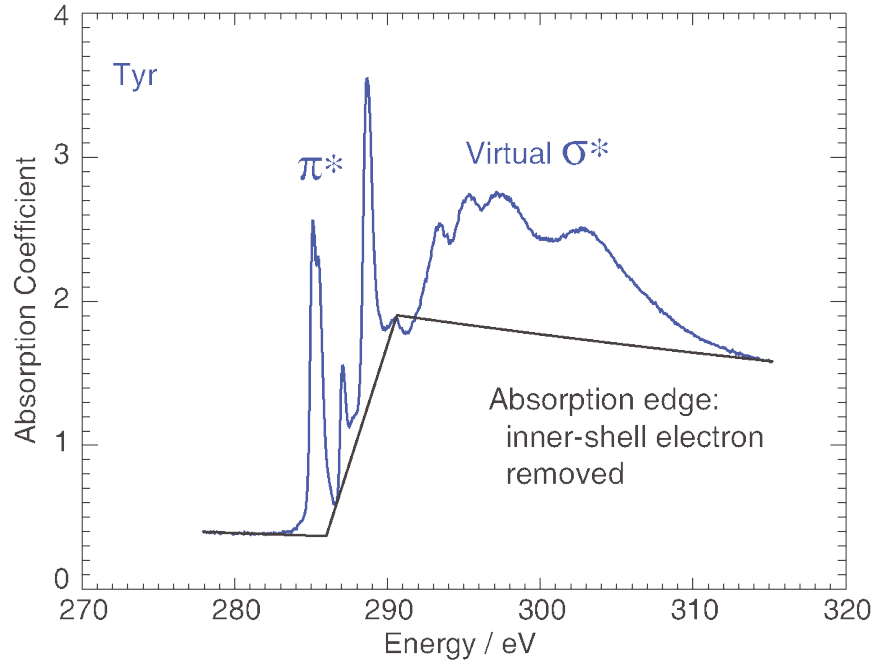

Compared with UV "tickling" of molecular orbitals, core-level electrons come from a single, well-defined state!

C-XANES of amino acids

- K. Kaznacheyev *et al.*, *J. Phys. Chem.* **A 106**, 3153 (2002)
- Experiment: K. Kaznacheyev *et al.*, Stony Brook (now CLS)
- Theory: O. Plashkevych, H. Ågren *et al.*, KTH Stockholm; A. Hitchcock, McMaster

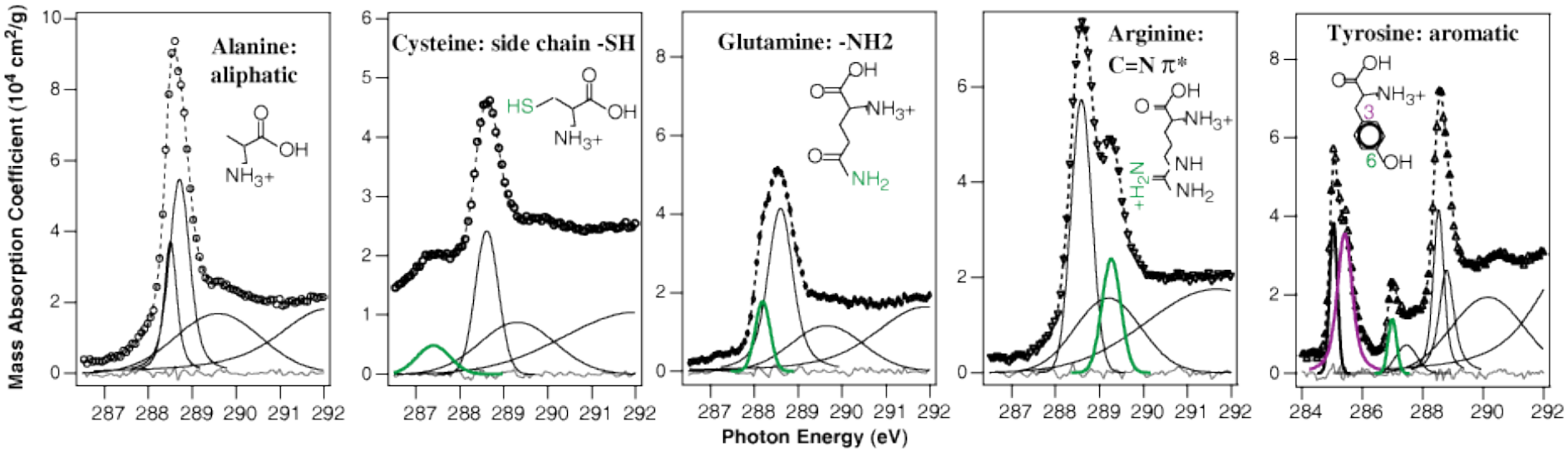

Polymers: see e.g., Dhez, Ade, and Urquhart, *JESRP* **128**, 85 (2003)

Spectromicroscopy: spectrum per pixel

(Aliases: spectrum imaging, hyperspectral imaging)

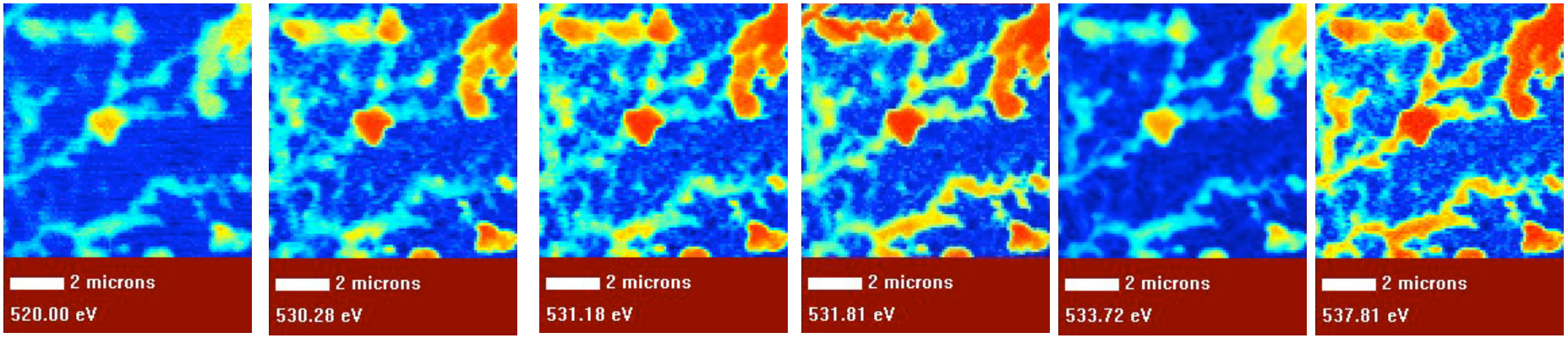

Lu in hematite (T. Schäfer)

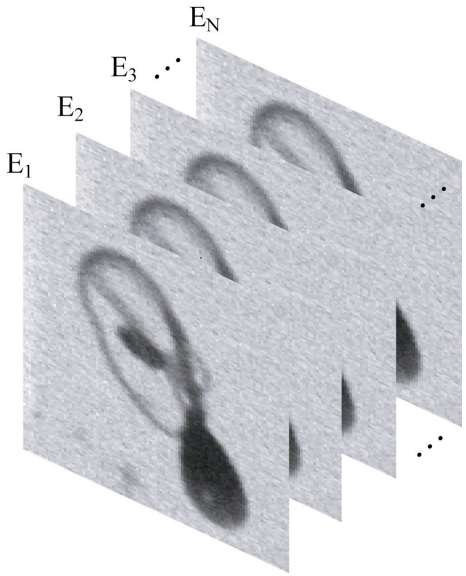

Elemental signals:

- Fluorescence microprobes (electron, x-ray, proton)
- Imaging mass spectrometry (e.g., TOF-SIMS)

Chemical signals:

- Near-edge electronic states with X rays (XANES, NEXAFS) and electrons (ELNES)
- Vibrational modes with infrared microspectroscopy, Raman (e.g., CARS)

Also satellite imaging...

Spectromicroscopy analysis

We have measured the optical density $D=\mu t$ from $I=I_0\exp[-\mu t]$, which gives us a matrix over $n=1..N$ energies and $p=1..P$ pixels of the data:

$$D_{N\times P} = \begin{bmatrix} D_{11} & \text{pixels} & D_{1P} \\ \text{spectra} & & \vdots \\ D_{N1} & \dots & D_{NP} \end{bmatrix}$$

What we have

We wish we could interpret this in terms of a set of $s=1..S$ components. We would then have a matrix of their spectra

$$\mu_{N\times S} = \begin{bmatrix} \mu_{11} & \text{components} & \mu_{1S} \\ \text{spectra} & & \vdots \\ \mu_{N1} & \dots & \mu_{NS} \end{bmatrix}$$

We would also have a matrix of their thicknesses

$$t_{S\times P} = \begin{bmatrix} t_{11} & \text{pixels} & t_{1P} \\ \text{components} & & \vdots \\ t_{S1} & \dots & t_{SP} \end{bmatrix}$$

What we wish we had

Doing the math

- We measure the data but want to interpret it as spectra times thicknesses:

$$\begin{bmatrix} D_{11} & \text{pixels} & D_{1P} \\ \text{spectra} & & \vdots \\ D_{N1} & \dots & D_{NP} \end{bmatrix} = \begin{bmatrix} \mu_{11} & \text{components} & \mu_{1S} \\ \text{spectra} & & \vdots \\ \mu_{N1} & \dots & \mu_{NS} \end{bmatrix} \cdot \begin{bmatrix} t_{11} & \text{pixels} & t_{1P} \\ \text{components} & & \vdots \\ t_{S1} & \dots & t_{SP} \end{bmatrix}$$

or $$D_{N\times P} = \mu_{N\times S} \cdot t_{S\times P}$$

- If we know all S components and their spectra $\mu_{N\times S}$, we can obtain thickness maps:

$$t_{S\times P} = \mu^{-1}_{S\times N} \cdot D_{N\times P}$$

- Matrix $\mu_{N\times S}$ of all spectra can be inverted using singular matrix decomposition (SVD). See *e.g.*, Zhang *et al.*, *J. Struct. Biol.* **116**, 335 (1996); Koprinarov *et al.*, *J. Phys. Chem. B* **106**, 5358 (2002).

The "organizer": components S

- If we know the $s=1\ldots S$ components (*e.g.*, known pure compounds) and their spectra, we know $\mu_{N\times S}$ and thus $t_{S\times P} = \mu^{-1}_{S\times N} \cdot D_{N\times P}$

$$\begin{bmatrix} D_{11} & \ldots & D_{1P} \\ \vdots & & \vdots \\ D_{N1} & \ldots & D_{NP} \end{bmatrix} = \begin{bmatrix} \mu_{11} & \ldots & \mu_{1S} \\ \vdots & & \vdots \\ \mu_{N1} & \ldots & \mu_{NS} \end{bmatrix} \cdot \begin{bmatrix} t_{11} & \ldots & t_{1P} \\ \vdots & & \vdots \\ t_{S1} & \ldots & t_{SP} \end{bmatrix}$$

- And if not? Can we uncover an "organizer" for our data anyway? General problem: find S!

$$\begin{bmatrix} D_{11} & \ldots & D_{1P} \\ \vdots & & \vdots \\ D_{N1} & \ldots & D_{NP} \end{bmatrix} = \begin{bmatrix} C_{11} & \ldots & C_{1S} \\ \vdots & & \vdots \\ C_{N1} & \ldots & C_{NS} \end{bmatrix} \cdot \begin{bmatrix} R_{11} & \ldots & R_{1P} \\ \vdots & & \vdots \\ R_{S1} & \ldots & R_{SP} \end{bmatrix}$$

Eigenspectra and eigenimages

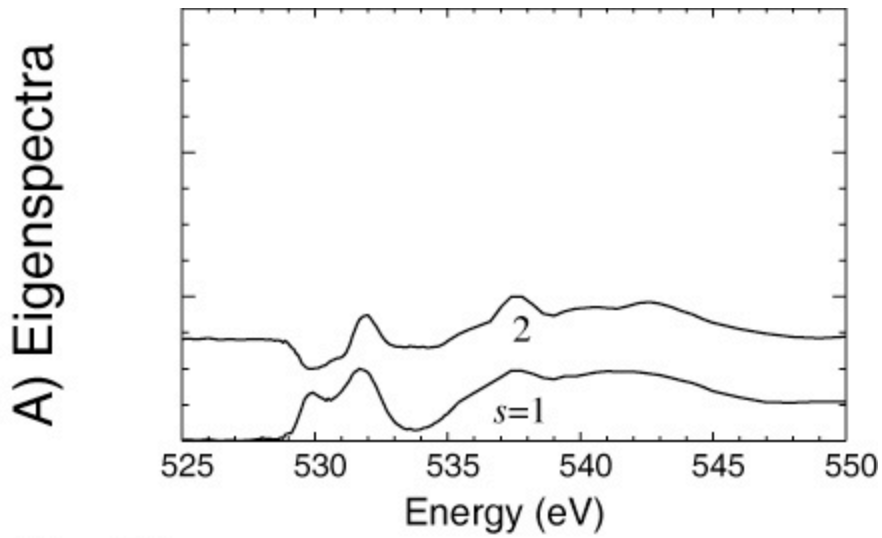

Find reduced number $\bar{S}_{abstract}$ of **significant** components

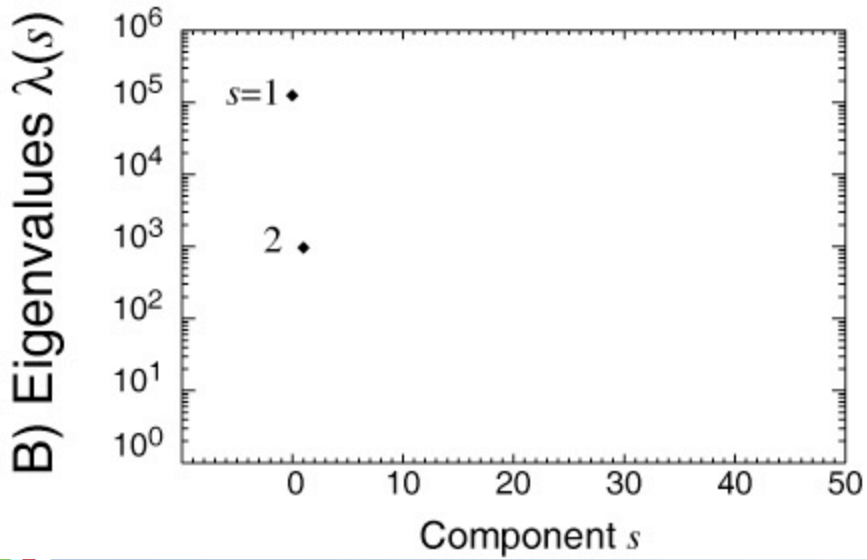

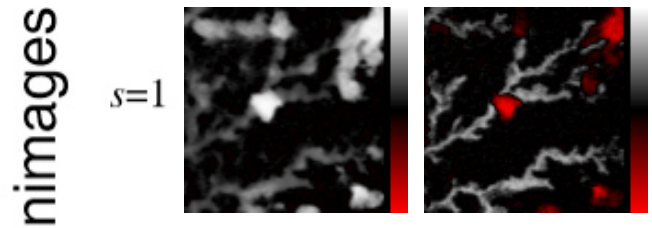

Eigenspectra and eigenimages

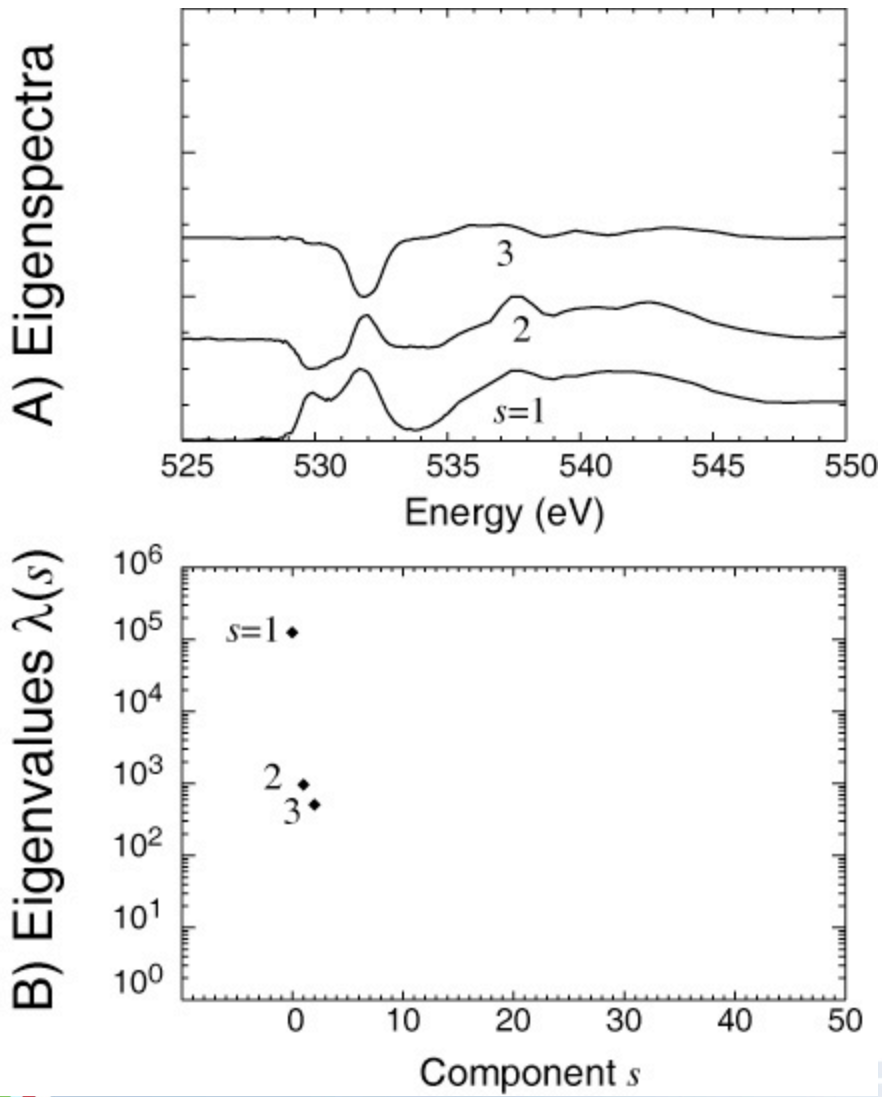

Find reduced number $\bar{S}_{abstract}$ of **significant** components

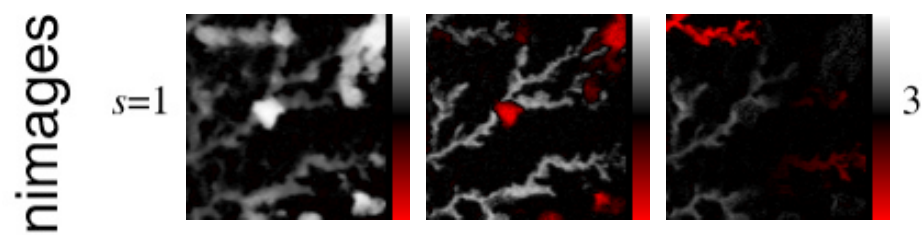

Eigenspectra and eigenimages

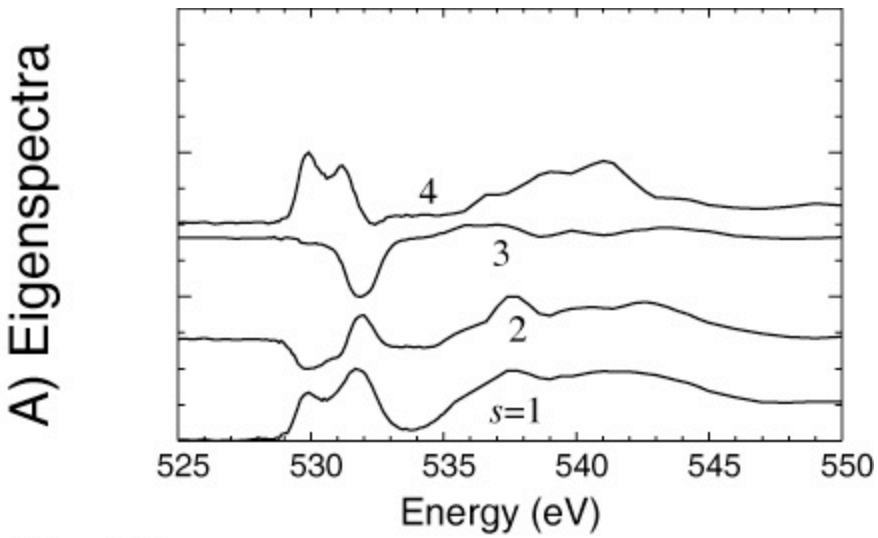

Find reduced number $\bar{S}_{abstract}$ of **significant** components

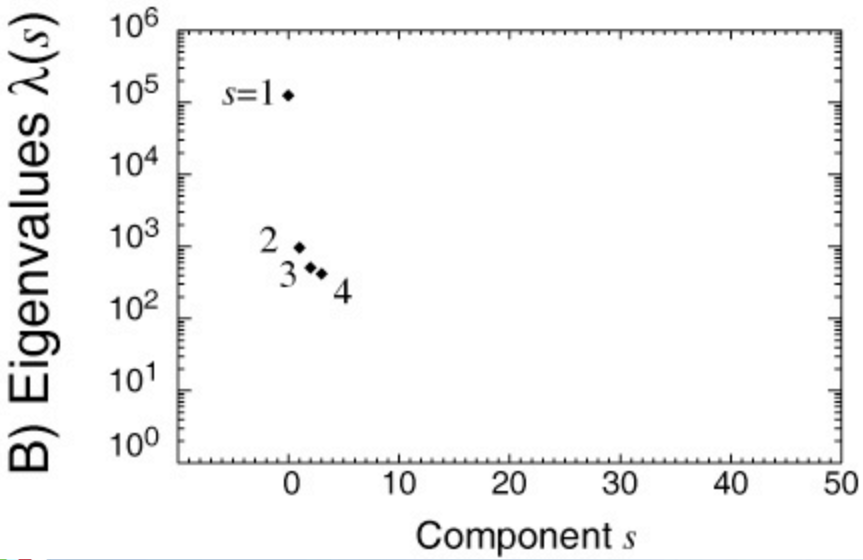

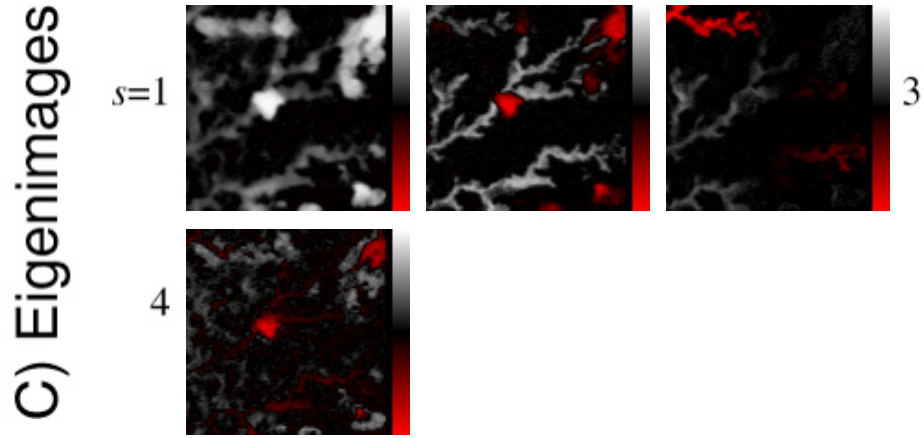

Eigenspectra and eigenimages

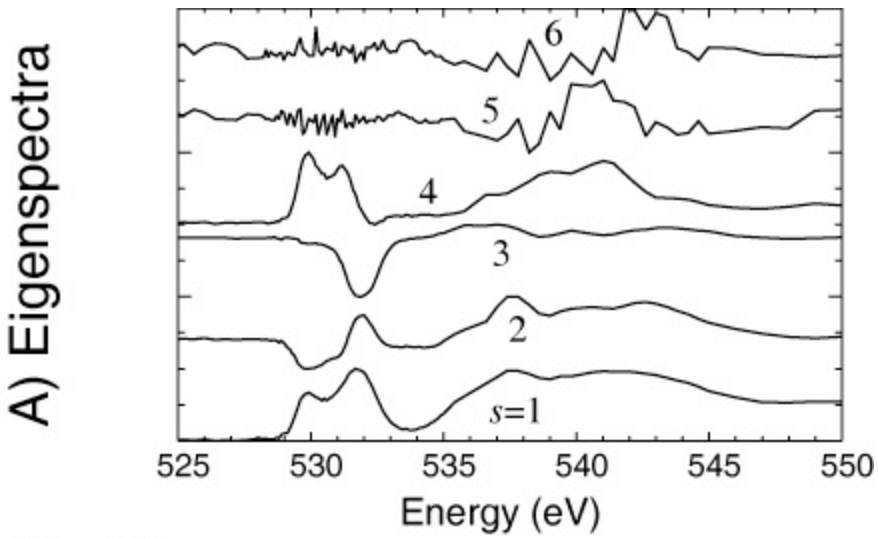

Find reduced number $\bar{S}_{abstract}$ of **significant** components

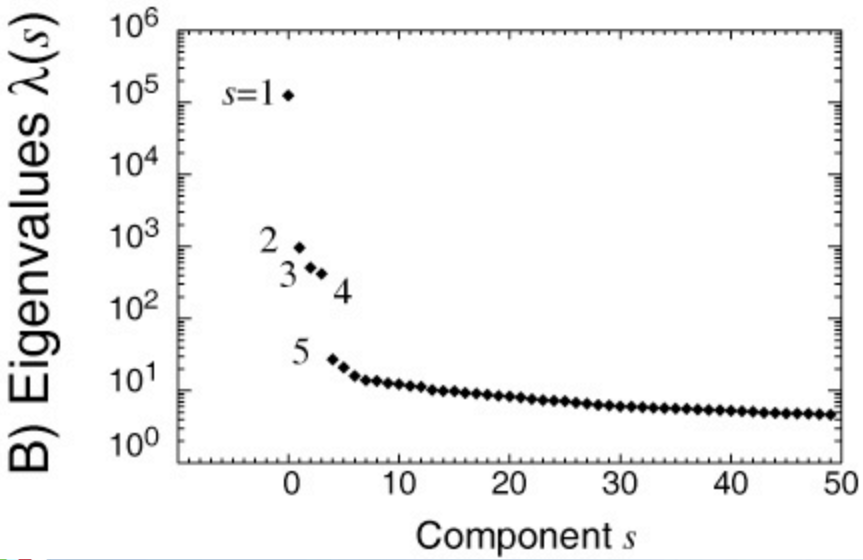

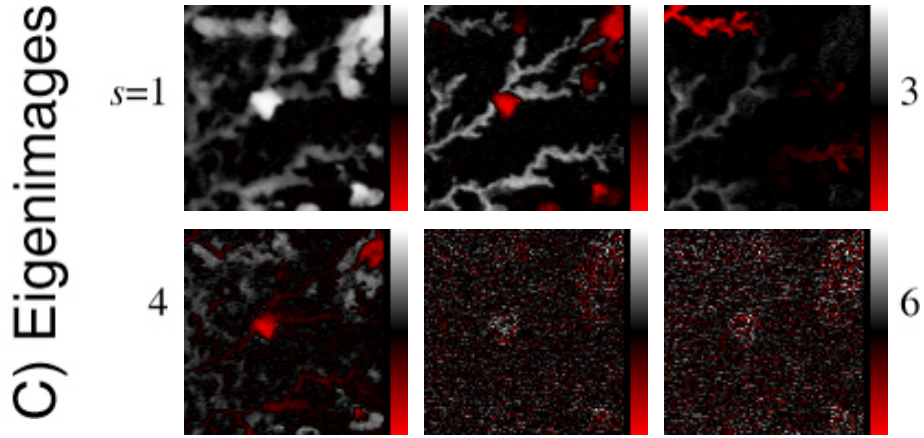

PCA gets us *something*…

- Principal component analysis lets you reduce and orthogonalize the data set!
- Reduction: filter out spectral variations that are poorly correlated throughout the dataset (smells like photon noise!). We went from N=140 energies to $\bar{S}_{\text{abstract}}$ =4 components
- Orthogonality might have nice consequences

But we have a problem…

- Eigenspectra > 1 are abstract. They have negative optical densities, so they are not readily interpretable.

A well-known problem

We chose to follow an approach which is well known in the literature:

"You can't always get what you want; but if you try sometimes, well you just might find you get what you need"

M. Jagger, K. Richards *et al.*, *Let it Bleed* **1**, 1 (1969)

Cluster analysis: Euclidian distance learning algorithm

- Kohonen, *Proc. IEEE* **78**, 1464 (1990)
- Pixels are scattered according to weighting of each component

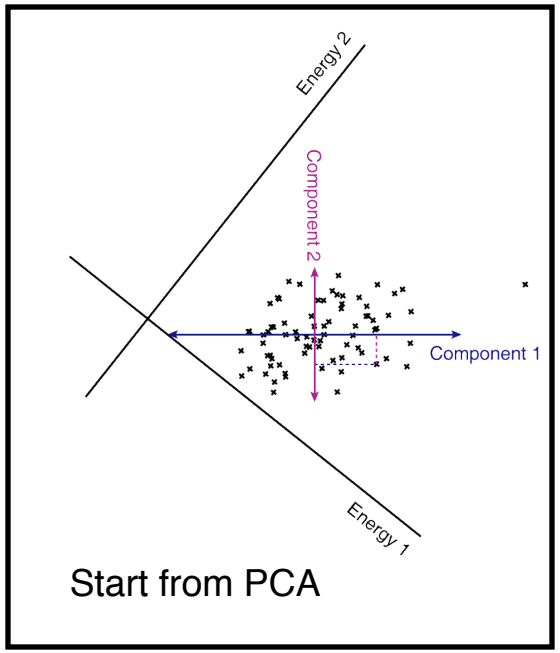

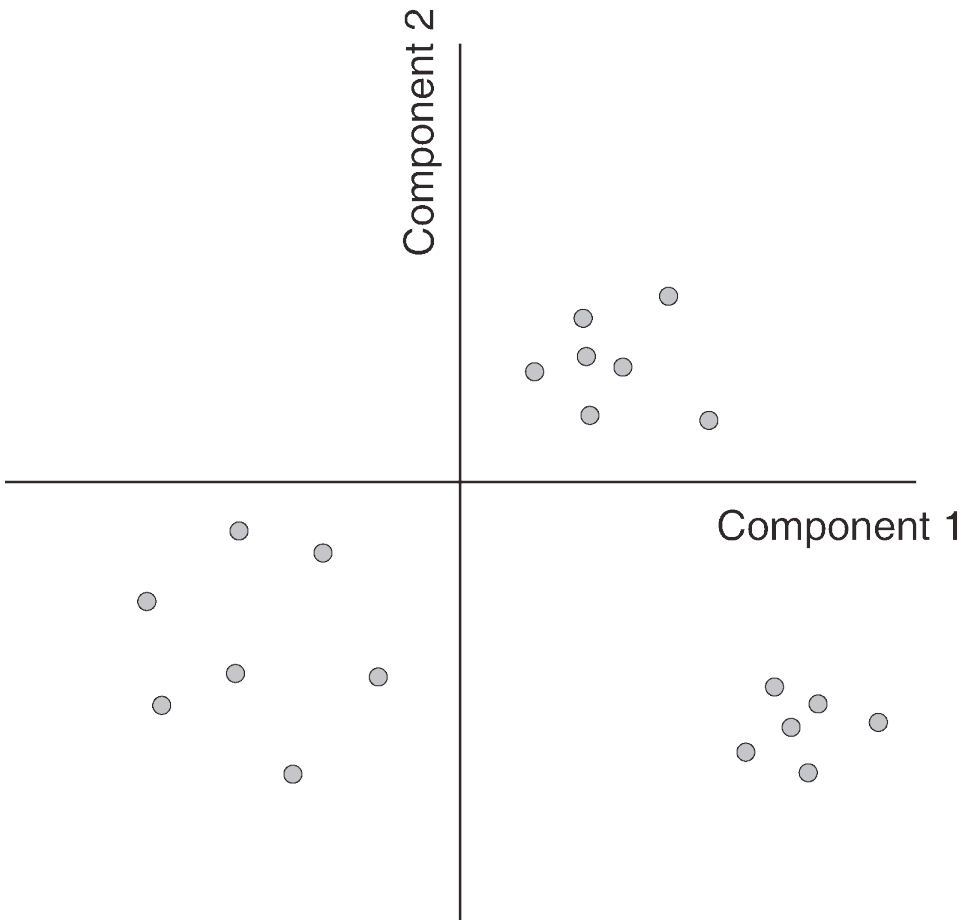

Cluster analysis: Euclidian distance learning algorithm

- Kohonen, *Proc. IEEE* **78**, 1464 (1990)
- Pixels are scattered according to weighting of each component
- Put down cluster centers at random positions.

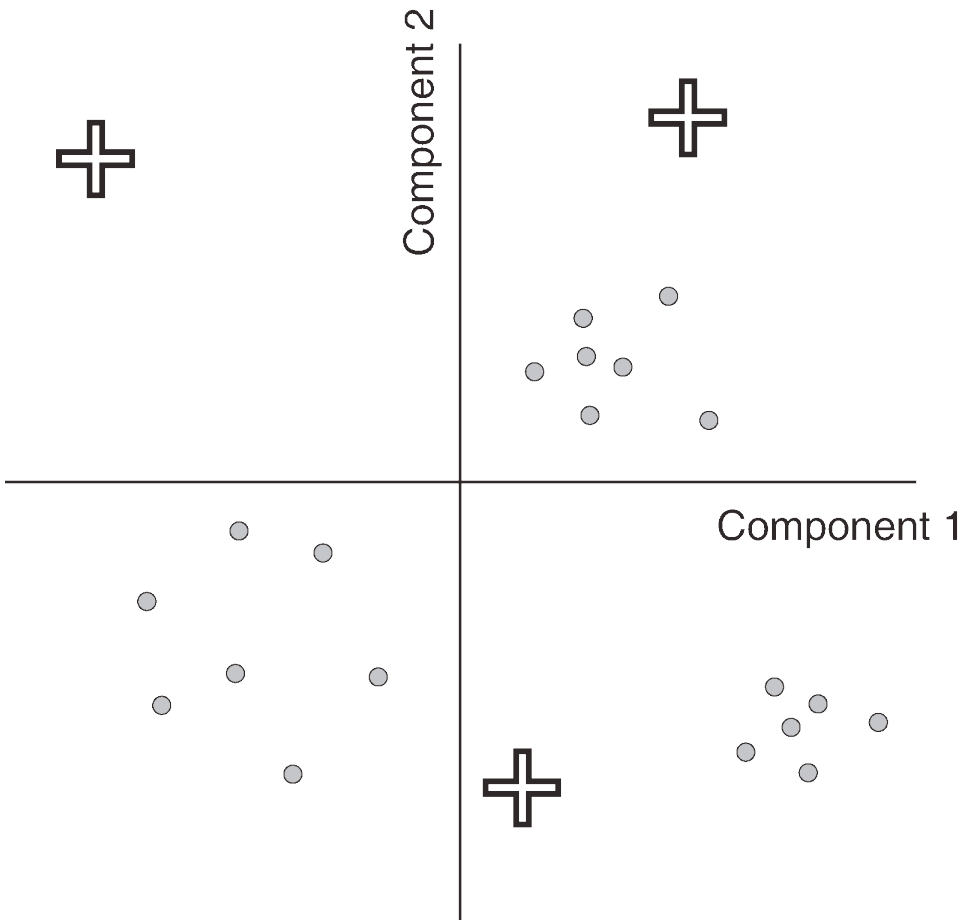

Cluster analysis: Euclidian distance learning algorithm

- Kohonen, *Proc. IEEE* **78**, 1464 (1990)
- Pixels are scattered according to weighting of each component
- Put down cluster centers at random positions.
- Iterate through all pixels, several times:
  - Calculate distances from one pixel to all cluster centers.
  - Pick shortest distance.

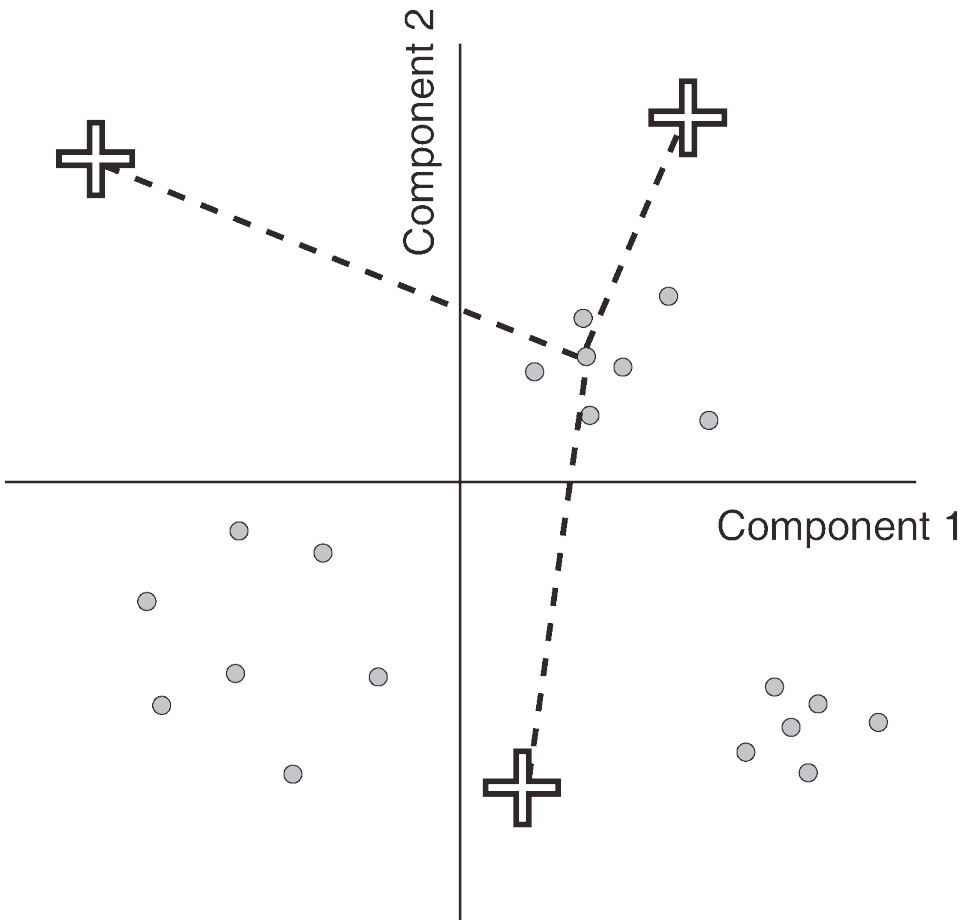

Cluster analysis: Euclidian distance learning algorithm

- Kohonen, *Proc. IEEE* **78**, 1464 (1990)
- Pixels are scattered according to weighting of each component
- Put down cluster centers at random positions.
- Iterate through all pixels, several times:
  - Calculate distances from one pixel to all cluster centers.
  - Pick shortest distance.
  - Move cluster center partway to pixel.

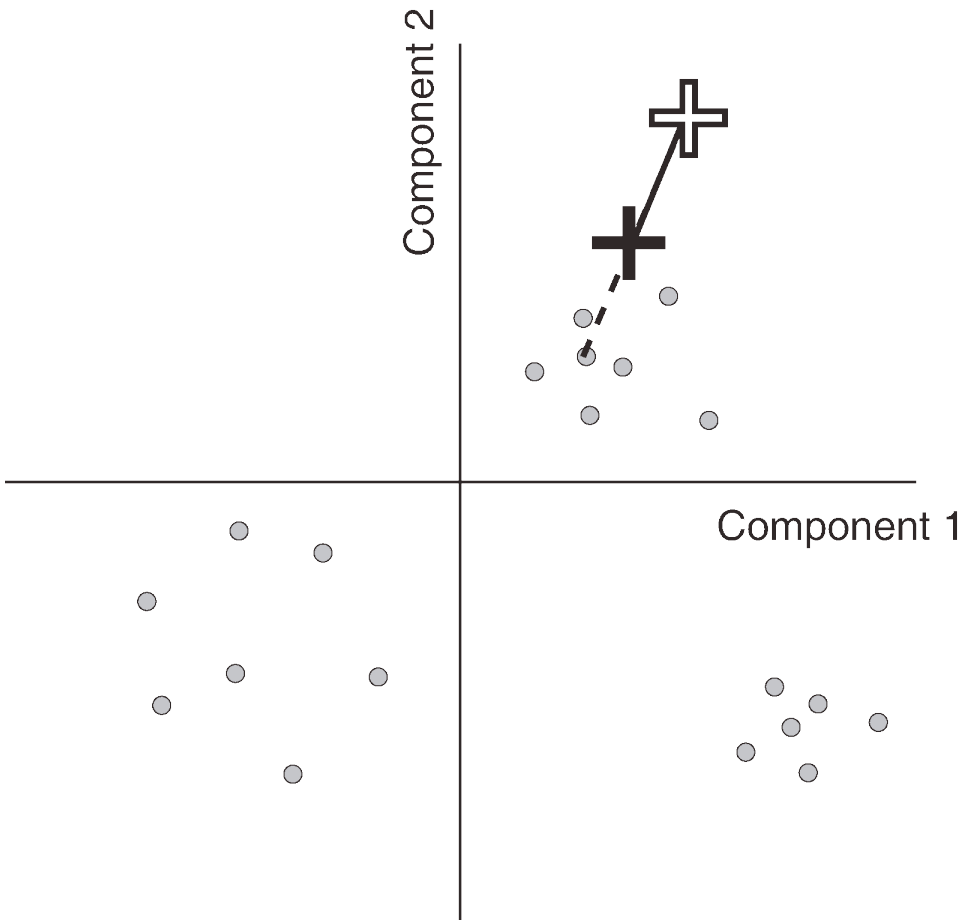

Cluster analysis: Euclidian distance learning algorithm

- Kohonen, *Proc. IEEE* **78**, 1464 (1990)
- Pixels are scattered according to weighting of each component
- Put down cluster centers at random positions.
- Iterate through all pixels, several times:
  - Calculate distances from one pixel to all cluster centers.
  - Pick shortest distance.
  - Move cluster center partway to pixel.
- Cluster pixels with their nearest cluster center

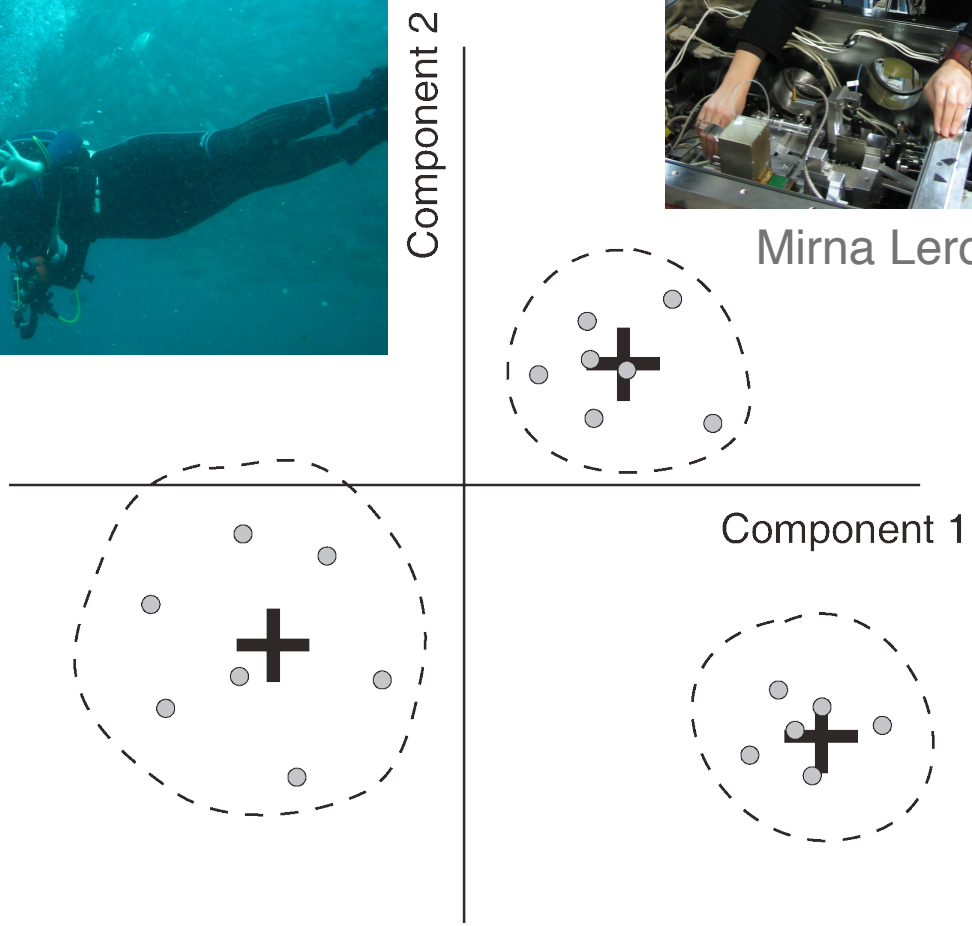

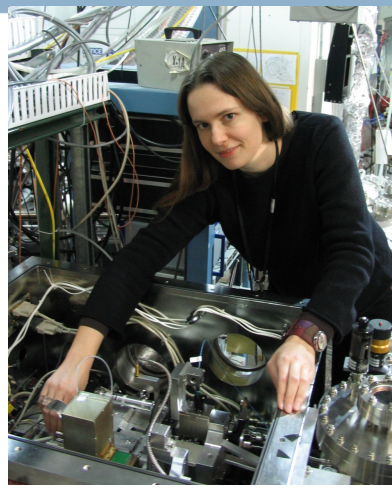

Mirna Lerotić

Cluster analysis: simplifying complexity

- Reference spectra only work for simple samples. What if we have complex, reactive chemistry, with unknown compounds?
- Can't do single molecule detection, but can uncover biochemical themes.
- This example: part of a study of the evolution of tree types, including now-extinct species that dominated in the "coal age" (carboniferous)

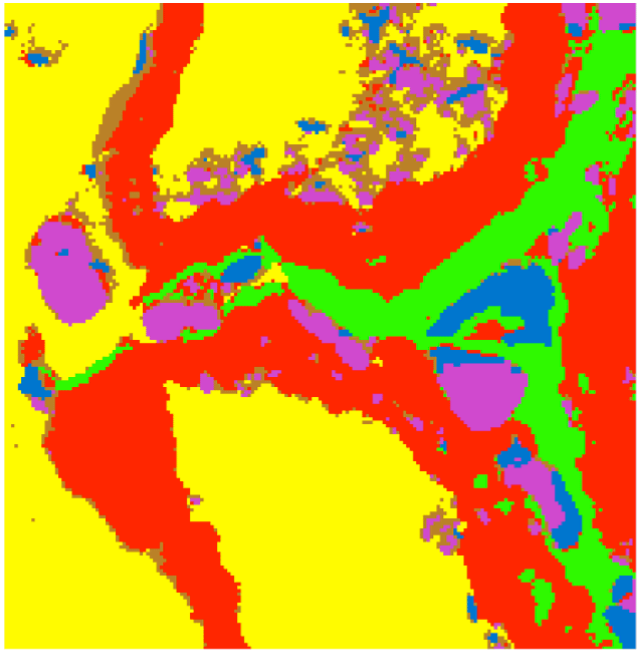

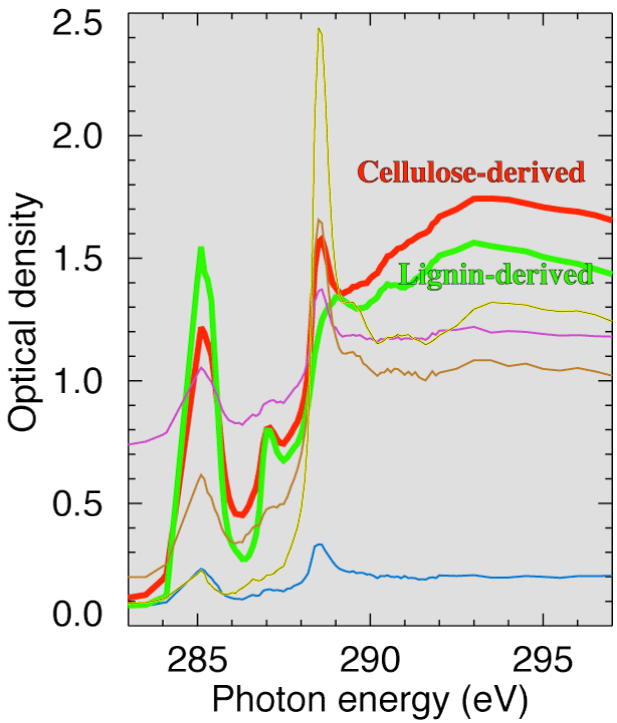

Lignin and cellulose in 400 million year old chert: Boyce *et al.*, *Proc. Nat. Acad. Sci.* **101**, 17555 (2004), with subsequent pattern recognition analysis by Lerotic *et al.*, *Ultramicroscopy* **100**, 35 (2004).

Organic carbon in soils: C-XANES

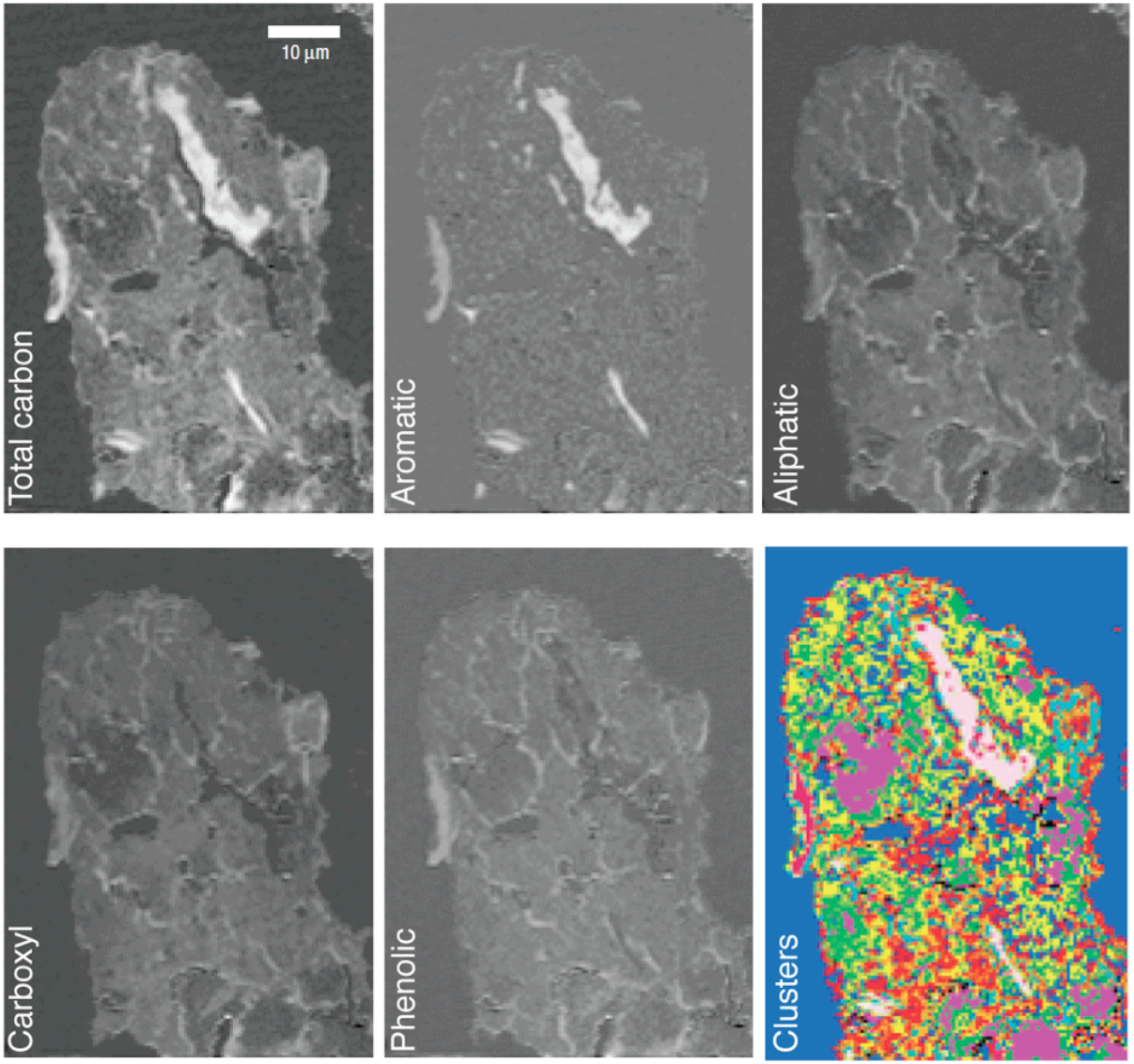

J. Lehmann, D. Solomon, J. Kinyangi, L. Dathe, S. Wirick, and C. Jacobsen, *Nature Geoscience* **1**, 238 (2008)

Cluster analysis: human sperm

Biochemical organization of sperm revealed directly from data: enzyme-rich region, DNA+histones, mitochondria and flagellar motor, lipid

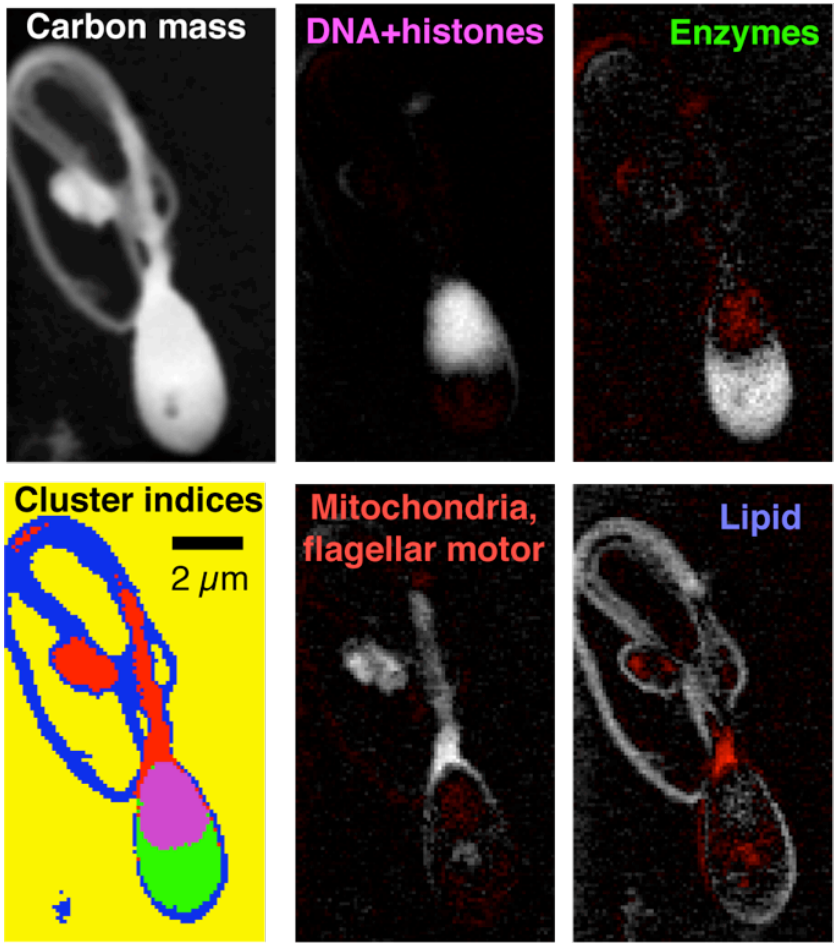

H. Fleckenstein, M. Lerotic, Y. Sheynkin *et al.*, Stony Brook. Human sperm, air-dried.

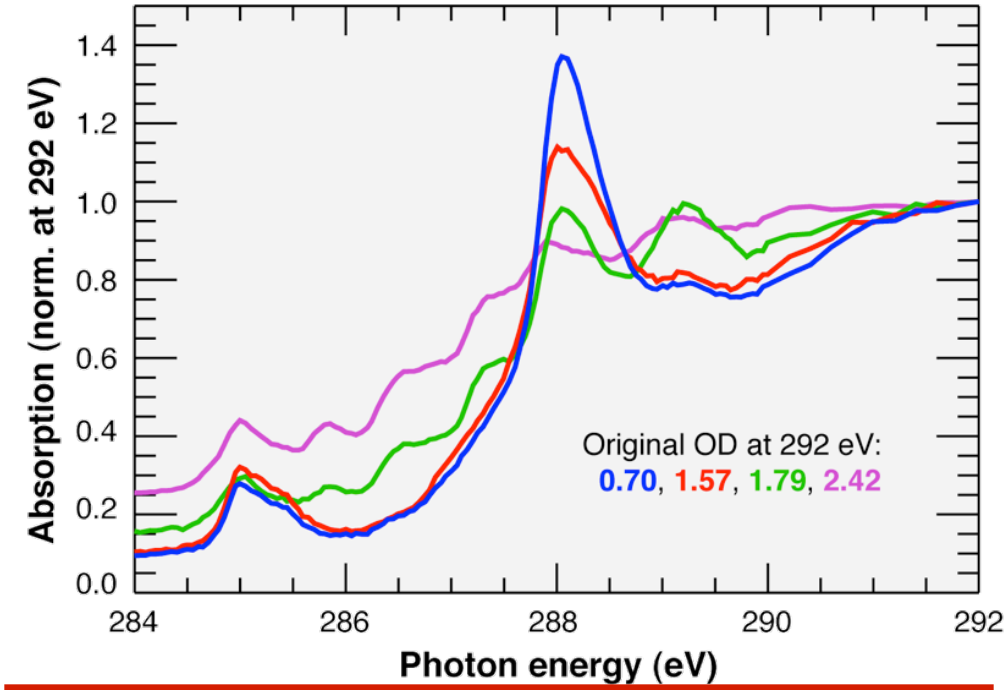

Red spots: negative values, because cluster spectra are not guaranteed to “span the set”

Avoiding negativity: non-negative matrix factorization

PCA

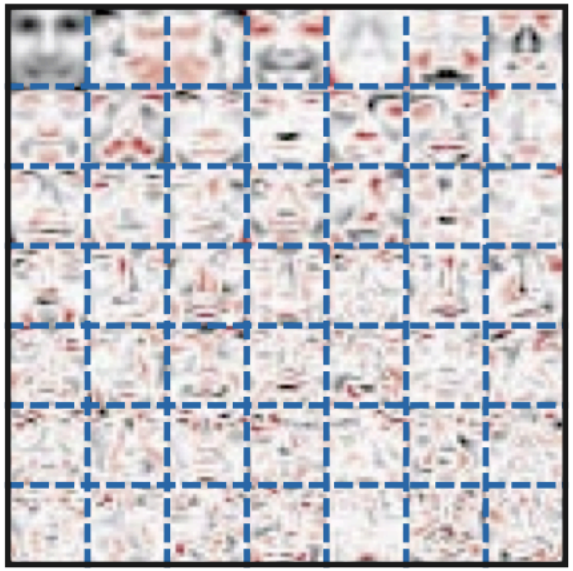

Lee and Seung, *Nature* **401**, 788 (1999)

Principal component analysis

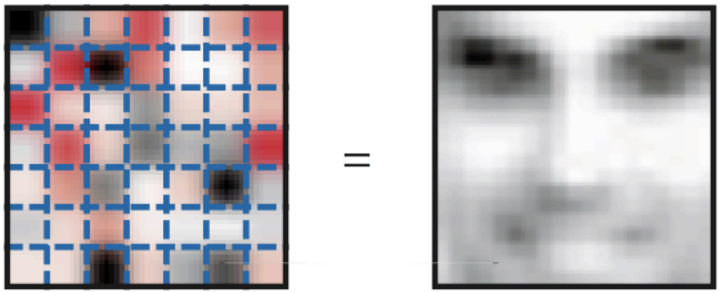

NMF

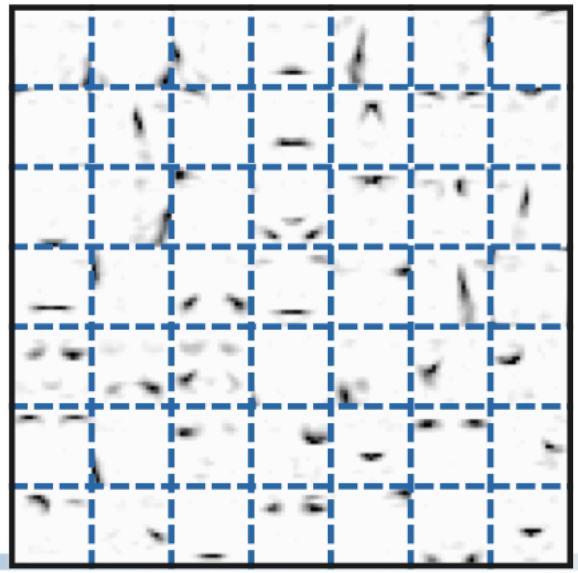

Non-negative matrix factorization

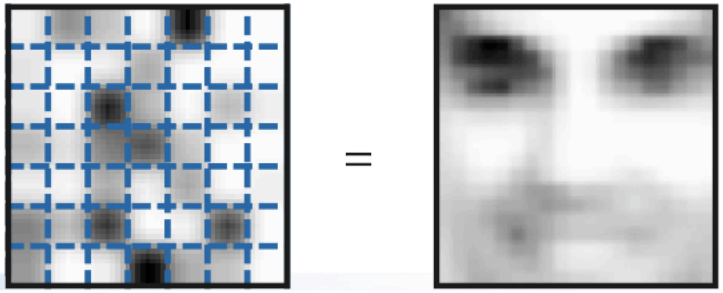

NMF analysis of sperm

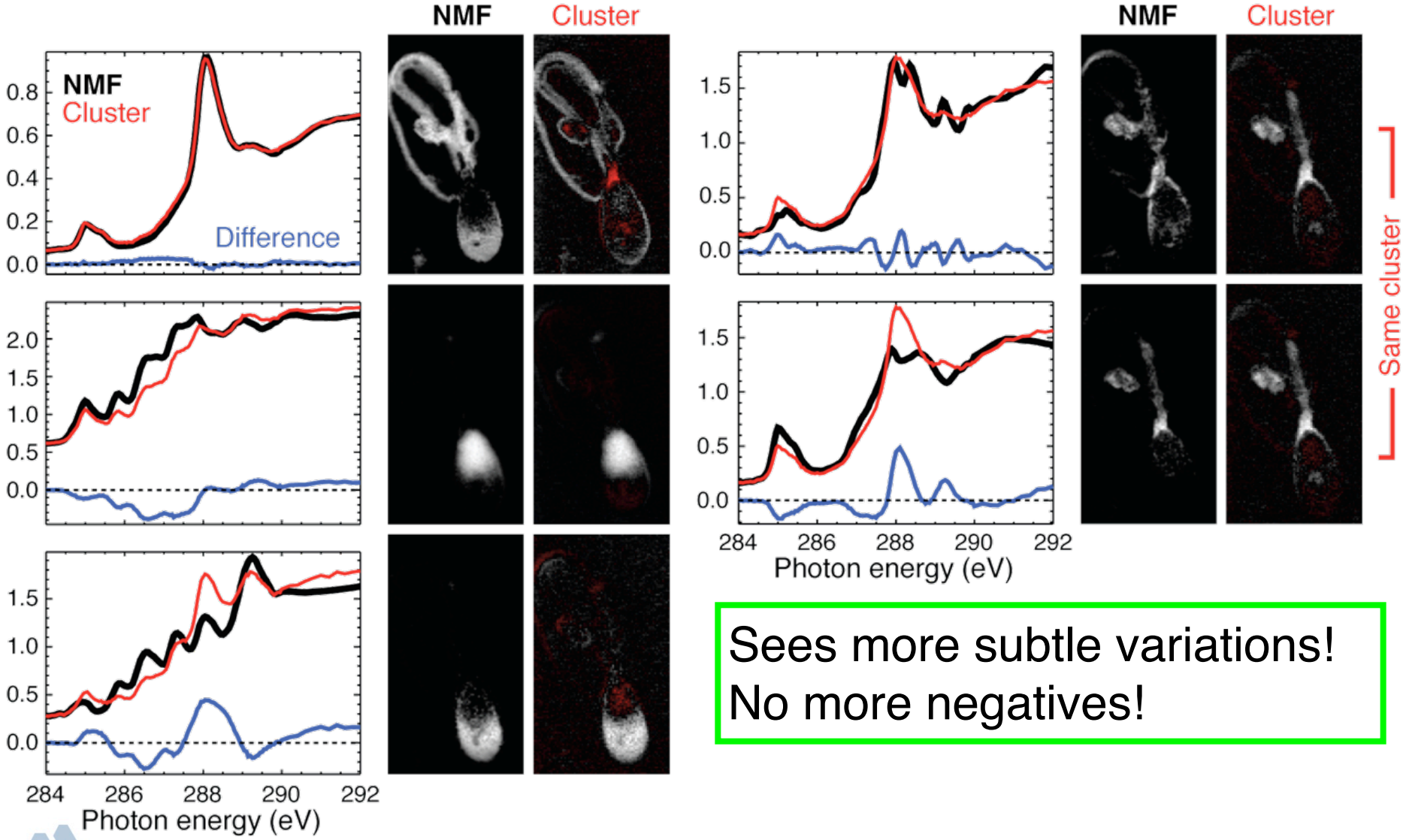

Sees more subtle variations!
No more negatives!

NNMA: many, many iterations

- On a single processor, Lee and Seung NMF algorithm can be slow!

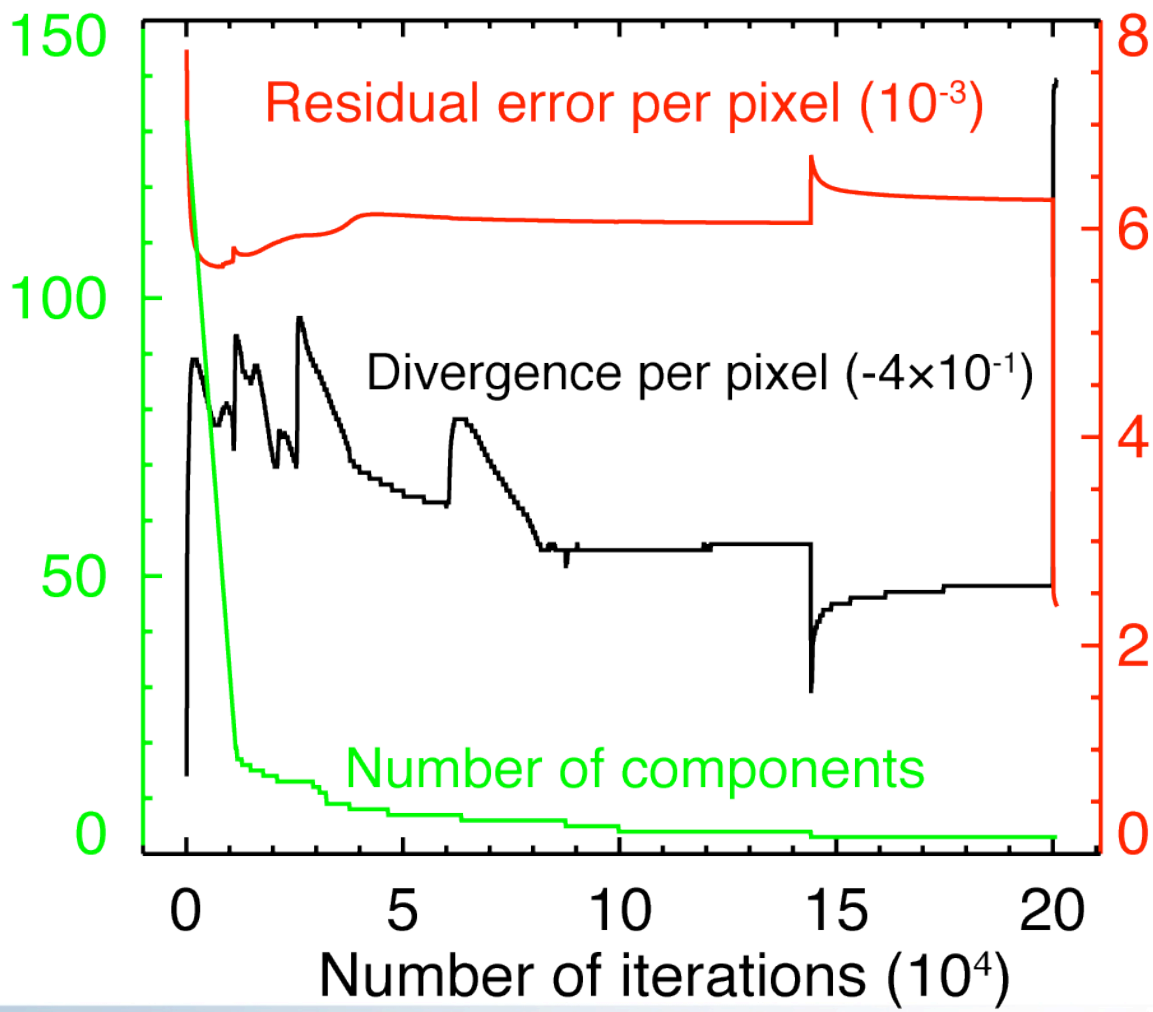

Cheap parallel computing

- Parallel nature of FC-NNLS algorithm may be well-suited to parallel computing architecture: NVidia CUDA, or OpenCL
- Each inverse calculation for each “group” of columns is independent.
- Each inverse calculation can be computed by a “block” of “threads”.
- Many blocks can execute in parallel, thus potentially speeding up the parallel algorithm even more...

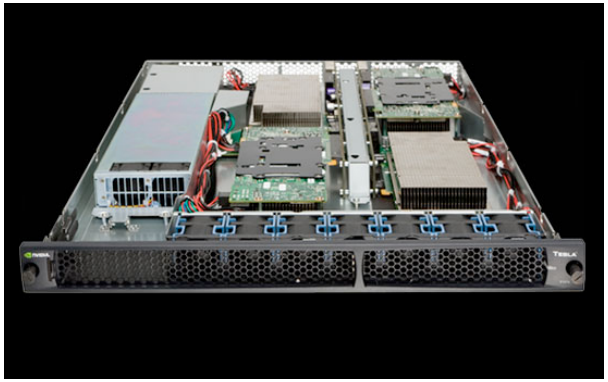

NVidia Tesla S1070

Coherent diffraction imaging

- For many specimens, radiation damage sets the ultimate limit on achievable resolution.
- Lenses phase the signal, but lose the signal. Example: 20 nm zone plate with 10% efficiency, 50% window transmission, 20% modulation transfer function (MTF) for 15 nm half-period:

  net transfer of 1% for high spatial frequencies
- Can we avoid this ~100x signal loss, and also go beyond numerical aperture limit of available optics?

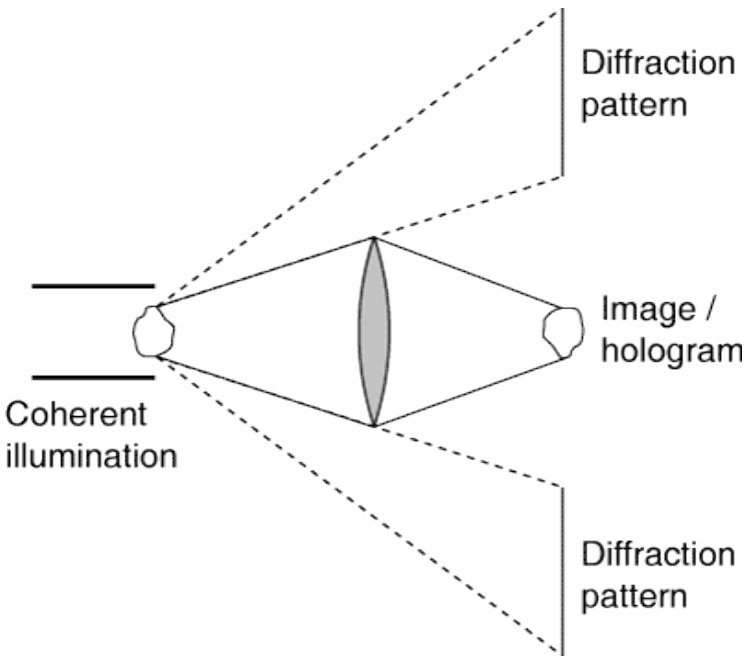

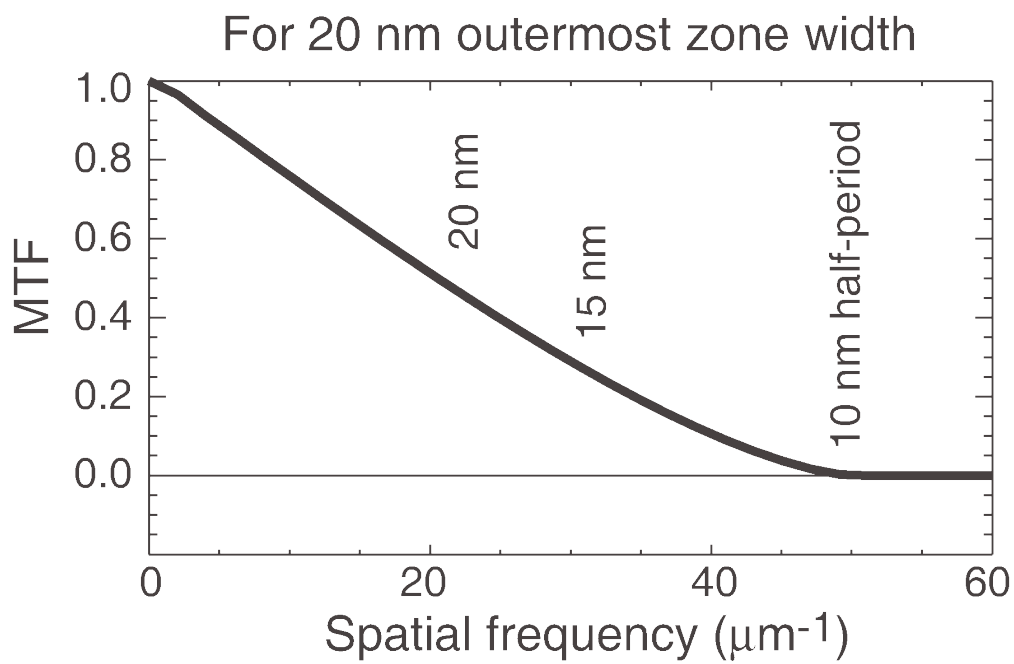

Phase matters

Image→ Fourier transform→ set either magnitude or phase to a constant→ inverse Fourier transform

Malcolm Howells at La Clusaz

Image using only Fourier magnitudes

Image using only Fourier phases

Phase matters

Image→ Fourier transform→ set either magnitude or phase to a constant→ inverse Fourier transform

Malcolm Howells at La Clusaz

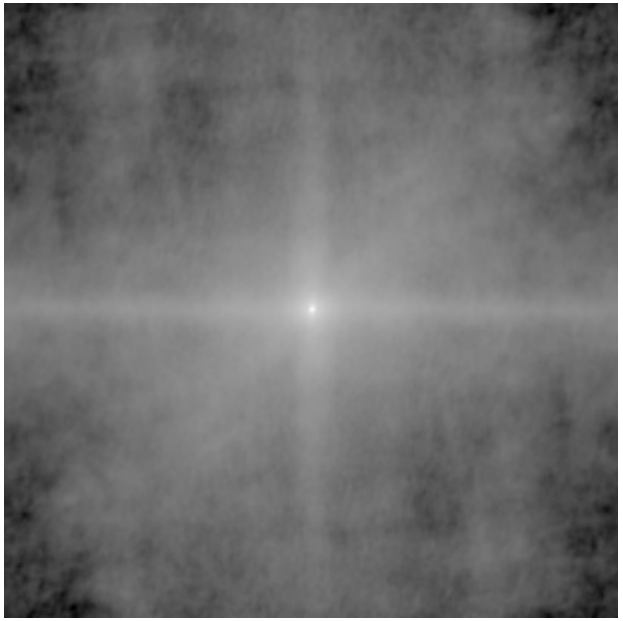

Image using only Fourier magnitudes

Image using only Fourier phases

Phase matters

Image→ Fourier transform→ set either magnitude or phase to a constant→ inverse Fourier transform

Malcolm Howells at La Clusaz

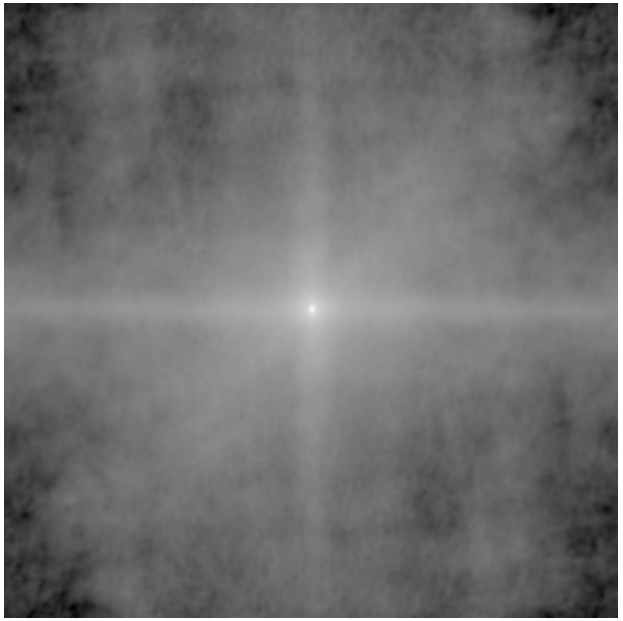

Image using only Fourier magnitudes

Image using only Fourier phases

Who else might be interested?

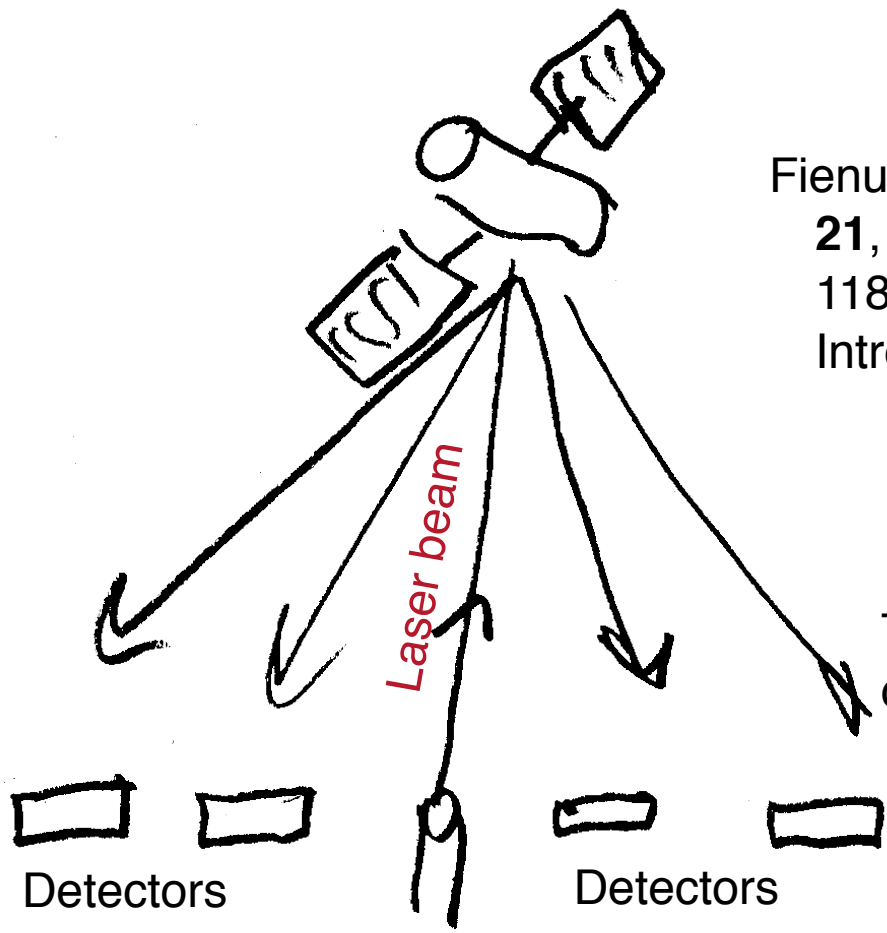

Fienup, *Opt. Lett.* **3**, 27 (1978); *Appl. Opt.* **21**, 2758 (1978); *J. Opt. Soc. Am. A* **4**, 118 (1987); and other papers. Introduces the use of a “finite support”.

Turbulent atmosphere degrades phase

Cartoon based on presentations by Fienup from ERIM (Environmental Research Institute of Michigan). Fienup is now at U. Rochester

Imaging without lenses

- Avoid losses of lens efficiency and transfer function
- Must phase the diffraction intensities

Real space: finite support (or other constraints)

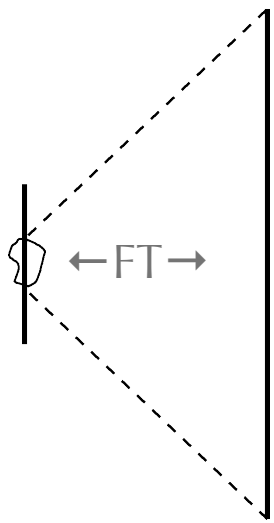

Fourier space: magnitudes known, but phases are not

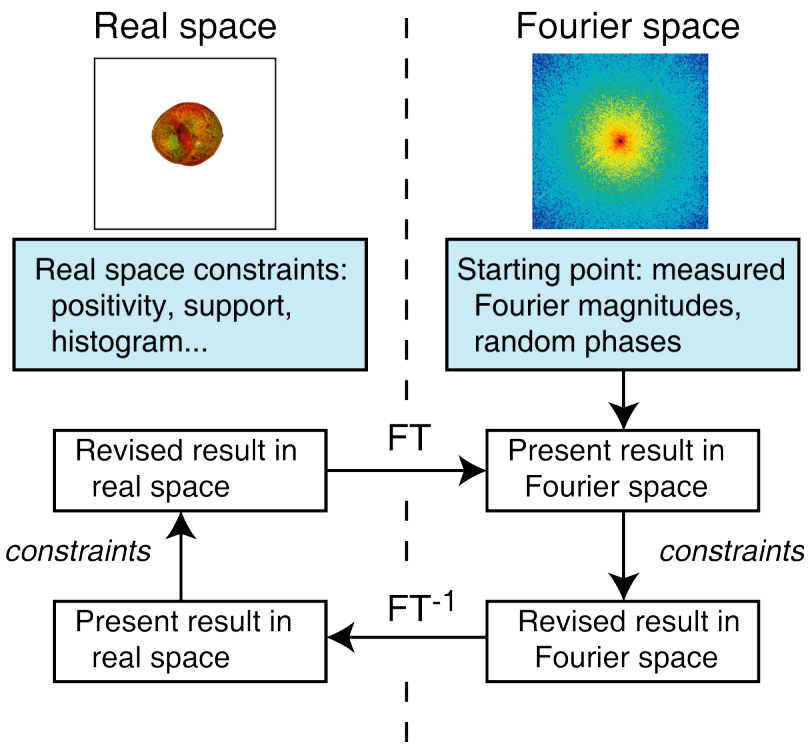

Phasing algorithms: Feinup, *Opt. Lett.* **3**, 27 (1978); Elser, *JOSA A* **20**, 40 (2003); and others. First x-ray demonstration: Miao *et al.*, *Nature* **400**, 342 (1999).

Iterative phasing: simple example

- High harmonic generation of XUV radiation from femtosecond lasers, illuminating two pinholes.
  - R. Bartels, A. Paul, H. Green, H.C. Kapteyn, M.M. Murnane, S. Backus, I.P. Christov, Y. Liu, D. Attwood, C. Jacobsen, *Science* **297**, 376 (2002)

Data

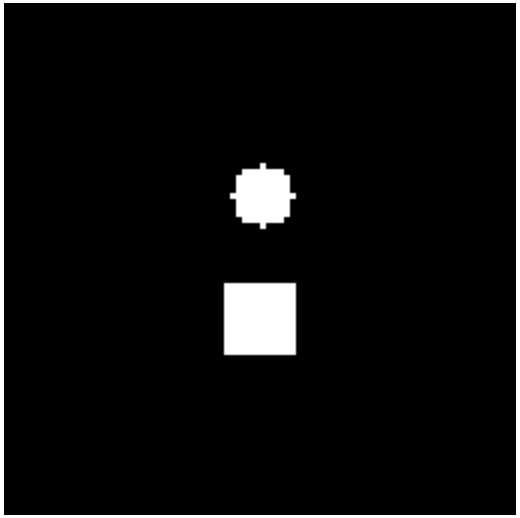

Support constraint (very loose)

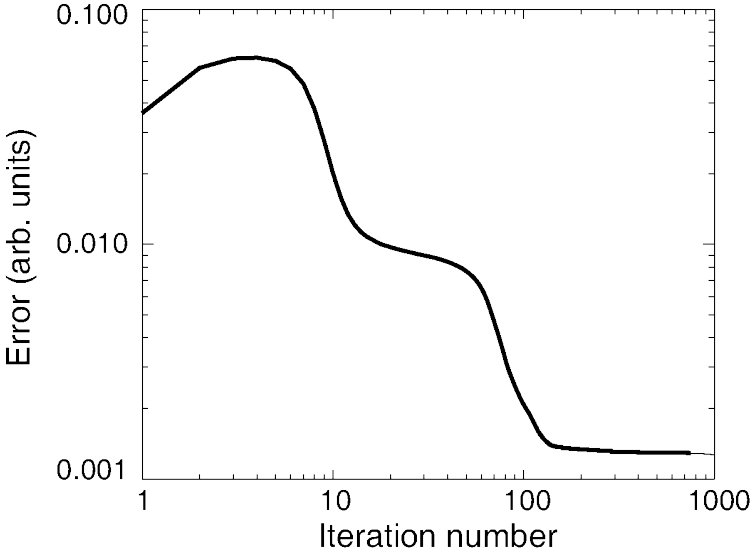

Reconstruction error

The reconstruction

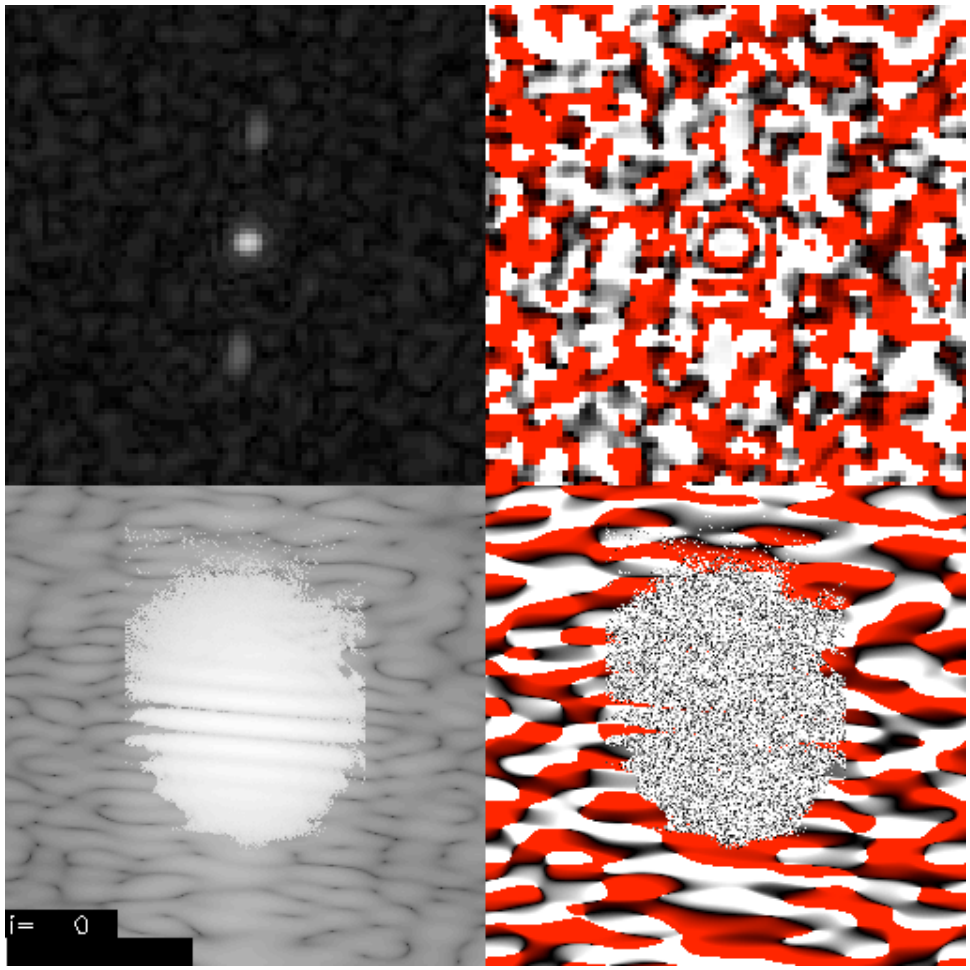

Real space Magnitude	Real space Phase
Far field Magnitude	Far field Phase

Coherent diffraction imaging: lower radiation dose than full-field zone plate imaging

Phasing in coherent diffraction imaging does not introduce extra noise; potential signal gain versus transmission x-ray microscopy (TXM; here assuming 10% efficient 20 nm zone plate)

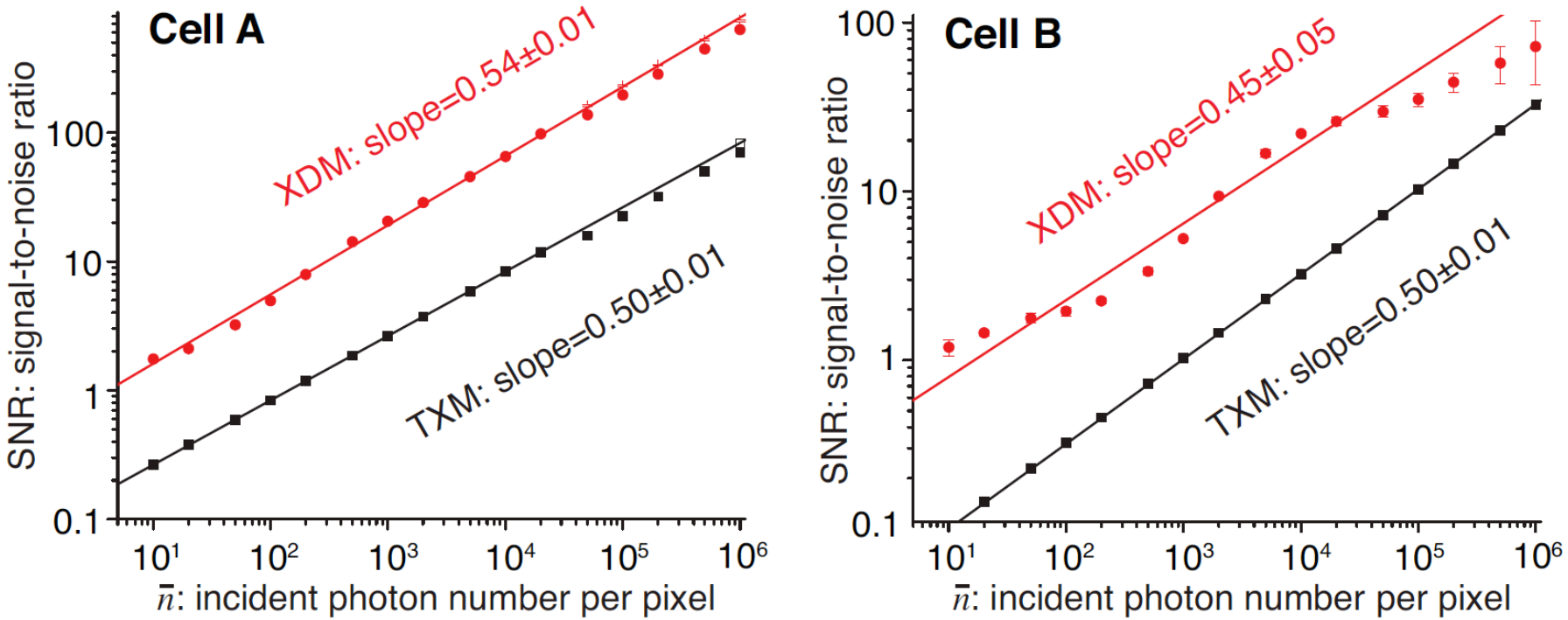

X. Huang *et al.*, *Optics Express* **17**, 13541 (2009)

Gold-labeled yeast

1.8 nm gold labeled for membrane sugars, silver-enhanced, dehydrated: J. Nelson *et al.*, *Proc. Nat. Acad. Sci.* **107**, 7235 (2010). 13 nm resolution x-ray diffraction microscopy.

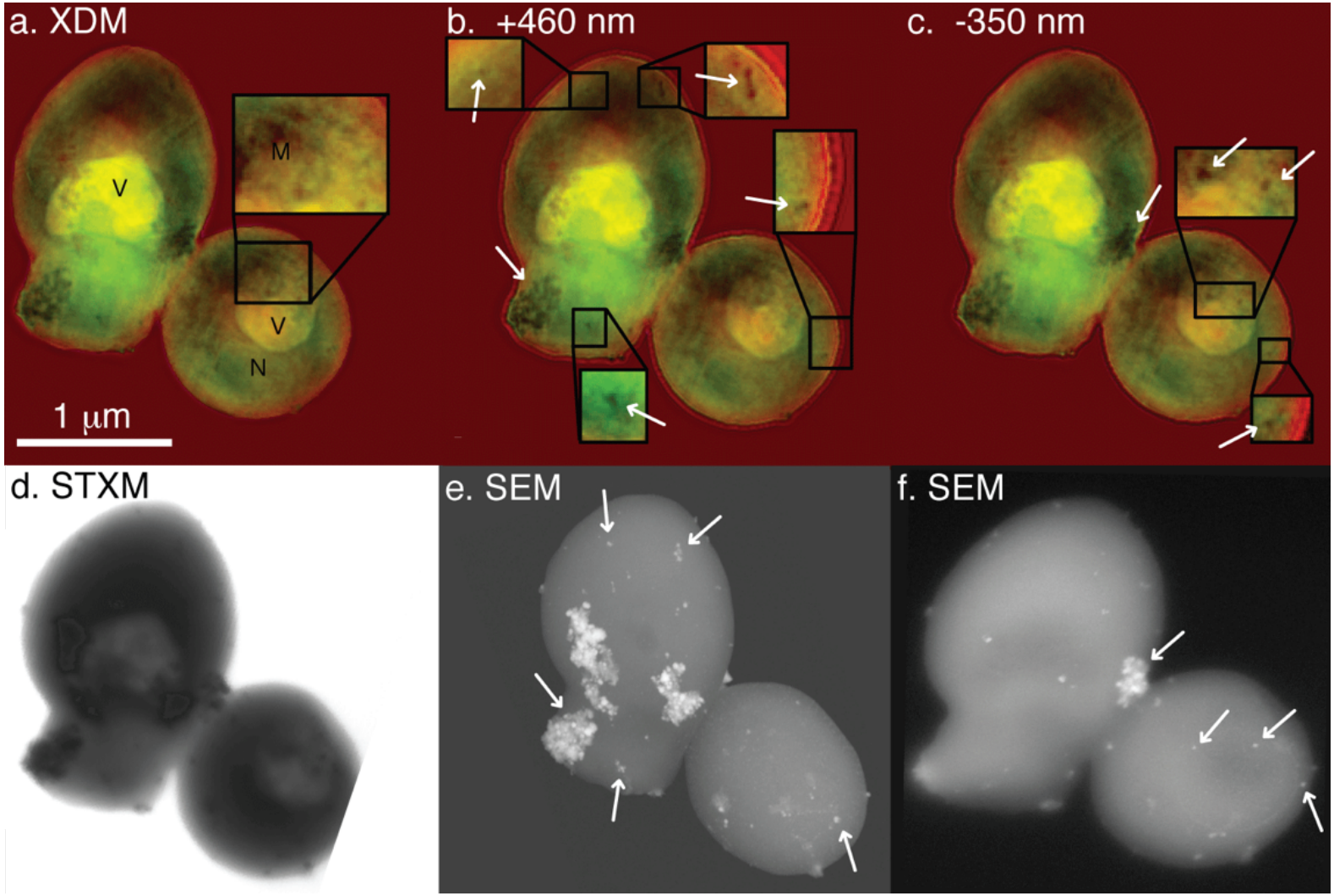

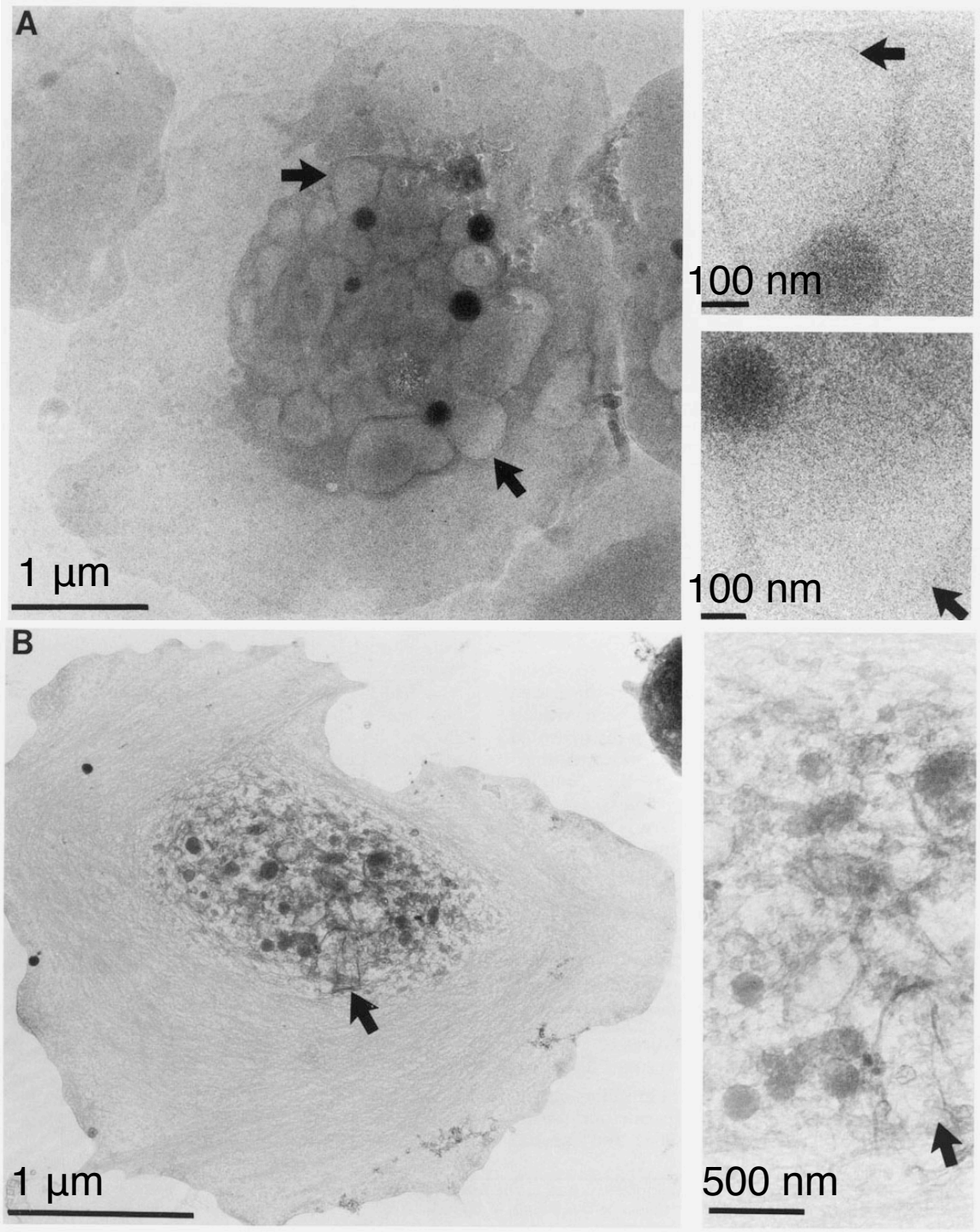

Frozen hydrated

2% glutaraldehyde fix
1% OsO_4 postfix
critical-point dry

- Human blood platelets
- 1 MeV transmission electron microscope (JEOL-1000)
- O'Toole, Wray, Kremer, and McIntosh, *J. Struct. Bio.* **110**, 55 (1993)

Cryo prep lab at the Advanced Photon Source

Instec/Nikon cryo light microscope

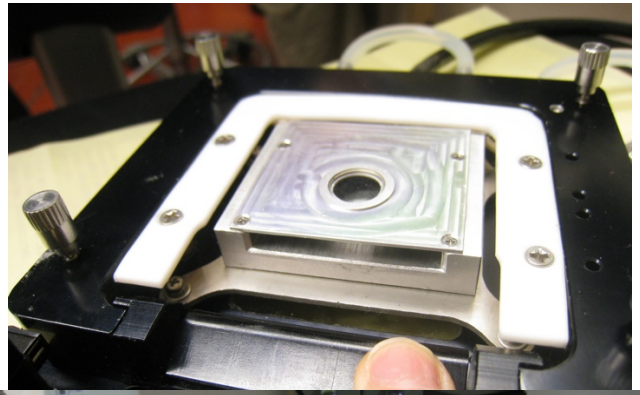

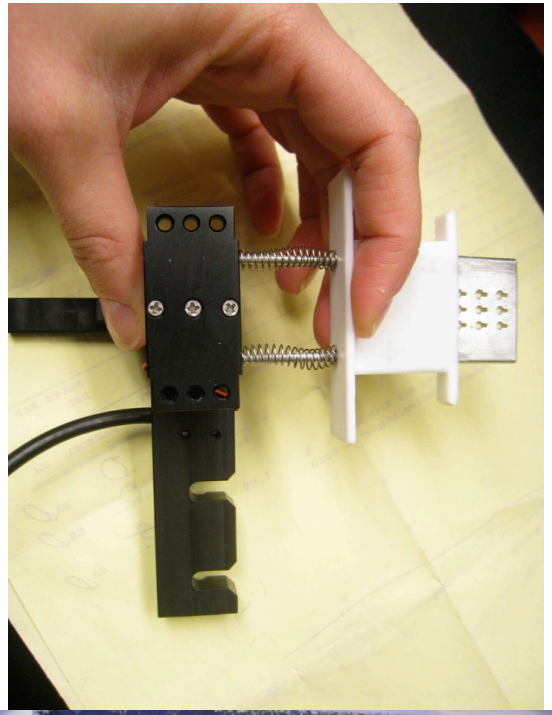

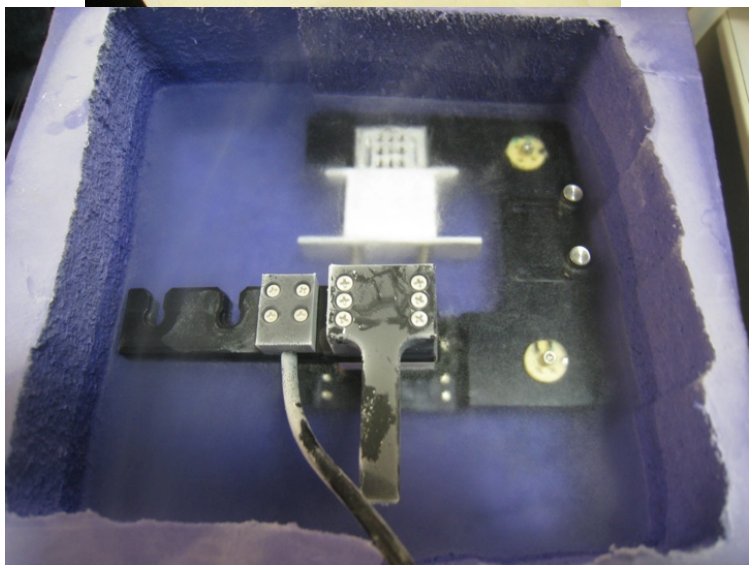

Complexity: confidence through correlation

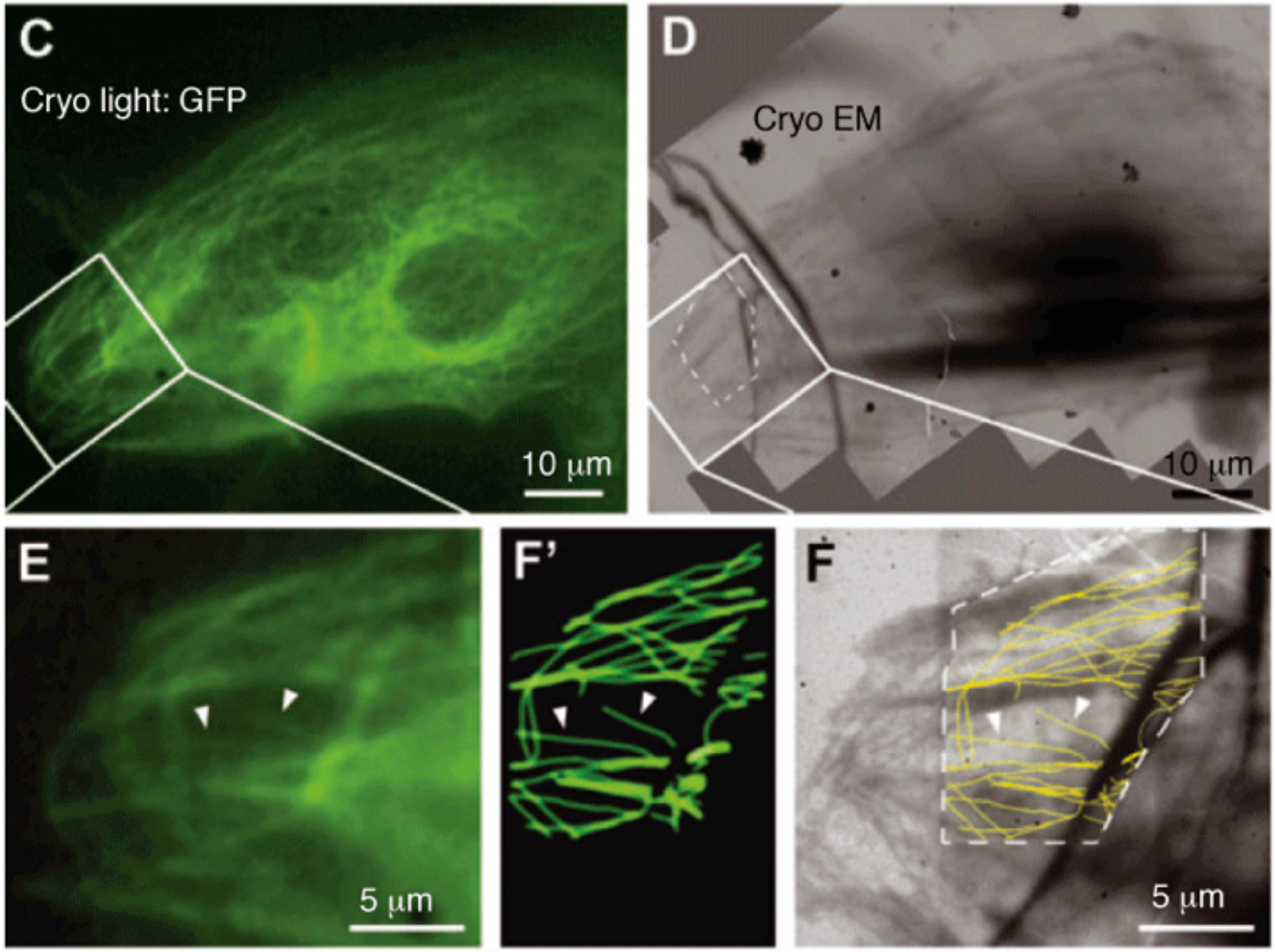

Schwartz et al., *J. Micros.* **227**, 98 (2007)

BioNanoprobe

- Energy range: 5 – 20 keV
- resolution: Mapping: δ <=30 nm; Spectroscopy: δ =50 nm

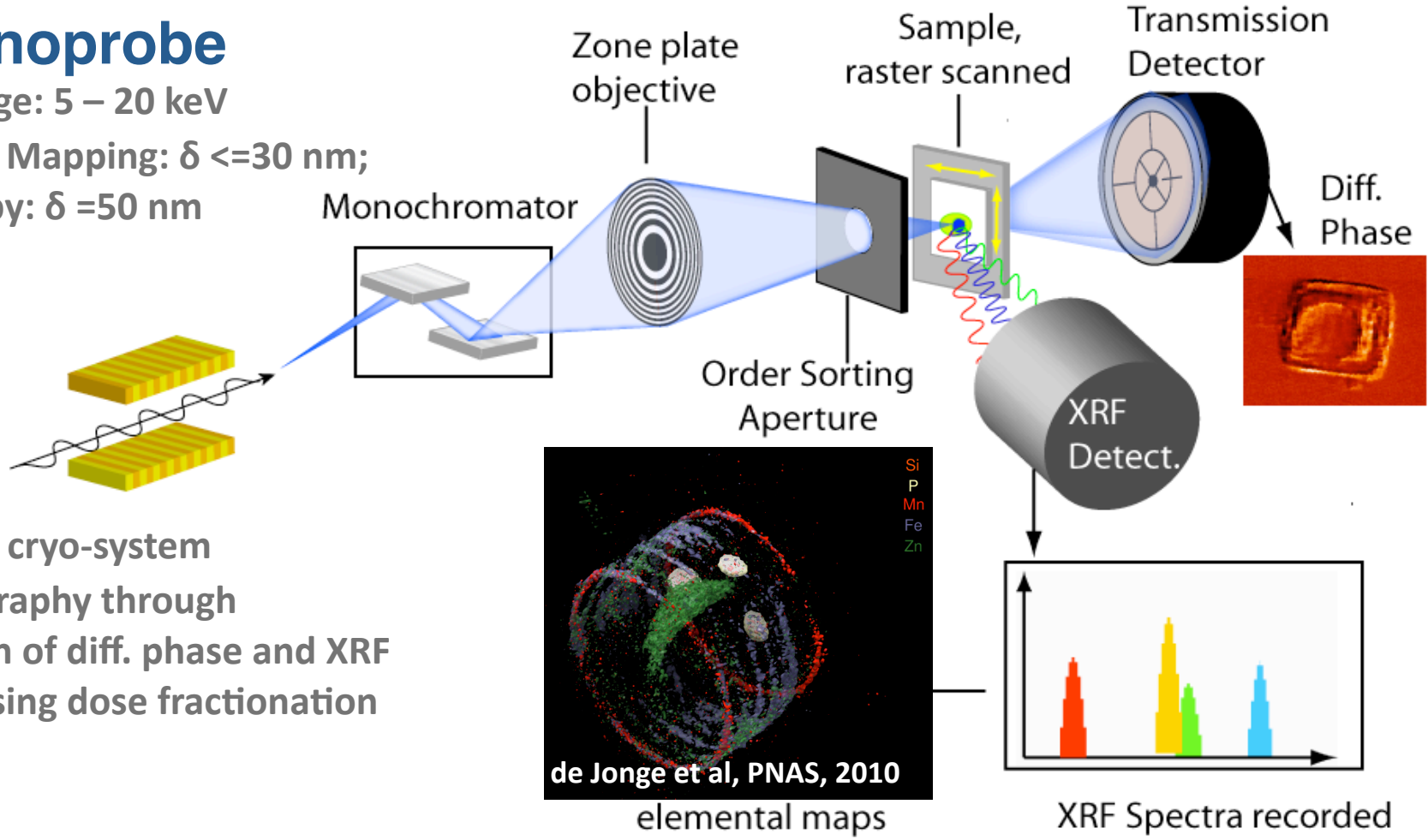

- in vacuum, cryo-system
- fast tomography through combination of diff. phase and XRF mapping, using dose fractionation

Received NIH funding May 2010 (PI: G. Woloschak, Northwestern University). BioNanoprobe will be built by Xradia, installed at APS: LS-CAT (sector 21), start commissioning in June 2011

co-Investigators: S. Vogt (tech lead), T. Paunesku, K. Brister (LS CAT tech lead), B. Lai, J. Maser, C. Jacobsen, W. Anderson, *et al*

Argonne NATIONAL LABORATORY

NORTHWESTERN UNIVERSITY FEINBERG SCHOOL OF MEDICINE

xradia insight in 3D

Summary

- X rays complement electrons:
  - lower spatial resolution (30-100 nm today, 5-10 nm goal)
  - thicker specimens (10-100 µm)
  - better trace element sensitivity
  - better chemical speciation.
- Lab systems for tomography
- Synchrotrons for faster tomography, trace element mapping, and spectromicroscopy
- Cryo is only starting to become available on a routine basis
  - Soft x-ray cryo tomography: Advanced Light Source in Berkeley, BESSY in Berlin (soon ALBA in Barcelona)
  - Hard x-ray cryo nanoprobe: Advanced Photon Source at Argonne, ESRF in Grenoble (lower resolution)

The university team

Jan Steinbrener, Lisseth Gavilan, Xiaojing Huang, Christian Holzner, Rachel Mak, Josh Turner, Johanna Nelson, Chris Jacobsen, Robert Towers. Not shown: Sue Wirick, Chris Peltzer.

Phase contrast and fluorescence
Spectromicroscopy
XDM/CXDI

Funding: DoE, NIH, NSF, ANL, NYSTAR

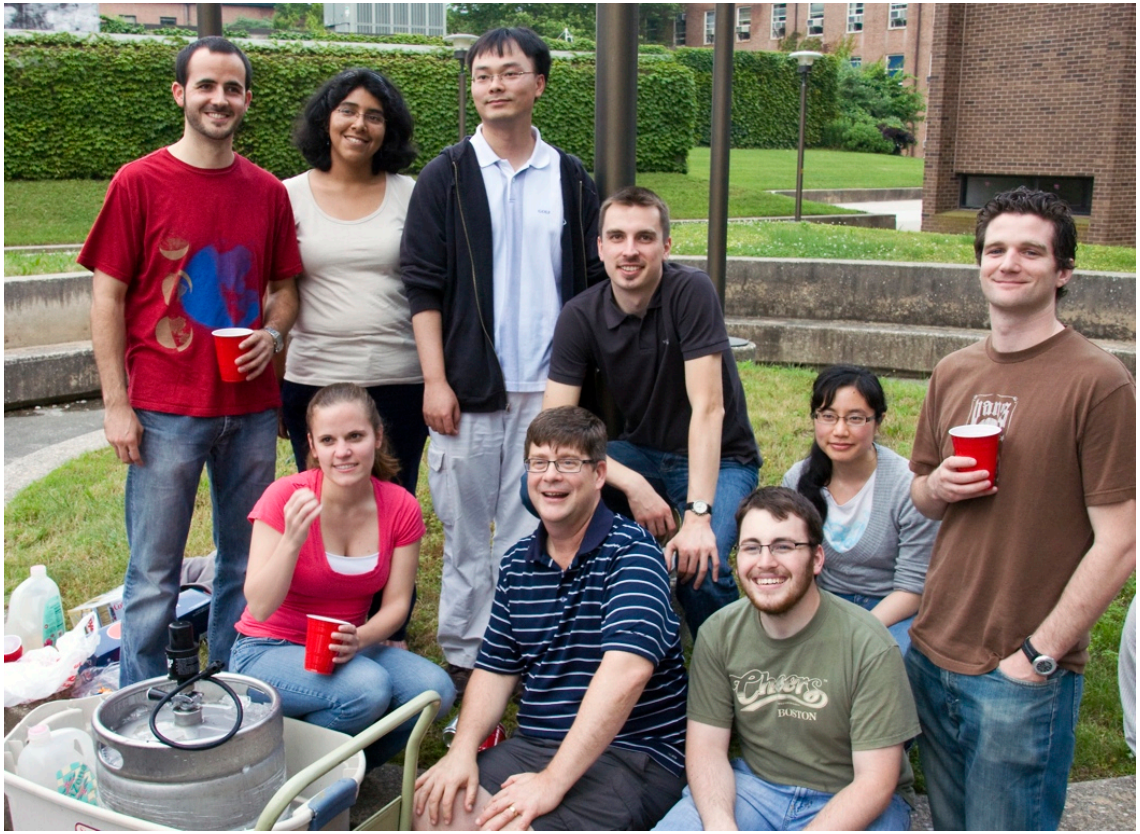

August 2009 at Stony Brook; now Argonne and Northwestern!

Argonne National Lab: Zhonghou Cai, Francesco De Carlo, Kamel Fezzaa, Lydia Finney, Charlotte Gleber, Ross Harder, Barry Lai, Wah-Keat Lee, Joerg Maser, Ian McNulty, David Vine, Steve Wang